

Fritz-Haber-Institut der Max-Planck-Gesellschaft Berlin

13th Meeting of the Fachbeirat

Berlin, 13th - 15th November 2005



Poster Abstracts

**Fritz-Haber-Institut der
Max-Planck-Gesellschaft
Berlin**

**13th Meeting of the Fachbeirat
Berlin, 13th – 15th November 2005**

Poster Abstracts

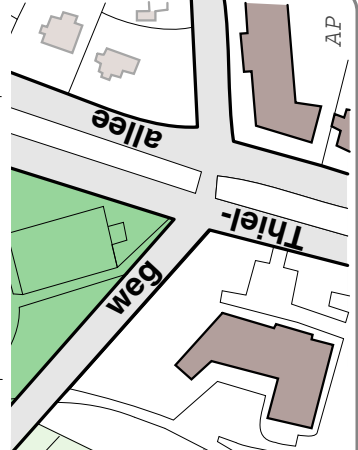
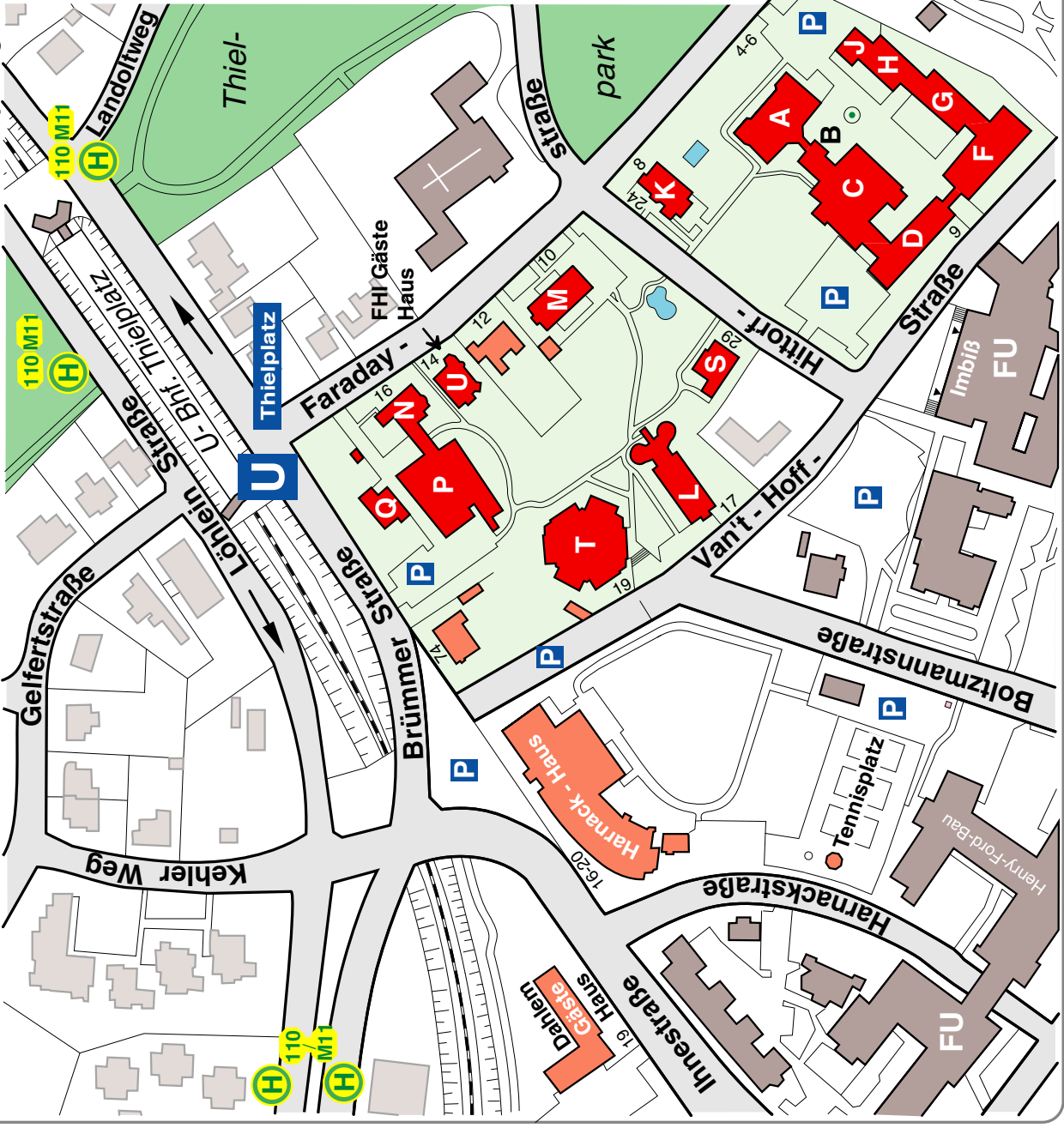
The posters can be found in the following buildings:

	Building
Department of Inorganic Chemistry	HH (W)*
Department of Chemical Physics	N, P, Q
Department of Molecular Physics	C, D
Department of Physical Chemistry	A
Theory Department	T

* Explanation: Harnack-Haus (Wintergarten), Ihnestrasse 16-20

Fritz-Haber-Institut der Max-Planck-Gesellschaft, Faradayweg 4-6, D-14195 Berlin

- A** Physikalische Chemie (G. Meijer)
- B** Haupteingang - Telefonzentrale
- C** Zentrale Dienste
- D** Haber-Linde
- E** Molekülphysik (G. Meijer)
- F** Physikalische Chemie (G. Meijer)
- G** Molekülphysik (G. Meijer),
Feinwerktechnik
- H** Anorganische Chemie (R. Schlögl),
Physikalische Chemie (G. Meijer)
- I** Bibliothek, Verwaltung
- J** Hörsaal, Holztechnik
- K** Zentrales Beschaffungswesen
- L** Maschinenbau
- M** Haber-Villa: Seminarraum
- N** Ernst-Ruska-Bau:
- O** Anorganische Chemie (R. Schlögl),
Elektroniklabor
- P** Richard-Willstätter-Haus:
Theorie [Geb. II] (M. Scheffler),
Seminarraum
- Q** Chemische Physik (H.-J. Freund)
- R** Seminarraum
- S** PP&B Personal Computer, Betriebsrat
- T** Theorie [Geb. I] (M. Scheffler),
GNZ Gemeinsames Netzwerkzentrum
- U** Gästehaus, Haustechnik



Department of Inorganic Chemistry

Poster List

- AC 1.0 Iron Oxides in Dehydrogenation**
- AC 1.1 Iron Oxide Based Model Catalysts - Preparation and Characterization**
S. Aburous, O. Shekhah, G. Ketteler, W. Ranke
- AC 1.2 Iron Oxide Based Model Catalysts – Adsorption and Catalysis**
O. Shekhah, A. Schüle¹, G. Kolios¹, W.X. Huang², W. Ranke
- AC 2.0 Zirconia and Heteropoly Acids in Hydrocarbon Activation**
- AC 2.1 Initiation of Alkane Isomerization on Sulfated Zirconia Catalysts**
B.S. Klose, R.E. Jentoft, T. Ressler, P. Joshi, A. Trunschke, F.C. Jentoft, R. Schlögl, I.R. Subbotina,* V.B. Kazansky*
- AC 2.2 Probe Molecule Investigations on Zirconia Powders**
J. Kröhnert, S. Wrabetz, A. Sauvage, F.C. Jentoft, R. Schlögl, I.R. Subbotina,* V.B. Kazansky*
- AC 2.3 Sulfated Zirconia Model Thin Films**
R. Lloyd, H. Sauer, F.C. Jentoft, R. Schlögl
- AC 3.0 Vanadium Oxides in Selective Oxidation**
- AC 3.1 Vanadia in n-Butane Selective Oxidation**
M. Haevecker, E. Kleimenov, K. Weiss, H. Sack-Kongehl, D. Wang, N. Pinna*, R.E. Jentoft, U. Wild, D. Teschner, M.E. Vass, J. Urban, D. Su, A. Knop-Gericke, R. Schlögl
- AC 3.2 Electronic Structure of Vanadium-Phosphorus Oxides**
M. Willinger, D. Su, R. Schlögl
- AC 3.3 SBA-15 Supported Vanadia: Spectroscopic Characterization and Reactivity**
C. Hess, U. Wild, R. Herbert, R. Schlögl

- AC 4.0 Molybdenum Oxide Based Catalysts in C3 Selective Oxidation**
- AC 4.1 Mo₅O₁₄ Model Catalyst for Oxidation of Propene to Acrylic Acid**
E. Rödel, P. Schnörch, P. Beato, T. Ressler, A. Knop-Gericke, A. Trunschke, R. Schlögl
- AC 4.2 Investigations on Synthesis and Activation of MoVTeNbO_x Catalysts**
A. Celaya Sanfíz, A. Blume, V. Makwana, F. Girgsdies, A. Trunschke, M. H. Looi*, S.B.A. Hamid*, R. Schlögl
- AC 4.3 Synthesis of Highly Dispersed Ru Oxide Species Hosted in Mo Oxide Based Matrices as Catalysts for Selective Oxidation of Propane**
O. Timpe, A. Trunschke, R. Schlögl
- AC 5.0 Copper in C1 Chemistry**
- AC 5.1 Microstructural Modifications of Cu/ZnO Catalysts as a Function of Precipitate Ageing**
B.L. Kniep, E.N. Muhamad, F. Girgsdies, T. Ressler, R. Schlögl
- AC 5.2 Cu/ZrO₂ catalysts for methanol steam reforming**
A. Szizybalski, F. Girgsdies, J.H. Schattka*, Y. Wang*, R.A. Caruso*, M. Antonietti*, T. Ressler, R. Schlögl
- AC 5.3 Combined in situ XPS and in situ XAS Study of Cu/ZnO Based Catalysts for Methanol Steam Reforming**
M. Hävecker, B.L. Kniep, E. Kleimenov, P. Schnörch, D. Techner, S. Zafeiratos, H. Bluhm, A. Knop-Gericke, T. Ressler, R. Schlögl
- AC 6.0 Introduction to Research Area 6: Palladium in Model Reactions**
- AC 6.1 Selective Hydrogenation of 1-pentyne on Pd Catalysts**
D. Teschner, A. Knop-Gericke, E. Vass, S. Zafeiratos, A. Pestryakov*, E. Kleimenov, M. Hävecker, H. Bluhm+, R. Schlögl
- AC 6.2 Oxidation of C₂H₄ and CH₄ on Pd (111): Characterization of the Active Phase by in situ XPS**
H. Gabasch, W. Unterberger*, E. Kleimenov, S. Zafeiratos, D. Zemlyanov+, B. Aszalos-Kiss+, A. Knop-Gericke, B. Klötzer*, K. Hayek*, R. Schlögl

- AC 6.3 Active-site isolated Pd-Ga Intermetallic Compounds for Selective Acetylene Hydrogenation**
J. Osswald, M. Armbrüster, K. Kovnier*, R.E. Jentoft, Y. Grin*, R. Schlögl, T. Ressler
- AC 7.0 Carbon in Catalysis**
- AC 7.1 Optimisation of Reaction Conditions for the Oxidative Dehydrogenation of Ethylbenzene to Styrene**
J.J Delgado, D. S. Su, N. Keller*, G. Mestl**, M.J. Ledoux*, R. Schlögl
- AC 7.2 Synthesis of Carbon Tube-in-tube Nanostructure**
D.S. Su, Z- P. Zhu*, X. Liu, G. Weinberg, R. Schlögl
- AC 7.3 Carbon Nanofibers Nested inside and Immobilized on Activated Carbon**
D.S.Su, X.W. Chen, G. Weinberg, A. Klein-Hofmann, O. Timpe, S.B. Abd. Hamid*, R. Schlögl
- AC 8.1 Catalytic Wall Reactor for Partial Alkane Oxidation with Molecular Beam Mass Spectrometer Interface**
R. Horn,* K. Ihmann, J. Ihmann, M. Geske, A. Taha, F.C. Jentoft, R. Schlögl
- AC 8.2 Ethylene Epoxidation over Silver**
A. Knop-Gericke, M. Hävecker, S. Zafeiratos, E. Kleimenov, E. Vass, V. Bukhtiyarov*, B. Jacobi, B. Steinhauer, B. Kubias, R. Schlögl

Iron Oxides in Dehydrogenation

Introduction

This research area deals with the non-oxidative and oxidative dehydrogenation of ethylbenzene (EB) to styrene (St) over iron oxide based catalysts. The study of the oxidative dehydrogenation of EB over carbon catalysts is part of the research area “Carbon in Catalysis” (D.S. Su).

Poster (AC 1.1): FeO(111), Fe₃O₄(111), α -Fe₂O₃(0001) and K-promoted Fe₃O₄ model catalyst films were prepared on Pt(111) substrates. In an attempt to determine their surface termination experimentally, a study using ISS was started. ISS is sensitive to the topmost layer composition. Further, it was tried to prepare thick stepped oxide surfaces by film growth on a stepped Pt substrate.

Poster (AC 1.2): The studies of EB dehydrogenation with our home made single-crystal flow reactor with pre- and post-reaction surface analysis on model catalysts (unpromoted Fe₂O₃(0001) and Fe₃O₄(111), K-promoted KFe_xO_y films) were completed. In cooperation with the University of Stuttgart, a microkinetic modeling of the data on unpromoted model catalysts was performed. The role of addition of traces of oxygen was systematically studied.

In the past, the interaction of the relevant gases EB, Sty and H₂O with model catalysts surfaces was investigated. Now also the interaction with hydrogen was studied. Atomic H causes oxygen removal with autocatalytic reaction kinetics. However, also surface phases were found which are quite resistant towards H.

Iron Oxide Based Model Catalysts - Preparation and Characterization

S. Aburous, O. Shekhah, G. Ketteler, W. Ranke

Introduction

Well-ordered iron oxide based model catalyst surfaces have been prepared in the form of thin epitaxial layers on Pt substrates and have been characterized concerning composition and structure [1-4]. Mainly the two following questions were addressed in the last two years.

Results: Surface termination

In order to confirm surface structure models developed in our laboratory and elsewhere, ISS (ion scattering spectroscopy) was applied to study the surface termination (composition of the topmost layer) of very thin FeO and thick Fe₃O₄, α -Fe₂O₃ and KFe_xO_y films. It was confirmed that FeO(111) is O-terminated, Fe₃O₄(111) is Fe-terminated and α -Fe₂O₃(0001), oxidized at high pressure, is O-terminated. A new information is that KFe_xO_y films contain K and O but no Fe in the top layer. The only Fe containing surface is thus Fe₃O₄ which has low catalytic activity. We state that Fe is necessary but should not be in the top layer because it binds both EB and St too strongly. In connection with the study of catalytic activity, K-promoted films with a wide range of K-contents were prepared.

Results: Fe_xO_y on stepped Pt substrates

Since the catalytic properties had been found to be related to surface defects, it was tried to prepare model catalyst surfaces with atomic steps by growing them on a stepped Pt(9 11 11) substrate. While relatively well-defined steps form on very thin FeO(111) films, the growth of catalytically relevant thicker Fe₃O₄ films turned out to be independent of the topography of the substrate[5].

References

1. W. Weiss, W. Ranke, Progr. Surf. Sci. **70**, 1 (2002).
2. Y. Joseph, G. Ketteler, C. Kuhrs, W. Ranke, W. Weiss, R. Schlögl, Phys. Chem. Chem. Phys. **3**, 4141 (2001).
3. G. Ketteler, W. Ranke, R. Schlögl, J. Catalysis **212**, 104 (2002).
4. W. Ranke and O. Shekhah, Recent Res. Developm. in Surf. Sci. **1**, 75 (2004).
5. G. Ketteler, W. Ranke, J. Vac. Sci. Technol. A **23**, 1055 (2005).

Iron Oxide Based Model Catalysts – Adsorption and Catalysis

O. Shekhah, A. Schüle*, G. Kolios*, W.X. Huang**, W. Ranke

Reactivity studies - bridging the „pressure gap“

Studies of EB dehydrogenation under realistic conditions over epitaxially grown model catalysts were completed. The results can be summarized as follows [1,2]:

Most active is Fe^{3+} in Fe_2O_3 or KFe_xO_y .

- Fe_3O_4 is less active, probably because of a too strong bonding of EB and St.
- Deactivation of unpromoted catalysts occurs by reduction to Fe_3O_4 and by coking.
- Both can be prevented by admixture of some oxygen to the feed.
- K itself is not active but suppresses reduction and catalyses carbon removal.
- The stable phases $\text{K}_2\text{Fe}_{22}\text{O}_{34}$ and especially KFeO_2 are K-reservoir phases.
- Coke has a non-negligible catalytic activity.
- “Steaming” (reaction in steam without EB) accelerates K-loss considerably.

In cooperation with A. Schüle and G. Kolios (Stuttgart), a microkinetic modeling of the reactivity and the deactivation behavior of unpromoted catalysts was performed. Excellent agreement was reached using basic adsorption data for EB, St and water from earlier measurements and adjusting the remaining parameters to measured reactivities. [3].

Interaction with atomic H

In order to close the catalytic cycle, the produced hydrogen must be removed from the surface. It may react with lattice oxygen and desorb as H_2O . The oxygen would then have to be replaced in an oxidation step (Mars-Van-Krevelen mechanism). Alternatively, the hydrogen may desorb as H_2 . Adsorption studies should clarify this question.

Since molecular H_2 does not interact with the model catalyst surfaces, a source for atomic H was constructed. The interaction was studied by TDS, XPS and LEED. A thin $\text{FeO}(111)$ film is partially reduced by H_2O desorption during exposure. The process starts at oxygen vacancies, accelerates autocatalytically and stops when a composition of $\text{FeO}_{0.75}$ is reached. This final film desorbs only H_2 . On thicker $\text{Fe}_3\text{O}_4(111)$ films, autocatalytically accelerated bursts of H_2 and H_2O desorption occur. They are also defect-related [4-6].

References

1. O. Shekhah, W. Ranke, A. Schüle, G. Kolios, R. Schlögl, *Angew. Chem., Int. Ed.* **42**, 5760 (2003).
2. O. Shekhah, W. Ranke, R. Schlögl, *J. Catal.* **225**, 56 (2004).
3. A. Schüle, O. Shekhah, W. Ranke, R. Schlögl, G. Kolios, *J. Catal.* **231**, 172 (2005).
4. W. Huang, W. Ranke, R. Schlögl, *J. Phys. Chem. B* **109**, 9202 (2005).
5. W. Huang, W. Ranke, *Surf. Sci.*, submitted (2005).

* Institut f. Chem. Verfahrenstechnik, Universität Stuttgart, Böblinger Str. 72, D-70199 Stuttgart

** Dept. of Chem. Phys., Univ. of Science and Technology of China, Hefei, 230036, P.R. China

Zirconia and Heteropoly Acids in Hydrocarbon Activation

Introduction

Despite intense research no consistent picture has evolved yet as to how sulfated zirconia materials activate and isomerize small alkanes at low temperatures. The nature of the active sites—possibly more than one type—is still debated. After creating procedures for the reliable synthesis of highly active sulfated zirconia catalysts¹ and understanding the solid state chemistry,² specifically the interaction of promoters (Mn, Fe) with zirconia,³ we are now addressing the issues of sites and mechanism of alkane activation in detail.

Various initial steps, all of which lead to carbenium ions, have been discussed for alkane isomerization. When sulfated zirconia first was believed to be a solid superacid, protonation of the alkane by a Brønsted site or hydride abstraction by a Lewis site were favorite reaction paths. In order to explain the promoting effects of iron or manganese, a redox initiation has alternatively been proposed. The alkane is oxidatively dehydrogenated and the produced alkene subsequently protonated by an acid site. We use in situ UV-vis, IR, and XAS spectroscopies to identify the promoter valence (Mn), the state of the surface functional groups, and surface species formed during *n*-butane isomerization (Poster AC 2.1).

As long as the nature of the active sites is not clear, it is difficult to select appropriate probe molecules to characterize them. We employ reactant, product and chemically similar molecules to ensure that we are probing relevant sites. Besides the classical quantities used in probe molecule methods such as band shifts (IR spectroscopy) and differential heats of adsorption (calorimetry) we seek to develop new analytical procedures, which take advantage of the change of IR band intensities upon adsorption of a probe. Furthermore, we have identified carbon dioxide as a probe for “bare”, non-sulfated zirconia surface and try to assess the interaction of alkanes with exposed (inactive?) zirconia (Poster AC 2.2).

In order to be able to apply surface science methods to the investigation of sulfated zirconia catalysts, we have developed a model system consisting of a thin nanocrystalline film of sulfated zirconia on a silicon substrate. The thermal treatment, key step in the preparation of powders, has been studied in more detail and probe molecule experiments have been started using ammonia and *n*-butane. (Poster AC 2.3).

The activities on heteropolyacids in the past two years were largely limited to data evaluation and finalization of manuscripts. Hence, no poster will be presented.

References

1. A. Hahn, T. Ressler, R.E. Jentoft, F.C. Jentoft, Chem. Commun. 537 (2001).
2. B.S. Klose, R.E. Jentoft, A. Hahn, T. Ressler, J. Kröhnert, S. Wrabetz, X. Yang, F.C. Jentoft, J. Catal. **217**, 487 (2003).
3. F.C. Jentoft, A., J. Kröhnert, G. Lorenz, R.E. Jentoft, T. Ressler, U. Wild, R. Schlögl, C. Häßner, K. Köhler, J. Catal. **224**, 124 (2004).

* Institut f. Chem. Verfahrenstechnik, Universität Stuttgart, Böblinger Str. 72, D-70199 Stuttgart

** Dept. of Chem. Phys., Univ. of Science and Technology of China, Hefei, 230036, P.R. China

Initiation of Alkane Isomerization on Sulfated Zirconia Catalysts

B.S. Klose, R.E. Jentoft, T. Ressler, P. Joshi, A. Trunschke, F.C. Jentoft, R. Schlögl, I.R. Subbotina,* V.B. Kazansky*

Sulfated zirconia (SZ) and Mn-promoted SZ were studied in situ during activation in different atmospheres and during *n*-butane isomerization. DRIFT spectra show that activation at 773 K leads to about 90% dehydration (60–125 $\mu\text{mol H}_2\text{O/g}$ remain). Comparison of SO single and double bond vibrations in the activated state with results from DFT calculations¹ suggests $\text{S}_2\text{O}_7^{2-}$ as predominant surface species. Spectra of Mn-promoted SZ after activation in N_2 or O_2 reveal slightly different OH band intensities. Strong Lewis acid sites capable of adsorbing N_2 at 358 K were present after activation in N_2 . XAFS and UV-vis spectra indicate significant reduction of Mn (valence before activation 2.65) in inert and slight reduction in oxidizing atmosphere.

All catalysts showed an induction period before they reached maximum conversion to isobutane. With increasing Mn valence after activation, the maximum rate of butane isomerization increased, seemingly suggesting that oxidative dehydrogenation (ODH) plays a role in the reaction initiation. However, there was no evidence for reaction initiation by stoichiometric ODH via reduction of Mn, neither in the XAFS nor in the UV-vis spectra. It is thus concluded that Mn^{2+} in comparison to Mn^{3+} (or Mn^{4+}) has no promoting effect. DRIFT spectra recorded of SZ or Mn-promoted SZ during *n*-butane isomerization show several bands growing between 1720–1550 and at 5200 cm^{-1} , and a shift of the S=O vibration at 1400 cm^{-1} to lower wavenumbers. The new bands may arise from adsorbed water, potentially a product of ODH, but other species cannot yet be excluded. At times on stream before maximum conversion is reached, the rate of isomerization is proportional to the area of the feature including the bands at 1630 and 1600 cm^{-1} . Hence, the absorbing species must be active intermediates or side products of the reaction producing the intermediates. It follows that the rate during the induction period depends on two factors: the number of active intermediates (reaction chain carriers) formed and the intrinsic turnover per such species. The presence of Mn enhances this intrinsic turnover frequency.

Formation of water indicates ODH, but Mn is not the oxidizing agent. Alkanes can be activated in absence of promoters, and sulfate has oxidizing power. Indeed, after exposure of SZ to *n*-butane at 573 K H_2O , CO_2 , H_2S and olefinic species were detected with DRIFTS. At higher temperatures, the sulfate can be completely reduced with concomitant complete oxidation of the hydrocarbon. At the lower isomerization reaction temperatures (323–378 K), partial oxidations and reductions may occur. Deactivation was often rapid, depending on catalyst and test conditions. However, full recovery was possible, excluding significant sulfate loss via formation of volatile compounds.

References

1. A. Hofmann, J. Sauer, J. Phys. Chem. B **108**, 14652 (2004), and personal communication.

*N.D. Zelinsky Institute of Organic Chemistry, Russian Academy of Sciences, Leninsky Prospect 47, Moscow 117913, Russia

Probe Molecule Investigations on Zirconia Powders

J. Kröhnert, S. Wrabetz, A. Sauvage, F.C. Jentoft, R. Schlögl,
I.R. Subbotina,* V.B. Kazansky*

Carbon dioxide is a probe for basic sites but can also adsorb weakly in a linear manner on Lewis acid sites. In TPD experiments CO₂ was retained on the surface of pure zirconia up to 823 K. Sulfated samples adsorbed little or no CO₂; specifically in presence of enough sulfate and calcination at a moderate temperature of 773 K all zirconia basic sites were found covered by sulfate. After exposure of this sample to *n*-butane at 773 K and subsequent evacuation, a small amount of CO₂ could be adsorbed, presumably on sulfate-free patches. That sulfate may be removed is proven by the IR spectroscopic results of Poster 2.1, which indicate conversion of sulfate into volatile compounds such as H₂S already at 573 K. DRIFTS experiments showed that a sulfated zirconia catalyst adsorbs more CO₂ in a linear fashion (at 313 K) after being partially desulfated through water-washing. Sulfate is known to increase the strength of Lewis acid sites on zirconia; here, we see that it blocks Lewis sites and thus reduces their number. CO₂ is identified a useful and sensitive probe for “bare” patches of zirconia in a sulfated material. The importance of the sulfate coverage becomes evident from adsorption isotherms of isobutane. On a number of sulfated and non-sulfated zirconia samples higher coverages of isobutane at equal pressures were consistently observed on non-sulfated materials. For samples with sub-monolayer sulfate coverage, alkanes may have to be classified as unselective probes because of adsorption also on presumably inactive surface. However, their strong affinity to pure zirconia could also play a role for catalysis.

The interaction of hydrocarbons with sulfated zirconia was investigated by a new method. Polarization of molecules upon adsorption should lead to a redistribution of charges and changes of dipole moments during vibrations should be different in comparison to the free molecule in the gas phase. Intensities of vibrational bands can thus serve as a measure of the activation of certain bonds. Extinction coefficients of the CH stretching vibrations of neopentane, an inert model alkane, after adsorption on sulfated zirconia samples and acidic reference materials (H-Mordenite) were determined. The integral molar extinction coefficient of the CH vibrations was almost always larger in the adsorbed state than in the gas phase. Adsorption on sulfated zirconia samples produced significantly higher extinction coefficients than interaction with zeolites. Unfortunately, the data were found to be obscured by scattering of the thin self-supporting wafers that were used for the transmission measurements. The influence of variations in scattering abilities of different samples on the extinction coefficients of adsorbate vibrations is currently investigated.

*N.D. Zelinsky Institute of Organic Chemistry, Russian Academy of Sciences,
Leninsky Prospect 47, Moscow 117913, Russia

Sulfated Zirconia Model Thin Films

R. Lloyd, H. Sauer, F.C. Jentoft, R. Schlögl

The SZ thin films, which have been developed within the department,¹ were prepared by aqueous deposition onto a self assembled monolayer functionalized silicon substrate, followed by thermal treatment. The effects of atmosphere during thermal treatment of the films have been studied to optimize this procedure. The surfaces of the films have been characterized by reactant and probe molecule adsorption experiments.

Thermal treatment of the SZ films at 823 K for 2 h was investigated both in synthetic air (analogous to powder preparation) and an inert atmosphere (in order to prevent possible damage to the film from combustion of precursors), at various heating rates. Transmission and scanning electron micrographs and electron diffractograms show the films to exhibit similar physical and crystal properties after the different treatments. X-ray photoelectron spectra show the chemical environments after the two different treatments to differ slightly; however, their overall compositions are comparable to typical SZ power catalysts.

Ammonia, probe molecule, thermal desorption experiments revealed fragments indicative of ammonia evolution at 373 to 423 K and at ca. 637 K with concomitant sulfate decomposition (induced by the presence of the basic probe). This is consistent with earlier reports of sulfated oxides undergoing oxidative decomposition upon exposure to basic probe molecules at elevated temperatures.²

Initial reactant, *n*-butane, thermal desorption and isobaric studies of the SZ thin films show no significant adsorption sites exceeding those from a blank (oxidized silicon wafer) experiment. This suggests there are no detectable amounts of strongly adsorbed butane species on the SZ surface, which is consistent with SZ powder calorimetric measurements showing the interaction of *n*-butane with the majority of sites on SZ is weak ($\approx 45\text{--}60$ kJ/mol).³ In order to test whether the thin films are active in *n*-butane isomerization and thus a valid model system, a suitable reactor is now being developed. The stainless steel construction allows for flow and batch mode operation, heating to the temperature necessary for activation (≈ 673 K) and pressures of a few atmospheres.

References

1. F.C. Jentoft, A. Fischer, G. Weinberg, U. Wild, R. Schlögl, *Stud. Surf. Sci. Cat.* **130**, 209 (2000).
2. X. Song, A. Sayari, *Catal. Rev. - Sci. Eng.* **38**, 329 (1996).
3. X. Li, K. Nagaoka, L.J. Simon, J.A. Lercher, S. Wrabetz, F.C. Jentoft, C. Breitkopf, S. Matysik, H. Papp, *J. Catal.* **230**, 214 (2005).

Vanadium Oxides in Selective Oxidation

Introduction

Vanadium oxides and vanadium-phosphorus oxide (VPO) systems are extensively used as catalysts in selective oxidation of hydrocarbons. The synthesis of maleic anhydride (MA) from *n*-butane over VPO is as yet the only industrial application of alkane selective oxidation and is based on the presence of vanadyl pyrophosphate (VPP). Besides that, vanadium-containing catalysts are of considerable scientific and industrial interest due to their importance for the direct synthesis of acrylic acid.

Results

Previous research activities up to the 12th Fachbeirat meeting in 2003 revealed the dynamic nature of the VPO surface using mainly *in situ* NEXAFS. These studies were extended by applying the complementary *in situ* XPS technique to characterize the surface of VPO catalysts at different depths using synchrotron radiation as a tuneable X-ray source. The experimental results suggest that in VPO the structure of the catalytically active species is only weakly related to the average bulk structure. Therefore, it seems necessary to study model systems with simplified structure but with relevant catalytic properties, e.g. nanostructured materials. To this end, V_xO_y nanoparticles were studied towards changes in the electronic and geometric structure during the selective oxidation of *n*-butane towards MA using a micro-reactor for catalyst testing in the micrometer regime (*Poster 3.1*).

VPO catalysts consist of the main V^{4+} phase $(VO)_2P_2O_7$ and a mixture of pentavalent $VOPO_4$ phases. These phases are crucial for the conversion and selectivity rate of the final catalyst. It is believed that only a specific combination of V^{4+} and V^{5+} phases leads to the high catalytic performance. Therefore, the electronic structure of VPO phases was investigated by means of a combined theoretical and experimental approach. TEM, EELS and XRD were used to study the geometric structure of VPO phases prepared with different routes and of the standard V^{5+} phases. Ab-initio band structure calculations based on density functional theory (DFT) were performed in order to evaluate the bulk electronic structure (*Poster 3.2*).

Due to the structure complexity of vanadium oxides and VPO systems, fundamental catalysis research benefits from uniform materials, which offer the opportunity to study selective oxidation reactions on model systems with well-defined structure. Therefore, vanadium oxides supported on mesoporous silica SBA-15 were prepared using a novel grafting/ion-exchange method. The individual steps of the synthesis to highly dispersed vanadia on mesoporous SiO_2 were elucidated using a combination of complementary spectroscopic techniques (XPS, DRIFTS, Raman), which allowed us to propose a detailed mechanism for the synthesis. The final vanadium oxide catalysts were tested in methanol and propane selective oxidation (*Poster 3.3*).

Vanadia in *n*-Butane Selective Oxidation

M. Haevecker, E. Kleimenov, K. Weiss, H. Sack-Kongehl, D. Wang, N. Pinna*, R.E. Jentoft, U. Wild, D. Teschner, M.E. Vass, J. Urban, D. Su, A. Knop-Gericke, R. Schlögl

Introduction

Previous results revealed the dynamic nature of the VPO surface using mainly *in situ* NEXAFS. These studies were extended by applying the complementary *in situ* XPS technique to characterize the surface of VPO catalysts at different depths using synchrotron radiation as tuneable X-ray source. The experimental results suggest the structure of the catalytically active species is only weakly related to the average bulk structure. Therefore, model systems with simplified structure but with relevant catalytic properties, e.g. V_xO_y nanoparticles were studied towards changes in the electronic and geometric structure during the selective oxidation of *n*-butane towards MA.

Results

For the oxidation of *n*-butane to MA the technical catalyst is vanadium-phosphorus-oxide (VPO), representing a complex material being composed of a variety of phases. We extended our previous *in situ* NEXAFS study by applying the complementary *in situ* XPS technique. Spectroscopic data for two mean information depths (1.0 nm and 1.8 nm) have been obtained using synchrotron radiation as a tunable X-ray source. The catalysts showed the same vanadium oxidation state at the outer surface (approx. +4.0) while the electronic structure was different at deeper layers. These experimental results suggest that in VPO the structure of the catalytically active species is only weakly related to the average bulk structure. Therefore, approaches to establish a structure/activity relationship for VPO that are based on bulk structural data would be at least ambiguous. It seems to be necessary to study model systems with simplified structure but with relevant catalytic properties, e.g. nanostructured materials. These materials need support to provide stability but self-supporting might be suitable as well.

Unsupported V_xO_y nanocrystals were synthesized in a controlled way via a simple non-aqueous process. The evolution of the electronic and geometric structure of the material was characterized by XPS, EELS, TEM and electron diffraction before and after the reaction at different temperatures. It was found that the particles did undergo a radical modification of the geometric and electronic structure. Pure V^{5+} is ineffective and the co-existence of V^{5+} and V^{4+} as a consequence of structural defects is essential for selective oxidation function. A selectivity change from acetic acid to MA was observed, which is ascribed to an acidic functionality forming acetic acid at low temperature. This function is missing at high temperatures and instead butane gets oxidized resulting in MA.

Finally a series of V_xO_y/Al_2O_3 catalysts was investigated for *n*-butane oxidation. A combination of *in situ* NEXAFS and XPS showed that the initial vanadium species was dependent upon catalyst loading. Under reaction conditions MA was detected among the products while the oxidation state of vanadium was a mixture of 4+ and 5+.

* Universität Halle-Wittenberg, Institut für Anorganische Chemie, Kurt-Mothes-Str. 2, 06120 Halle

Electronic Structure of Vanadium-Phosphorus Oxides

M. Willinger, D. Su, R. Schlögl

Introduction

Vanadium phosphorus oxides (VPO) are a very complex and fascinating system, which is characterized by an easy formation and inter-conversion of several crystalline phases. They are commercially used as catalysts for the synthesis of MA in the partial oxidation of n-butane. VPO catalysts consist of the main V^{4+} phase $(VO)_2P_2O_7$ and a mixture of pentavalent $VOPO_4$ phases. These phases are crucial for the conversion and selectivity rate of the final catalyst. It is believed that only a specific combination of V^{4+} and V^{5+} phases leads to the high catalytic performance.

To get a more profound understanding of the working catalyst and the role of the different phases we reduced the complexity of the system by investigating specific phases in depth on their own. VPO phases have been chosen according to their applicability as model substances for the investigation of the relation between geometric and electronic structure by means of a combined theoretical and experimental approach. TEM, EELS and XRD were used to study the geometric structure of VPO phases prepared with different routes and of the standard V^{5+} phases. Ab-initio band structure calculations based on density functional theory (DFT) were performed in order to evaluate the bulk electronic structure. Core level spectroscopic methods were applied to experimentally probe the electronic structure at the ionized species. The effect of structural variations on the electronic structure was investigated for three different $VOPO_4$ phases.

Results

The results point out the close agreement in their electronic structure and show that differences in the total energy of the polymorph are very small. The variations in the density of states are mainly related to variations in the geometry and distortion of the VO_6 and PO_4 structural units, while their relative arrangement has only a minor effect on the electronic structure. Observed differences in the stability and hydration behavior as well as the reduction and re-oxidation properties are, on the other hand, determined by the way in which these structural units form the three dimensional structure.

Simulations performed for the case of V^{4+} phases revealed a strongly localized electron in a HOMO state located at the equatorial plane of the VO_6 polyhedron. As the Fermi level is shifted upwards with respect to the V^{5+} phases and the lowest vanadium $3d$ state is occupied with one electron, the band gap is determined by the splitting of this state from the remaining $3d$ states and hence, related to the distortion of the VO_6 polyhedron. Due to the close agreement between simulation and the experimentally recorded electron energy loss spectra, characteristic features of differently coordinated oxygen atoms can be identified and traced back to the underlying transitions. Spectral features are hence well understood and can be used for the interpretation of spectra recorded from samples of unknown phase composition.

SBA-15 Supported Vanadia: Spectroscopic Characterization and Reactivity

C. Hess, U. Wild, R. Herbert, R. Schlögl

Introduction

Due to the structure complexity of vanadium oxides and VPO systems, fundamental catalysis research benefits from uniform materials, which offer the opportunity to study selective oxidation reactions on model systems with well-defined structure. Therefore, vanadium oxides supported on mesoporous silica SBA-15 were prepared using a novel grafting/ion-exchange method. The individual steps of the synthesis to highly dispersed vanadia on SBA-15 were elucidated using a combination of complementary spectroscopic techniques. The final vanadium oxide catalysts were tested in methanol selective oxidation.

Results

The individual steps of our novel synthesis approach to highly dispersed vanadium oxide were elucidated using XPS and vibrational spectroscopy (DRIFTS, Raman): (1) The inner pores of the mesoporous matrix are functionalized via hydroxy groups leading to the formation of an organic framework consisting of ammonium propyl chains. Because of its structure it allows for a controlled introduction of vanadia into the nanopores. (2) The metal oxide precursor (butyl-ammonium decavanadate) is introduced intact into the nanopores via ion exchange without any changes in the organic framework. (3) During calcination the V_xO_y cluster are anchored to the surface and the organic residues are completely removed from the pores.

Catalytic experiments demonstrate that highly dispersed vanadia supported by SBA-15 is highly selective in methanol oxidation to formaldehyde between 300-400°C. Selectivity values range between 96% at low conversion and temperature and 83% at 400°C and 87% methanol conversion. We report the highest formaldehyde yield (72%) in the methanol oxidation over silica supported vanadium oxides. It is obtained for the vanadium oxide catalyst with the highest dispersion (7.2 wt% V) at 400°C. Raman characterization of this catalyst after reaction at high conversion indicates that dispersed vanadia partly agglomerates into vanadia crystallites during methanol oxidation.

These results demonstrate the potential of our novel approach for the controlled synthesis of nanostructured transition metal model catalysts. The high specific surface area (800 m²/g) and small pore size distribution of the mesoporous support allow for a high dispersion of uniform active vanadium oxide sites within the nanopores. Our reactivity results demonstrate the excellent catalytic performance of this catalyst. Therefore, it seems very well suited for studying structure-activity relationships of selective oxidation reactions of small alkanes.

Molybdenum Oxide Based Catalysts in C3 Selective Oxidation

Introduction

The manifold catalytic properties of MoO_3 have been applied in a wide range of industrially important reactions including selective oxidation of olefins¹. Further improvements and the ongoing need for new catalysts transforming light alkanes directly and selectively into more valuable products require a fundamental understanding of oxidation catalysis and the identification of relations between catalyst structure and product distribution. Generally, the selective oxidation of an alkane involves multiple steps like the activation of C-H bonds, hydrogen abstraction, oxygen activation, oxygen insertion and regeneration of active sites by incorporation of oxygen atoms into lattice vacancies. Such complex functionalities may be accomplished by coexistence of various active sites. Consequently, a certain structural complexity with respect to the molecular environment of the molybdenum atoms at the catalyst surface is indispensable. This local structure could be associated with the type of crystal plane on which the molybdenum ions are accommodated. It could be, however, also provided by ill-defined nano-structured surface clusters. In industrially applied systems optimized functionalities have been achieved by adding other components resulting in complex composed multi-metal oxides.

Addressing the relevance of specific phase structures in propene and propane activation, in particular Mo_5O_{15} like structural motifs, the mixed oxide $\text{Mo}_{0.68}\text{V}_{0.23}\text{W}_{0.09}\text{O}_x$ has been studied. An investigation of the crystallization process as well as the monitoring of bulk and surface characteristics under reaction conditions revealed a very dynamic character of the model catalyst.

Chemical as well as structural complexity is increased in MoVTeNbO_x catalysts that show high activity and selectivity in direct oxidation of propane to acrylic acid. Preparation and activation conditions strongly influence the phase composition of the final catalyst, which is, however, not reflected accordingly in the catalytic behavior.

New approaches for the preparation of noble metal containing molybdenum oxide based catalysts involve the application ion exchanged hetero-poly acids (HPA). The thermal decomposition of ruthenium exchanged HPA produces highly dispersed Ru oxide species in a MO_x (M=Mo, V, Te, Nb) matrix with potential for further developments.

References

1. J. Haber, E. Lalik; *Catal. Today* **33**, 119 (1997).

Mo₅O₁₄ Model Catalyst for Oxidation of Propene to Acrylic Acid

E. Rödel, P. Schnörch, P. Beato, T. Ressler, A. Knop-Gericke, A. Trunschke, R. Schlögl

Introduction

Industrial catalysts for the oxidation of propene to acrylic acid are based on mixed MoVW metal oxides. In order to reveal reliable structure-activity relationships, the complexity of the system needs to be reduced, preferably retaining a comparable catalytic activity. Hence, a detailed *in-situ* structural investigations of a Mo_{0.68}V_{0.23}W_{0.09} oxide was performed because (1) the preparation of the Mo_{0.68}V_{0.23}W_{0.09} oxide precursor (spray-drying) has been reasonably well understood^{1,2}, (2) the high catalytic performance of the resulting Mo₅O₁₄ type material for the selective oxidation of propene and acrolein was confirmed in a quartz tubular flow reactor¹, and (3) the elemental composition is close to that of industrial catalysts.

Results

The formation of crystalline Mo_{0.68}V_{0.23}W_{0.09} oxide was studied by *in-situ* XRD. *In-situ* XAS provided insight into the evolution of the local structure around each element in the mixed oxide material (Mo, V, W). The crystallization process strongly depends on the parameters of thermal activation, namely gas flow and dwell time, are important and have to be carefully adjusted to obtain a crystalline, phase-pure (Mo_{0.68}V_{0.23}W_{0.09})₅O₁₄ catalyst. The bulk structure of Mo_{0.68}V_{0.23}W_{0.09} oxide has been investigated during TPR in propene and oxygen with *in-situ* XRD and *in-situ* XAS. The results obtained are compared to the analysis of the catalyst surface.

The electronic surface structure of the Mo_{0.68}V_{0.23}W_{0.09} oxide was analyzed by *in-situ* XPS at 0.5 mbar in the presence of propene and oxygen at elevated temperature. Concentration profiles perpendicular to the surface of the working catalyst showed a different distribution of metal centers in the surface and the underlying layers strongly depending on temperature and atmosphere. The surface exhibited a higher concentration of vanadium, while a variation in the binding energy of molybdenum indicates a change in Mo oxidation state between surface and 'bulk'.

The structure of representative sections of the Mo_{0.68}V_{0.23}W_{0.09} oxide surface has been studied by *in-situ* Raman spectroscopy during partial oxidation of propene at atmospheric pressure. Reversible changes in the patterns of the M-O vibration bands between 623 and 713 K coincide with the onset of catalytic activity. Decreasing bandwidths indicate an increased local order of the oxide under working conditions. There is evidence that the active surface is actually a very dynamic one.

References

1. S. Knobl, G. A. Zenkovets, G. N. Kryukova, O. Ovsitser, D. Niemeyer, R. Schlögl, G. Mestl; *J. Catal.* **215**, 177 (2003).
2. S. Knobl, G. A. Zenkovets, G. N. Kryukova, R. I. Maksimovskaya, T. V. Larina, N. T. Vasenin, V. F. Anufrienko, D. Niemeyer, R. Schlögl; *Phys. Chem. Chem. Phys.* **5**, 5343 (2003).

Investigations on Synthesis and Activation of MoVTenbO_x Catalysts

A. Celaya Sanfiz, A. Blume, V. Makwana, F. Girgsdies, A. Trunschke,
M. H. Looi*, S.B.A. Hamid*, R. Schlögl

Introduction

Natural gas is a huge resource, which mainly consists of light alkanes. The utilization of these alkanes by selective oxidation has been widely investigated. Propane selective oxidation to acrylic acid is one of the recent challenges in the selective oxidation field. The most promising catalyst up-to-date for this reaction is a MoVTenbO_x mixed oxide originally developed by Mitsubishi Chemicals¹, generally comprising two different hexagonal phases referred to in the literature as M1 and M2, respectively. There is an ongoing debate about the function of the two phases². The preparation method and the calcination conditions seem to be crucial to achieve high catalytic performance. In the present work, chemical strategies have been applied to control the phase composition of the final catalyst. Proposed relations between phase composition and catalytic properties in selective oxidation of propane to acrylic acid have been reassessed.

Results

MoVTenbO_x mixed oxides have been prepared starting from slurries obtained by mixing aqueous solutions of the metal components followed by either spray-drying or hydrothermal treatment. Types of starting polyoxometalate species as well as concentrations have crucial effects on structural properties of the resulting materials. Conditions of calcination of the dried precursors at about 573 K and activation in He at about 873 K also play an important role. By spray-drying, mixtures of M1 and M2 have been obtained. The M1 content ranges from traces to 80 % depending on the nature of the vanadium precursor and the conditions of thermal activation. Certain hints have been given by *in-situ* XRD that amorphous precursors of the finally formed crystalline phases are established in the calcination process and changes during heat treatment in inert gas are mainly related to the establishment of long range order (crystallization) of these phases. A clear correlation between the fraction of a specific phase and catalytic properties was not observed. Hydrothermal synthesis results in materials that solely consist of M1. (XRD and HRTEM). These phase-pure catalysts have been obtained after various activation procedures. Surprisingly, activation in nitrogen at 873 K with previous calcination in air at 548 K produces a catalyst that is less active and less selective than a catalyst obtained after activation at 923 K with previous calcinations in air at 623 K indicating that catalytic properties of MoVTenbO_x mixed oxides are controlled rather by the nanostructure of the catalyst surface than by the phase composition of the bulk. Analyzing composition and molecular structure of the outermost surface layers of MoVTenbO_x catalysts under the conditions of propane oxidation is a challenging task upon which our recent research efforts are focused.

References

1. M. Hatano and A. Kayou, United States Patent No. 5,049, 692, (1991).
2. R.K. Grasselli, D.J. Buttrey, P. DeSanto, Jr., J.D. Burrington, C.G. Lugmair, A.F. Volpe, Jr., T. Weingand, Catal. Today **91-92**, 251 (2004).

* Combinatorial Technology and Catalysis Research Centre (COMBICAT), University Malaya, 50603 Kuala Lumpur, Malaysia

Synthesis of Highly Dispersed Ru Oxide Species Hosted in Mo Oxide Based Matrices as Catalysts for Selective Oxidation of Propane

O. Timpe, A. Trunschke, R. Schlögl

Introduction

The tuning of catalysts for direct conversion of light alkanes to partially oxidized products is a challenging task. For the conversion of propane to acrylic acid, efforts of some groups over the past decade yielded a catalyst consisting of Mo, V, Nb and Te oxide (MO_x). The classic approach to achieve further improvement is the addition of promoters such as ruthenium that has attracted much attention in the past as heterogeneous catalyst for oxidation reactions. To prevent formation of larger agglomerates of added Ru species during preparation and reaction, linkage on a molecular scale is desirable. Accordingly, cation exchanged hetero-poly acids (HPA) have been used as container to introduce Ru ions into the MO_x host matrices

Results

A series of HPA with varying heteroatom (Si, P) and addenda atoms (Mo, W, V, Nb) has been prepared. The complex compound $[[\text{Ru}(2,2'\text{-Bipyridine})_3](\text{NO}_3)_2]_{\text{aq}}$ was synthesized according to a published procedure¹. The dropwise addition of the complex cation dissolved in water to an aqueous solution of the HPA evokes the formation of a precipitate immediately. The isolated solid has the stoichiometry of one complex cation per Keggin unit. Solid mixtures (ball milled) of conventional MO_x with the Ru-HPA compounds were co-calcined to introduce the additive into the catalyst.

The Ru-HPA compounds show XRD patterns closely related to the parent HPA and decompose at temperatures around 700 K. Ru forms small clusters in the range of 5 nm located in the remaining oxide matrix as probed by TEM. The Ru complex itself decomposes in the same temperature range, losing the bipyridine ligands. If the decomposition is driven in oxygen containing atmosphere, the process is exothermic and the metals remain thereby in their highest oxidation state. In inert atmosphere, the weight loss associated to the decomposition is smoother and not exothermic (TG/DTA) and the metals in the generated Ru- MO_x are distinctly reduced. In the catalytic oxidation of propane as test reaction the Ru-HPA decomposition products behave superior by large with respect to the parent HPA, both in conversion and in the yield of acrolein, acrylic acid being generated only in traces. The Ru-HPA- MO_x mixtures tend to be of lower activity if the load of Ru-HPA is high. For low loadings, the results are ambiguous and depending on the nature of the HPA an increase of the yield to acrylic acid was observed. The catalysts generated by decomposition of $[\text{Ru}(2,2'\text{-Bipyridine})_3]\text{-HPA}$ compounds in inert atmosphere show a distinct higher selectivity to acrolein compared to the catalysts activated in oxygen containing atmosphere. We estimate this new family of catalysts as promising, even more as these compounds are versatile and might have the potential for further evolution.

References

1. R.A. Palmer, T.S. Piper, *Inorg.Chem.* **5**, 864 (1966).

Copper in C1 Chemistry

Copper based catalysts are extensively used for methanol synthesis and the conversion of methanol to hydrogen and carbon dioxide (reforming) or formaldehyde (selective oxidation). The work performed in this research area focuses on revealing structure-reactivity relationships of various copper systems and rationalizing copper catalyst synthesis in terms of tailoring particular bulk and surface properties to accomplish an improved catalytic performance. The results shown demonstrate that elucidating structure-activity relationships is a necessary prerequisite for a rational catalyst design, together with a detailed knowledge about appropriate preparation and treatment conditions resulting in the right target structure of the desired copper based catalyst.

Recently, we were able to show that the catalytic activity of binary Cu/ZnO catalysts correlates with the microstrain in the copper particles. The strain in the copper particles is an indicator for an improved Cu-ZnO interface and a homogeneous microstructure of the corresponding catalyst. Ageing of precipitates at a very early state of catalyst preparation exerts a pronounced effect on the microstructure of the resulting precursors, the final copper catalyst (“chemical memory”) and structure-activity relationships. (*AC 5.1*)

The structural and catalytic properties of novel CuO/ZrO₂ catalysts in the methanol steam reforming process were investigated by various characterization methods. The CuO/ZrO₂ catalysts can be activated by an oxidation procedure resulting in partially oxidized copper clusters supported on ZrO₂ which exhibit improved catalytic properties (e.g. stability, selectivity, etc.) compared to a commercial Cu/ZnO/Al₂O₃ catalyst. Moreover, the effect of various preparation procedures on the catalytic properties of Cu/ZrO₂ catalysts was studied. Precipitation of small copper clusters in a concentration of less than 10 wt-% on a pre-formed nanostructure ZrO₂ support yielded superior catalysts in terms of stability and selectivity compared to co-precipitation procedures. (*AC 5.2*)

In addition to analyzing correlations between the bulk structure of copper-zinc oxide catalysts and their activity in the steam reforming of methanol we investigated the surface properties of differently prepared Cu/ZnO catalysts by combined in situ X-ray photoelectron (XPS) and in situ X-ray absorption (XAS) under methanol steam reforming reaction conditions. (*AC 5.3*)

Microstructural Modifications of Cu/ZnO Catalysts as a Function of Precipitate Ageing

B.L. Kniep, E.N. Muhamad, F. Girgsdies, T. Ressler, R. Schlögl

Introduction

Microstructural characteristics of Cu/ZnO catalysts such as microstrain, impurities and particle size affect the catalytic activity for methanol steam reforming¹. Here we report on tailoring microstructural characteristics of “real Cu/ZnO catalysts” by appropriate ageing of freshly precipitated precursors^{2,3}. Furthermore, we compare the effect of the precipitation agent (sodium carbonate or ammonium hydroxide) on the ageing process and the resulting microstructure of the catalyst. Microstructural properties of the active catalysts were elucidated using in-situ X-ray absorption spectroscopy (XAS) and in-situ X-ray-diffraction (XRD) combined with mass spectrometry, and electron microscopy (TEM).

Results

Precipitation using ammonium hydroxide leads to the formation of a single phase Cu₂Zn hydroxynitrate precursor (HN), whereas the standard precipitation using sodium carbonate results in a mixture of several Cu₂Zn-hydroxycarbonates (HC). The characteristic crystallization during ageing of HC precipitates and the accompanying increase in catalytic activity was not observed for the Cu/ZnO catalysts obtained from aged HN precipitates. Ageing of HN precursors results in large, separated, and less strained Cu and ZnO particles with an inferior catalytic activity. Conversely, increased HC ageing leads to nanostructured Cu/ZnO catalysts which exhibit a characteristic “real” structure that significantly deviates from that of fcc Cu metal (e.g. microstrain). While the less active Cu/ZnO catalysts comprise a heterogeneous mixture of large and isolated Cu and ZnO particles, the more active catalysts show small and intimately mixed Cu and ZnO particles (homogeneous microstructure)⁴. The structure-activity correlations indicate that crystallinity, phase composition, and homogeneity of the resulting precursor strongly influence the microstructural properties of the final copper catalyst. The characteristic transformation during ageing from originally amorphous HC precipitates into crystalline products is transmitted over the entire multi-step preparation including calcination and reduction (“chemical memory”). Hence, the structural characteristics of the precipitates as adjusted by an appropriate ageing procedure govern the properties of the final catalyst and are not annihilated by subsequent treatment procedures.

References

1. M. M. Günter, T. Ressler, R.E. Jentoft, B. Bems, *J. Catal.* **203**, 133 (2001)
2. B.L. Kniep, T. Ressler, F. Girgsdies, A. Rabis, M. Baenitz, F. Steglich, R. Schlögl, *Angew. Chem.* **43**, 112 (2004)
3. B.L. Kniep, F. Girgsdies, T. Ressler, *J. Catal.*, submitted
4. T. Ressler, B.L. Kniep, I. Kasatkin, R. Schlögl, *Angew. Chem.* **117**, 2 (2005)

Cu/ZrO₂ Catalysts for Methanol Steam Reforming

A. Szizybalski, F. Girgsdies, J.H. Schattka*, Y. Wang*, R.A. Caruso*, M. Antonietti*,
T. Ressler, R.Schlögl

Introduction

Steam reforming of methanol can be employed to produce hydrogen for fuel cells in mobile applications. [1] Recently, we described a binary Cu/ZrO₂ catalyst which is more active compared to a commercial Cu/ZnO/Al₂O₃ catalyst, more stable during time on stream, and produces less CO. [2] Detailed structure-activity relationships of the Cu/ZrO₂ material and the influence of various preparation methods on the catalytic performance are subject of this work.

Results

Structure-activity relationships of a nanostructured Cu/ZrO₂ catalyst for the steam reforming of methanol (MSR) were investigated under reaction conditions by in situ X-ray absorption spectroscopy (XAS) and X-ray diffraction (XRD) combined with on-line mass spectrometry (MS) and corroborated by TG/DSC/MS measurements. After extended time on stream and treatment at 673 K in hydrogen, no significant sintering of the copper particles or deactivation of the reduced Cu/ZrO₂ catalysts was detected indicating a superior stability of the material. The initially low steam reforming activity of the Cu/ZrO₂ catalyst after reduction in hydrogen could be significantly increased by a temporary addition of oxygen to the feed. This increased activity after oxidative treatment is correlated to an increasing amount of oxygen in the copper particles. ⁶³Cu NMR studies detected only a minor degree of microstrain in the active copper phase of the Cu/ZrO₂ catalyst. The structure-activity correlations revealed indicate a different metal support interaction compared to Cu/ZnO catalysts.

Using various starting materials and templates, nanostructured, mesoporous, and macroporous Cu/ZrO₂ catalysts were prepared by precipitation, impregnation, and templating techniques. The properties of the final Cu/ZrO₂ catalysts strongly depend on the preparation conditions. Calcination and reduction of the various precursor materials do not annihilate the structural differences in the precursors (“chemical memory”), and, hence, the different preparation routes employed result in differently active catalysts for the steam reforming of methanol. In order to ensure a good metal support interaction and, hence, good catalytic performance, a copper concentration in the materials of less than ~ 15 % had to be chosen. Possibly because of reduced metal support interaction, coprecipitation routes resulted in large copper particles and inferior catalytic properties. Conversely, impregnation of a pre-formed ZrO₂ support resulted in small Cu particles, and a superior activation behavior and catalytic performance.

References

1. P.J. de Wild, M.J.F.M. Verhaak, Catal. Today **60**, 3 (2000).
2. H. Purnama, F. Girgsdies, T. Ressler, J.-H. Schattka, R.A. Caruso, R. Schomäcker, R. Schlögl, Catal. Lett. **94**, 61(2004).

Combined in situ XPS and in situ XAS Study of Cu/ZnO Based Catalysts for Methanol Steam Reforming

M. Hävecker, B.L. Kniep, E. Kleimenov, P. Schnörch, D. Techner, S. Zafeiratos,
H. Bluhm, A. Knop-Gericke, T. Ressler, R. Schlögl

Introduction

Copper-zinc oxide (alumina) catalysts are active for the steam reforming of methanol.¹ An important application could be the onboard production of hydrogen for fuel cell application. The surface properties play a decisive role for the understanding of a catalyst. Here, we report a combined in situ X-ray photoelectron (XPS) and in situ X-ray absorption (XAS) surface study of differently prepared Cu/ZnO catalysts under methanol steam reforming reaction conditions.

Results

Cu/ZnO catalysts (molar ratio Cu:Zn = 70:30) were prepared by co-precipitation of mixed copper zinc hydroxyl carbonates. The precipitates were aged under constant stirring in their mother liquor for different times (0 min – 120 min), washed and calcined. XP core level spectra were taken in a temperature range of 25 °C – 250 °C in the presence of 0.25 mbar H₂ and in the H₂O/CH₃OH reaction mixture (p_{tot}=0.25 mbar), respectively. Cu L_{2,3} - and Zn L_{2,3} - near edge X-ray absorption fine structure (NEXAFS) spectra were taken under these conditions as well. Synchrotron radiation of the undulator U49 at the storage ring BESSY was used. Changes in the gas phase composition were monitored by on-line mass spectrometry simultaneously to the spectroscopic characterization of the catalyst surface.

The reduction of the catalyst is crucial for its structure under methanol steam reforming conditions. A sequential two-step reduction process at the surface (CuO → Cu₂O → Cu) was found. The Zn/Cu3p core level intensity ratio altered strongly during the reduction in H₂. In the first reduction step (CuO → Cu₂O), an increase was observed. Further reduction caused a decrease of this intensity ratio. This observation stresses the dynamic behavior of the surface and the presence of strong surface modifications during the activation process. Residual carbon species (carbonates and others) were observed on the surface even after prolonged calcination in air. The Zn L₃-NEXAFS indicates the presence of a zinc species different to ZnO. This modification is likely caused by the residual carbonates. These carbonate species decomposed during the reduction of the catalyst. Furthermore, a surface oxygen species was found that is primarily located in the outermost surface layers of the reduced catalyst. Comparison to reference compounds and literature data suggests the presence of OH-species that are known to create a modified, defective surface on single phase ZnO.

References

1. P.J. Wild, M.J.F.M. Verhaak, Catal. Today **60** (2000) 3.

Introduction to Research Area 6: Palladium in Model Reactions

Pd catalysts supported on alumina have been investigated in hydrogenation- and in oxidation reactions. The hydrogenation of pentyne investigated with in situ XPS showed clear indication for the formation of subsurface C. The influence of this C on the selectivity and the conversion will be described in Poster 6.1.

The formation of subsurface carbon was observed in Pd(111) surfaces in the frame of ethene oxidation. At temperature higher than 480 K the formation a carbidic phase is observed. This phase is stable up to 670 K. The surface is metallic at elevated temperature. The maximum of the selectivity is at CO₂ at temperature below 480K and it changes to CO in the temperature range from 480-670 K and it switches back to CO₂ at temperatures higher than 670 K. Details on this study are shown on Poster 6.2.

Pd is known to show high catalytic activity, but the selectivity and stability of Pd based catalyst is rather poor. Poster 6.3 summarizes activities to improve the selectivity and stability by following the active-site isolation approach. PdGa and Pd₃Ga₇ intermetallic compounds have been prepared and characterized. The selectivity was increased compared to a Pd/Al₂O₃ catalyst.

Selective Hydrogenation of 1-pentyne on Pd Catalysts

D. Teschner, A. Knop-Gericke, E. Vass, S. Zafeiratos, A. Pestryakov*, E. Kleimenov, M. Hävecker, H. Bluhm[†], R. Schlögl

Introduction

The removal of multiple unsaturated hydrocarbons has a crucial importance to produce polymer-grade alkene stream. This can be done by using catalysts showing high selectivity towards hydrogenating C≡C triple bond instead of C=C double bond. In this study we aimed to understand the governing factors of *selective triple C≡C* hydrogenation (i.e. only hydrogenating to alkene) on palladium by using our novel in-situ XPS setup.

Results

Four different palladium samples were investigated, two supported catalysts (5% Pd/carbon-nanotubes, 3% Pd/Al₂O₃) and two bulk palladium materials (Pd(111), Pd foil). All of them showed catalytic activity in the hydrogenation of 1-pentyne (~1 mbar). Both, single and total hydrogenation products were formed. Pentane is produced more in the early stage of the experiment at lower temperatures, whereas selective hydrogenation (to 1-pentene) occurred at steady 358 K. This latter is related with carbon retention as a special “Pd-C” phase builds up in the reaction, seen by a new Pd 3d component at 335.6 eV (Pd 3d_{5/2}). This component is surface related (shown by non-destructive depth profiling), calculation revealed its thickness as 2-3 atomic layer. A direct correlation between the “Pd-C” component and the 1-pentene yield could be established; therefore the active surface in selective triple bond hydrogenation is a non-metallic Pd phase. Valence band spectra point also to a massive charge redistribution. It is important to mention that in the hydrogenation of trans-2-pentene this 335.6 eV Pd 3d component does not form.

HRTEM experiments on a post-reaction catalyst indicate lattice expansion which is more pronounced in the surface-near area. The reason is carbon incorporation during the catalytic experiment. Depth-profiling XPS experiment on Pd foil during catalytic run on both palladium and carbon core level reveals maximum carbon content with intermediate information depth. This clearly indicates that a significant amount of carbon is situated in the near-surface region i.e. in subsurface positions. The increase of palladium at the most surface sensitive energy suggests that the surface is not fully covered by any type of adsorbates and that the subsurface carbon is located below the 2-3 palladium-atom-thick “Pd-C” layer. By using “switching off” (H₂/C₅) experiments we conclude that the Pd-C phase is heterogeneous: a Pd rich layer builds the surface, below of which a Pd-to-C 2-to-1 layer is found. This latter decomposes and forms as pentyne is switched off respectively introduced, emphasizing the dynamics of the system.

At high temperature (523 K) in the reaction mixture hydrogen and pentyne desorb and/or decomposes, the double-layered Pd-C phase is destroyed, and a blocking surface/subsurface carbon layer builds up inhibiting any further reaction. Only after regeneration the active double-layer can be restored by the reaction itself.

Present address: * Tomsk Polytechnic University, Lenin ave., Tomsk 634034, Russia.

[†] Chemical Sciences Division, Lawrence Berkeley National Laboratory, USA

Oxidation of C₂H₄ and CH₄ on Pd (111): Characterization of the Active Phase by in situ XPS

H. Gabasch, W. Unterberger*, E. Kleimenov, S. Zafeiratos, D. Zemlyanov[†], B. Aszalos-Kiss[†], A. Knop-Gericke, B. Klötzer*, K. Hayek*, R. Schlögl

Introduction

Many studies address the role of Pd both in selective and total catalytic oxidation, but still a detailed understanding of intermediates, mechanism and the active phases present under “operation” has not yet been attained. It is still not clear which chemical phase of Pd is active during different oxidation processes^{1,2}. The interaction of the Pd surface with several adsorbates (e.g. oxygen, carbon, hydrogen), has been investigated experimentally under UHV conditions^{3,4}, but also by theory calculations⁵. These studies indicate that the gas-surface interaction is not limited to adsorption on the topmost atom layer, but involves also subsurface migration and bulk dissolution. If such species form only at a sufficiently high gas phase chemical potential, it is impossible to detect them under UHV conditions, and forces the investigation by *high pressure* in situ XPS.

Results

The oxidation of ethene (ethene:O₂ = 1:3, total pressure 1.6x10⁻³ mbar) was studied in a temperature-programmed reaction experiment. In the range from 440 K to 460 K the reaction takes place at the adsorbate-covered metal surface and the main product is CO₂, presumably formed via intermediate CO adsorbed with high lifetime. From [6] it is known that ethene decomposes in this temperature range on metal surface, whereas the bulk migration of carbon is inhibited. At higher temperatures (>480K), when C bulk migration sets in, a novel carbon-containing, non-metallic active phase is clearly identified by XPS. The main product of the reaction is now CO, and CO₂ formation is largely suppressed, most likely because of a lower lifetime of CO on this “carbide” Pd_xC_y phase. Above 670 K this phase decomposes towards a metallic Pd surface and the maximum selectivity switches back to CO₂. The formation and decay of this phase is responsible for a strong kinetic hysteresis in the *activity* and *selectivity*.

The oxidation of methane was performed at 0.3 mbar and at a CH₄: O₂ ratio of 5:1. During heating maximum conversion is observed at 650K, which can be attributed to the presence of a surface oxide. At high temperature oxygen atoms on or beneath the metal surface are responsible for the activity.

References

1. D. König, W.H. Weber, B.D. Poindexter, J.R. McBride, G.W. Graham, K. Otto, Catal. Lett. **29**, 9 (1994).
2. R.J. Farrauto, M. C. Hobson, T. Kennelly, E. M. Waterman, Appl. Catal. A **81**, 227 (1992).
3. M. Bowker, C. Morgan, J. Couves, Surf. Sci. **555**, 145 (2004).
4. B. Klötzer, K. Hayek, Ch. Konvicka, E. Lundgren, P. Varga, Surf. Sci. **482**, 237 (2001).
5. I.V. Yudanov, K.N. Neyman, N. Rösch, Phys. Chem. Chem. Phys. **6**, 116 (2004).
6. H. Gabasch, K. Hayek, B. Klötzer, A. Knop-Gericke, R. Schlögl, J. Phys. Chem B **2005**, submitted

* Universität Innsbruck, Institut für Physikalische Chemie, A-6020 Innsbruck, Austria

[†] University of Limerick, Materials and Surf. Sci. Institute and Physics Department, Limerick, Ireland

Active-site Isolated Pd-Ga Intermetallic Compounds for Selective Acetylene Hydrogenation

J. Osswald, M. Armbrüster, K. Kovnier*, R.E. Jentoft, Y. Grin*, R. Schlögl, T. Ressler

Introduction

Selective hydrogenation of acetylene in the presence of ethylene is an important method to remove traces of acetylene in the ethylene feed for polyethylene production¹. Typical Pd metal catalysts supported on oxides show high activity but only limited selectivity and long-term stability^{2,3}. The limited selectivity and stability is due to the presence of neighbouring Pd atoms at the surface and formation of Pd hydrides^{4,5}. Active-site isolation through selecting Pd-Ga intermetallic compounds increases selectivity and long-term stability. PdGa⁶ and Pd₃Ga₇⁷ provide well-defined crystallographic structures with isolated Pd atoms.

Results

Thermal analysis (TG/DSC), in situ X-ray diffraction (XRD) and in situ X-ray absorption spectroscopy (EXAFS) were performed to investigate thermal and structural stability in different gas atmospheres. PdGa and Pd₃Ga₇ show high thermal stability in helium, hydrogen, and oxygen in the temperature range from RT to 673 K. No hydride formation was detected in 50% hydrogen by in situ XRD and in situ EXAFS. In situ EXAFS measurements in 10% C₂H₂ and 20% H₂ showed no structural changes at the onset of catalytic activity. Surface characterization with XPS and ISS resulted in high gallium oxide content which cannot be significantly reduced by heating in hydrogen. Catalytic performance of PdGa and Pd₃Ga₇ was determined in 2% C₂H₂ + 4% H₂ and compared to Pd supported on alumina. Both Pd-Ga intermetallic compounds showed a higher selectivity compared to Pd/Al₂O₃. Isothermal catalytic investigations were performed in 0.5% C₂H₂, 5% H₂ and 50% C₂H₄ to determine selectivity and long-term stability under more industrial condition. PdGa and Pd₃Ga₇ are more selective in acetylene hydrogenation and show less deactivation compared to the supported palladium and a palladium-silver alloy (Pd₂₀Ag₈₀). Chemical etching of the Pd-Ga intermetallic compounds to remove the surface oxide resulted in a higher activity at similar selectivity. Because of the low surface area of PdGa and Pd₃Ga₇ a new preparation technique to obtain highly dispersed Pd-Ga intermetallic compounds was investigated. Mixed and alloyed Pd and Ga nanoparticles were prepared by this new synthesis method.

References

1. A.N.R. Bos, K. R. Westerterp, *Engin. and Process.* **32**, 1-7 (1993).
2. A. Molnar, A. Sarkany, M. Varga, *Journal of Molecular Catalysis A-Chemical* 2001, 173, 185.
3. Albers, P.; Pietsch, J.; Parker, S. F. *Journal of Molecular Catalysis A-Chemical* 2001, 173, 275.
4. Derouane, E. G. *Journal of Molecular Catalysis* 1984, 25, 51-58.
5. Coq, B.; Figueras, F. *Journal of Molecular Catalysis A-Chemical* 2001, 173, 117-134.
6. Hellner, E.; Laves, F. *Zeitschrift für Naturforschung* 1947, 2a, 177-183.
7. Pfisterer, H.; Schubert, K. *Zeitschrift für Metallkunde* 1950, 41, 433-441

* Max Plank Institute for Chemical Physics of Solids, 01187 Dresden, Germany

Carbon in Catalysis

D. S. Su, X.W. Chen, G. Weinberg, X. Liu, J.J. Delgado, R. Schlögl

Introduction

The classical carbon materials (active and activated carbon, carbon black and graphite) are old objects in catalysis research. Since the discovery of nanocarbons (fullerenes, nanotubes, nanofilaments), carbon draws more interest to heterogeneous catalysis. Nanocarbons are ideal as catalyst supports due to their high surface area. They are used as templates to prepare nanostructured catalysts like nanotubes of transition metal oxides. The project *Carbon in Catalysis* is conducted in the following three directions: i) optimisation of the oxidative dehydrogenation (ODH) of ethylbenzene (EB) to styrene (ST) over nanocarbon; ii) synthesis of carbon tube-in-tube nanostructure; iii) nano-architecturing of activated carbon.

Results

For the ODH of EB to ST, we take the first steps towards a later industrialisation of carbon catalysts. The activities are concentrated on i) the search for nanocarbons which can be produced in large scales and exhibit high styrene yield as well prolonged life times; ii) the role of oxygen partial pressure in the ODH of EB; iii) the influence of total flow on the catalytic activity. Our data confirms that nanostructures are very active and promising alternative catalysts to potassium promoted iron oxides. The nanocarbons remain stable in an oxidative atmosphere; the reaction temperature is decreased for about 200°C in respect to the commercial process, whereas the yield to styrene is as high as 50%, similar to the industrial catalyst. (*Poster 7.1*).

Carbon tube-in-tube (CTIT) nanostructures, built by a narrower inner tube inside an outer tube, exhibit multiple intramolecular channels and surfaces and should be beneficial for the improvement of their properties. Unlike its counterpart CNTs that can be fabricated in many ways, the CTIT structure is difficult to assemble. Our strategy for the synthesis is based on a two-step process. First, the graphitic nanoparticles are disintegrated into small fragments by an HNO₃-based oxidation at defective sites, a process previously used to purify, cut, or open nanotubes. Secondly, the small graphene fragments are reintegrated around or inside pristine nanotubes to assemble CTITs by acid-catalyzed esterification linkages between the carboxyl/hydroxyl groups. (*Poster 7.2*).

Selective chemisorption of unwanted species from drinking water (Mn, As, Hg, Fe), modification of the properties of polymers and the use as catalysts are potential applications of CNT/CNFs in chemistry. Loose CNT/CNFs are unsuitable for such purpose as they cannot be controlled in their suprastructural properties and are difficult to handle. A hierarchical organisation of the nanocarbons on a robust carrier structure in larger dimensions is needed. We choose activated carbon from natural sources as substrate. Carbon nanofibers are successfully nested inside or immobilized onto modified activated carbon. A simple, cheap method suitable for production in large scale is used. (*Poster 7.3*)

Optimisation of Reaction Conditions for the Oxidative Dehydrogenation of Ethylbenzene to Styrene

J.J. Delgado, D. S. Su, N. Keller*, G. Mestl**, M.J. Ledoux*, R. Schlögl

Introduction

During the last years, our research was focussed on the optimisation of reaction conditions for the oxidative dehydrogenation (ODH) of ethylbenzene (EB) to produce styrene. We have studied the effect of the reaction temperature, O₂:EB ratio and total flow rate over the conversion and selectivity to styrene. This is the first step to use CNTs as catalyst in the industrial process of styrene synthesis.

Results

The catalytic tests show that at low temperatures, below 400°C, the selectivity is not strongly affected by the oxygen pressure in the line, but the conversion increases significantly when working at high O₂:EB ratios. Similarly, the selectivity is slightly reduced when the total flow is decreased. At low temperatures and high retention time, high conversion with high selectivity can be achieved. The characterization of the used catalysts before and after reaction indicates that the different materials (nanofibers, nanotubes and onion-like carbons) are stable under high oxidizing conditions and therefore exhibit high catalytic performances.

The effect of different pre-treatment over the catalytic activity of carbon nanomaterials of CNTs with HNO₃, LiAlH₄ in THF and thionylchloride, DSMO and oxalylchloride change the number of oxygenated species on the catalyst surface. All pre-treated samples exhibit higher activities than the initial sample, which was poor in oxygenated groups. The functionalized samples exhibit different activities during the initial induction period, but the final stable catalytic performance are quite similar for all the studied samples. The activities decrease from 50 to 25 %, indicating that the oxygenated species play an important role in the reaction mechanism. Therefore, the new oxygenated species are not stable under reaction condition and we have to find the way to create stable oxygenated species.

To overcome the shortage that nanostructured carbon is difficult to handle in real fixed-bed reactors, carbon nanofiber are grown on graphite felts by catalytic chemical vapour decomposition of ethane. The obtained composite is of macroscopic scale and mechanically stable, avoiding any limitations due to the fine powder form of the primary structure of nanocarbons. A stable yield of 38 % of ST in the ODH of EB to ST was obtained with a selectivity of 85 % towards ST. In addition, due to the open structure with large void volume of the supported nanocarbon no pressure drop was observed.

References

D.S. Su, N.I. Maksimova, J.J. Delgado, N. Keller, G. Mestl, M.J. Ledoux and R. Schlögl, *Catalysis Today* **102-103**, 110 (2005)

J.J. Delgado, R. Vieira, G. Rebmann, D. S. Su, N. Keller, M.J. Ledoux, R. Schlögl, submitted to *Carbon*.

* Laboratoire des Materiaux, Surface et Procédés pour la Catalyse, UMR 7515 CNRS, Strasbourg

** NanoScape AG, Munich

Synthesis of Carbon Tube-in-tube Nanostructure

D.S. Su, Z- P. Zhu*, X. Liu, G. Weinberg, R. Schlögl

Introduction

Carbon tube-in-tube (CTIT) nanostructures, built by a narrower inner tube inside an outer tube, exhibit multiple intramolecular channels and surfaces and should be beneficial for the improvement of their properties and for the application due to the doubled surface area. Unlike its counterpart CNTs that can be fabricated in many ways, the CTIT structure is difficult to assemble.

Carbonaceous impurities, amorphous and graphitic nanoparticles, are always present in as-synthesized samples of CNTs, independent of the synthesis methods. Most of the carbonaceous impurities exhibit structures similar to those of nanotubes and most of the grown nanotubes are highly defective. Conversely, the structural similarity between the carbonaceous impurities and nanotubes guides us to reorganize the external and internal impurities around and inside of pristine tubes to assemble CTIT structures. Our strategy for the reorganization is based on a two-step process. Firstly, the graphitic nanoparticles are disintegrated into small fragments by an HNO₃-based oxidation at defective sites, a process previously used to purify, cut, or open nanotubes. The oxidation concomitantly functionalizes the fragment edges with carboxyl/hydroxyl groups. Secondly, the small graphene fragments are reintegrated around or inside pristine nanotubes to assemble CTITs by acid-catalyzed esterification linkages between the carboxyl/hydroxyl groups.

Results

The obtained CTITs exhibit three types of distinct morphologies, likely associated with the different assembling mechanisms. One type exhibits relatively small and uniform interval spaces along the length and normally shows rather similar and matched shapes, windings, or nodes between the outer and inner tubes. The second type has large and highly irregular interval spaces; the winding of the inner tubes obviously differs from that of the outer tubes. Thin inner tubes of less than 50 nm are normally observed for this type of CTIT, meaning that they are newly formed from the reorganization of graphene fragments contained inside pristine tubes. More interestingly, another type of CTITs shows triple tubular structures. We believe that they are formed from integrating the carbon fragments both around and inside the pristine tubes.

Unlike the pristine tube moieties that show well-ordered fishbone-like graphene structures with interlayer distances of 0.34 nm, the newly formed outer or inner tube moieties exhibit pre-graphitic short-range-ordered structures, with larger interlayer distances of about 0.35 nm. Upon thermal treatment in inert atmosphere at 1000 °C, the involved oxygen-containing groups are decomposed and released as CO/CO₂. The remained carbon structures are significantly condensed and improved.

References

- Z.P. Zhu, D. S. Su, G. Weinberg, R. Jentoft, R. Schlögl, *Small*, No. **1**, 107 (2004)
Z.P. Zhu, D. S. Su, G. Weinberg, R. Schlögl, *Nano Letter* Vol. **4**, No. 11, 2257 (2004)

* State Key Laboratory of Coal Conversion, Institute of Coal Chemistry, CAS, Taiyuan, China

Carbon Nanofibers Nested Inside and Immobilized on Activated Carbon

D.S. Su, X.W. Chen, G. Weinberg, A. Klein-Hofmann, O. Timpe, S.B. Abd. Hamid*, R. Schlögl

Introduction

Carbon nanotubes or nanofibers (CNTs or CNFs) have attracted the interest of many researchers in the field of chemistry, physics and nanotechnology because of their extraordinary properties. Activated carbon (AC) is widely used to absorb unwanted species from drinking water, such as Mn, As, Hg, Fe and so on. In this work, carbon nanofibers were synthesized on activated carbon by means of chemical vapour decomposition (CVD) of ethylene.

Results

Palm kernel shell based activated carbon was mildly oxidized in air at 400 °C for 4 h. The oxidation removes the small debris of carbon and enlarges the pore size of activated carbon. The as-obtained activated carbon was impregnated with an aqueous solution of iron nitride, calcined at 500 °C in N₂ and reduced under H₂ at 700 °C. After catalytic decomposition of a mixture of C₂H₄ and H₂ at 700 °C over a Fe/AC catalyst, carbon nanofibers form and cover the activated carbon. They are entangled and randomly oriented. The diameters of the fibers range from 20 to 300 nm. Both TEM and SEM images show that the carbon nanofibers are nested inside of the pores and immobilized on the surface of activated carbon. The adsorption capability of heteropolymolybdate on as-synthesized CNFs/AC was greatly increased by 27 times of that on activated carbon. The deliberate nanostructuring carbon creates new functions on the surface of activated carbons.

The parameters for the CVD based synthesis of CNTs on AC such as temperature (500, 600, 700 and 800 °C) and reaction time (10, 30, 60 and 120 min) were varied. The morphology of nanostructured carbon on activated carbon depends on the synthesis temperature. Nanocarbons were obtained on activated carbon at 500 °C in a mixture of C₂H₄ and H₂ for 2 h. When the temperature is increased to 600 °C, short carbon nanofibers form on the activated carbon. Longer carbon nanofibers become are obtained at 700 °C. However, carbon nanofibers are more wound up when the temperature is increased to 800 °C. The product yield increases with the temperature increasing from 500 to 700 °C, however drops by 7 % at 800 °C. The reaction time also has a great influence on the product yield. It increases with increasing reaction time.

References

D.S. Su, X.W. Chen, G. Weinberg, A. Klein-Hofmann, O. Timpe, S.B. Abd. Hamid, R. Schlögl, *Angew. Chem. Int. Ed.*, in press

Catalytic Wall Reactor for Partial Alkane Oxidation with Molecular Beam Mass Spectrometer Interface

R. Horn,* K. Ihmann,[†] J. Ihmann, M. Geske, A. Taha, F.C. Jentoft, R. Schlögl

Introduction

Partial oxidations of hydrocarbons, conducted in high temperature and pressure conditions, are suspected to proceed through heterogeneous and homogeneous reactions, which may couple with each other by exchange of energy and reaction intermediates, predominantly radicals. To study these reactions in mechanistic detail, a Molecular Beam Mass Spectrometer (MBMS) attached to a high temperature catalytic wall reactor has been developed. The setup (first sketches presented during FB 2003, details described in FB report 2005) is now in the phase of final assembly and testing.

Results

First, the MBMS interface and the catalytic wall reactor were operated separately. As the reactions of interest proceed on a ms to μ s timescale via short lived reactive intermediates (e.g. radicals), an in situ mechanistic investigation requires quick removal and thermal quenching of any sample from the reaction zone. This is achieved by expansion of a small fraction of the reacting gases through a nozzle in the catalytically active wall into several differentially pumped vacuum stages. The interface was tested with a cylindrical reactor of about 25 ml volume with a 125 μ m pinhole. The pressure in the reactor could be adjusted up to 1.5 bar by variation of the inlet flow. The interface was successfully operated with various gas mixtures. Via threshold ionization radicals can be identified in presence of interfering molecules. Variation of the MS sensitivity with the overall composition prompted us to add equipment (gas chromatograph, non-dispersive infrared analyzer, paramagnetic oxygen analyzer) for accurate effluent gas analysis.

The wall reactor for alkane oxidation consists of a resistively heated 90%Pt-10%Rh tube (O.D. = 5 mm). As a first reactant, methane was used. Once lit, the oxidation reactions proceed autothermally (at 1000–1473 K). The temperature of the surrounding parts and the expansion of the tube were successfully controlled and compensated by the cooling and the reactor mounting units, respectively. Effluent gas analysis showed H₂, H₂O, CO, CO₂ and C₂ hydrocarbons. With different gas throughput, size and position of the hottest zone could be tuned (see report). In this way, samples can be taken from different reaction zones.

In the next step, the wall reactor will be coupled with the MBMS interface. Steady state experiments will be conducted at different flow rates to investigate the species above the catalyst surface. Further mechanistic information will be derived from transient experiments, for example from ignition studies or from periodic variation of the feed composition (frequency response). The advantage of our setup for transient studies is the negligible time between sampling and detection leading to a temporal resolution that is limited only by the mass spectrometer response (ms resolution possible).

*Present address: Chemical Engineering and Materials Science Department,
University of Minnesota, 421 Washington Avenue SE, Minneapolis MN 55455, USA

Ethylene Epoxidation over Silver

A. Knop-Gericke, M. Hävecker, S. Zafeiratos, E. Kleimenov, E. Vass, V. Bukhtiyarov*,
B. Jacobi, B. Steinhauer, B. Kubias, R. Schlögl

Introduction

Silver catalysts for ethylene epoxidation have been extensively studied in the past¹⁻⁵, but mostly with high-vacuum based surface science techniques under ex situ conditions. Here we present in-situ X-ray photoelectron spectroscopy (XPS) and proton-transfer reaction mass-spectrometry (PTRMS) studies from 300 to 520 K and in a pressure from 0.07 to 1 mbar on Ag foil as well batch experiments in a model reactor at <5mbar.

Results

The formation of ethylene oxide at $T \geq 420$ K was determined by releasing carbonaceous contaminants and carbonates from the silver surface. The total pressure value of 0.1 mbar was found to be exceeded to activate the silver surface for ethylene epoxidation. The active surface contains two oxygen species – the nucleophilic and electrophilic oxygen⁴. The observed correlation between abundance of the nucleophilic oxygen and the ethylene oxide yield is explained via “ionic silver” concept which suggests that the nucleophilic oxygen creates Ag^+ ions via formation of surface Ag_2O as sites for ethylene adsorption. Subsequent formation of ethylene oxide proceeds via Langmuir-Hinshelwood mechanism between adsorbed ethylene and the electrophilic oxygen. In full agreement with this mechanism, highest yields of ethylene oxide are observed for the Ag surfaces which are characterized by similar concentrations of the nucleophilic and electrophilic oxygen.

As shown by batch experiments, ethylene oxide is markedly adsorbed on the reactor walls at room temperature and tends to be oxidized if the reactor is heated to $>90^\circ\text{C}$. To avoid these undesired blank effects, the planned in situ STM-experiments¹⁾ for a study of the microscopic structural changes on the surface of an Ag single crystal under the influence of the reactants have to be carried out under flow conditions.

References

1. C.T Campbell, J. Catal. **94**, 436 (1985)
2. R.B. Grant, R.M. Lambert, J. Catal. **92**, 364 (1985)
3. R.A. van Santen, H.P.C.E. Kuipers, Adv. Catal. **35**, 265 (1987)
4. V.I. Bukhtiyarov, V.V. Kaichev, E.A. Podgornov, I.P. Prosvirin, Catal. Lett. **57**, 233 (1999)
5. B.S. Bal'zhinimaev, Kinet. Catal. **40**, 795 (1999)

¹⁾ DFG Projekt „Mikroskopische Strukturbildung von Katalysatoroberflächen unter Realbedingungen“ (Schl 332/8-1, Wi 1003/5-1)

Department of Chemical Physics

Poster List

- CP 1 Preparation of Thin Ordered MoO₃ and V₂O₅ Layers on Au(111) via Oxidation Under Elevated-pressure (~50 mbar) Conditions**
S. Guimond, Y. Romanyshyn, M. Abu Al-Haija, H. Kuhlenbeck, H.-J. Freund
- CP 2 Surface Structure and Chemical Activity of Thin V₂O₃(0001) Films**
M. Abu Al-Haija, S. Guimond, A. Uhl, Y. Romanyshyn, H. Kuhlenbeck, H.-J. Freund
- CP 3 Break Through in the SMART Project**
Th. Schmidt, H. Marchetto, U. Groh, H. Kuhlenbeck, H.-J. Freund, E. Umbach
- CP 4 Hydrogenation of Hydrocarbons on Supported Pd and Pd-Ag Particles**
N. Khan, A. Doyle, A. Uhl, S. Shaikhutdinov, H.-J. Freund
- CP 5 Iron Oxide Supported Gold Nanoparticles: Structure and Reactivity**
D. Starr, C. Lemire, R. Meyer, S. Shaikhutdinov, H.-J. Freund
- CP 6 Group Five Model Catalysts: Supported Vanadia Clusters and Thin Niobia Films**
S. Kaya, J.-L. Lu, A. Uhl, S. Guimond, D. Lahav, F. Mendes, D. Starr, J. Weissenrieder, H. Kuhlenbeck, S. Shaikhutdinov, H.-J. Freund
- CP 7 Frequency Modulated Atomic Force Microscopy: Atomic Resolution and Distance Dependence of Tip-sample Interaction**
M. Heyde, M. Sterrer, M. Kulawik, G. Thielsch, H.-P. Rust, H.-J. Freund
- CP 8 Atomic Chain Formation in the Early Nucleation Stage of Gold on Al₂O₃ Thin Films**
M. Kulawik, N. Nilius, H.-P. Rust, H.-J. Freund
- CP 9 Self-organization of Au Atoms on a Polar FeO Film**
E. D. Rienks, N. Nilius, H.-P. Rust, H.-J. Freund

- CP 10 Influence of Electromagnetic Interactions on Optical Properties of Ordered and Disordered Silver Particle Ensembles**
H. M. Benia, N. Nilius, N. Ernst, H.-J. Freund
- CP 11 Structure and Dynamics of Proteins on Planar Surfaces**
K. Jacobsen, T. Risse, W. L. Hubbell
- CP 12 Construction of an UHV Compatible W-band (94 GHz) ESR Spectrometer for the Characterization of Paramagnetic Surface Species**
W. Hänsel-Ziegler, E. Fischbach, T. Risse, H.-J. Freund
- CP 13 Color Centers on the MgO Surface**
M. Sterrer, E. Fischbach, M. Yulikov, M. Heyde, N. Nilius, H.-P. Rust, T. Risse, H.-J. Freund
- CP 14 Sum Frequency Generation Spectroscopy and Reactivity Studies under Ambient Conditions**
F. Höbel, A. Bandara, J. Silvestre-Albero, G. Rupprechter, H.-J. Freund
- CP 15 PM-IRAS and XPS Spectroscopy of Methanol Decomposition and Oxidation on Pd(111)**
M. Borasio, O. Rodriguez de la Fuente, G. Rupprechter, H.-J. Freund
- CP 16 Reaction Kinetics on Supported Pd Nanoparticles Prepared by e-Beam Lithography: Molecular Beam Experiments and Mikrokinetic Simulations**
M. Laurin, V. Johánek, S. Schauer mann, J. Hoffmann A. Grant, B. Kasemo, J. Libuda, H.-J. Freund
- CP 17 Reaction Kinetics on Oxide Supported Metal Nanoparticles: On the Role of Surface Oxygen, Subsurface Oxygen, Surface and Interface Oxides**
T. Schalow, B. Brandt, M. Laurin, S. Schauer mann, J. Libuda, H.-J. Freund
- CP 18 Two-photon Photoemission Study of Silver Nanoparticles on Thin Alumina Films**
F. Evers, K. Watanabe, D. Menzel, H.-J. Freund

**CP 19 Towards a Completely Self Consistent Embedded Cluster Approach:
Calculation of Adsorbates on Metal Surfaces**

D. Lahav, T. Klüner

**CP 20 Quantitative Surface Structure Determination Using Scanned-Energy
Mode Photoelectron Diffraction**

E. A. Kröger, D. I. Sayago, M. Polcik, D. P. Woodruff, F. Allegretti, M.
Knight, C. L. A. Lamont, G. Nisbet, K. Hogan

Preparation of thin ordered MoO₃ and V₂O₅ layers on Au(111) via oxidation under elevated–pressure (~50 mbar) conditions

S. Guimond, Y. Romanyshyn, M. Abu Al-Hajja, H. Kuhlenbeck, H.-J. Freund

Introduction

MoO₃ and V₂O₅ both exhibit catalytic activity for several reactions, most of them involving oxygen atoms. Therefore surfaces of these oxides are interesting targets for structural and chemical studies. Methods for the preparation of single crystal surfaces are known for V₂O₅ as well as for MoO₃. However, this requires single crystals which may not be easily available. Besides this the preparation and the handling of well ordered single crystal surfaces is not straight forward in both cases since this may involve cleavage and/or involved preparation methods to establish the appropriate surface structure and the correct oxidation state. At low temperature which may be required for adsorption experiments also charging effects may impair studies which involve charged particles like electron spectroscopy.

An easier path to the study of well ordered MoO₃ and V₂O₅ surfaces may be the use of thin films. Thin films are not expected to charge even at low temperature (if they are not too thick) and in case that a film is damaged by the experiments one may simply prepare a new one. However, preparation methods for well ordered MoO₃ and V₂O₅ films have not been published yet.

We have constructed a cell for oxygen treatment at elevated pressures and prepared thin films of MoO₃ and V₂O₅ on Au(111) by evaporation of the respective metal followed by oxidation at elevated pressures and temperatures. Layers of different thickness have been studied with STM, LEED, NEXAFS and XPS.

Results

For molybdenum as well as for vanadium well ordered monolayer thick oxide films could be grown. The Mo3d and V2p core level binding energies are slightly smaller than those of regular MoO₃ and V₂O₅ which may be attributed to screening of the ionic XPS final state by Au(111) substrate electrons. The films cover the whole substrate which makes them suitable for adsorption studies, but their structure differs from that of the respective bulk material. Additional layers on the first layer exhibit the structure of the respective bulk material as concluded from XPS and NEXAFS but they are less well ordered. LEED points towards the formation of rotationally disordered crystallites in both cases which is consistent with the significant dependence of the NEXAFS data on the polar light incidence angle.

Surface structure and chemical activity of thin $V_2O_3(0001)$ films

M. Abu Al-Haija, S. Guimond, A. Uhl, Y. Romanyshyn, H. Kuhlenbeck, H.-J. Freund

Introduction

Besides some interesting physical properties which are related to the phase transitions and the magnetic properties of some vanadium oxides, vanadium oxides also exhibit interesting chemical properties: they catalyze a number of reactions, most of them involving transfer of oxygen atoms. Propylene formation via oxy-dehydrogenation of propane and methanol oxidation to form formaldehyde may be named. With the chemical activity of vanadium oxides in mind we have prepared and investigated thin $V_2O_3(0001)$ films on Au(111). Two different terminations of $V_2O_3(0001)$ were prepared and investigated with respect to structure and adsorption properties using electron spectroscopy, vibrational spectroscopy and STM.

Results

Well ordered $V_2O_3(0001)$ layers were grown on Au(111) by evaporation of vanadium in an oxygen atmosphere with subsequent oxidation at elevated temperature. Usually 50 Å of vanadium were evaporated which leads to a 100 Å thick oxide film. Under typical UHV conditions the film is terminated by a layer of vanadyl groups which can be removed by electron irradiation. The vanadyl terminated surface as well as partially and fully reduced surfaces were imaged with STM. It could be shown that the fully reduced surface is terminated by a layer of vanadium atoms which results from the removal of the oxygen atoms of the vanadyl groups by electron irradiation.

Adsorption of several gases (H_2O , CO_2 , O_2 , Propane) was studied with vibrational spectroscopy, TDS, and electron spectroscopy using light from the BESSY II electron storage ring. In all cases the vanadyl terminated surface turned out to non-active whereas the vanadium terminated surface exhibited a strong interaction with the gases. H_2O forms a layer of hydroxyl groups and O_2 leads to re-establishment of the vanadyl layer via a negatively charged molecular intermediate. CO_2 adsorption also re-establishes the vanadyl groups. In this case a negatively charged bent precursor could be identified.

Break through in the SMART project

Th. Schmidt*, H. Marchetto, U. Groh*, H. Kuhlenbeck, H.-J. Freund, E. Umbach*

Introduction

The lateral resolution in photoelectron emission microscopy (PEEM) is basically limited by aberrations, which can be overcome by suitable correction techniques. The SMART[#] spectromicroscope [1] uses an electrostatic tetrode mirror combined with a highly symmetric magnetic beam-splitter [2] to compensate simultaneously for both, the chromatic and spherical aberrations. SMART aims at a lateral resolution of 2 nm with an energy resolution of 100 meV and is therefore the most ambitious project in the field of spectroscopic microscopy worldwide. The final setup of the SMART instrument started full operation at the UE52-PGM beamline at BESSY in November 2004.

Experimental

In 2004 the SMART microscope was completely reassembled, mechanically aligned and tested at the Fritz-Haber-Institute. The instrument was then transferred back to BESSY and the entire installation of the final SMART version, i.e. with aberration corrector, OMEGA-filter, and electron gun, all mounted on a vibration-damped frame, was finished at the end of October. Surprisingly the first preliminary measurements have shown a lateral resolution below 14 nm and an energy resolution of the imaging analyzer of 150 meV (world record in its field). The SMART allows a combination of different contrast mechanisms. Fig. 1 compares the imaging of nominal 5 ML thick PTCDA film on a Ag(111) surface with three different contrast mechanisms. The 3D islands appear bright in the LEEM image of reflected electrons (due to constructive interference in the crystallites), dark in the Hg-PEEM (high work function and strong attenuation of the electrons emitted from the substrate) and again bright in the NEXAFS-PEEM taken at a molecular C1s \rightarrow π -resonance. The instrument's versatility enables a detailed characterization of surfaces with respect to, e.g., topography, crystal structure, work function, electronic and chemical structure and molecular orientation; all of this on objects of a few tens of nanometers in size.

References

1. R. Fink et al., J. Electr. Spectrosc. Rel. Phen. **84**, 231 (1997)
2. D. Preikszas and H. Rose, J. Electr. Micr. **1**, 1 (1997)

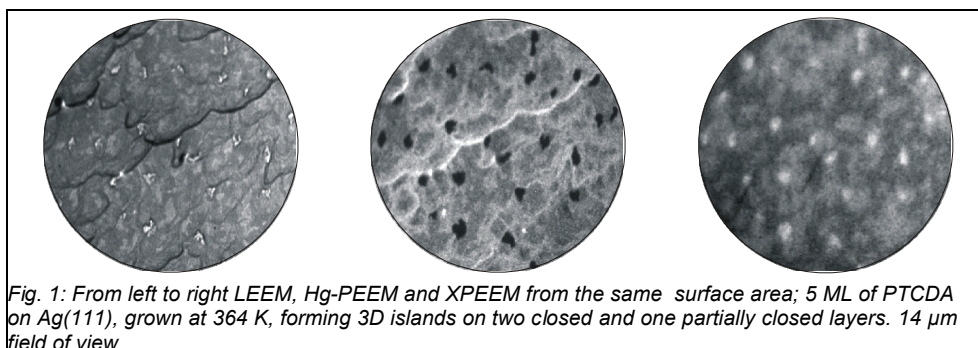


Fig. 1: From left to right LEEM, Hg-PEEM and XPEEM from the same surface area; 5 ML of PTCDA on Ag(111), grown at 364 K, forming 3D islands on two closed and one partially closed layers. 14 μ m field of view.

* Exp. Physik II, Am Hubland, Universität Würzburg

[#] Collaboration of E. Umbach (project coordinator, Univ. Würzburg) – H.-J. Freund, R. Schlögl (FHI, Berlin) – E. Bauer (ASU/USA), G. Lilienkamp (TU Clausthal) – H. Rose (TU Darmstadt) – R. Fink (Univ. Erlangen) – D. Preikszas (ZEISS, Oberkochen) – W. Eberhardt (BESSY, Berlin); funded by BMBF under contract 05KS4WWB/4.

Hydrogenation of Hydrocarbons on Supported Pd and Pd-Ag Particles

N. Khan, A. Doyle, A. Uhl, S. Shaikhutdinov, H.-J. Freund

Introduction

It is well documented that hydrogenation of unsaturated hydrocarbons occurs efficiently on Pd based catalysts. Model systems with a reduced complexity have been developed in order to elucidate mechanism of these reactions, which are believed to be structure insensitive. Here, we report on comparative studies of alkene (ethylene, 2-pentene, acetylene) hydrogenation reactions on Pd(111) single crystal and Pd and Pd-Ag particles supported on alumina films.

Results

Using temperature programmed desorption (TPD), we have observed that a number of hydrocarbon transformations, such as dehydrogenation and H-D exchange reaction, occur on both Pd(111) single crystal and Pd particles. However, the hydrogenation to alkane is only observed on particles, which is rationalized on the basis of accessibility of subsurface hydrogen facilitating hydrogen addition to alkene [1].

The adsorption of trans-2-pentene on Pd particles is shown to exhibit site-specific behavior, which results in a strong increase in hydrogenation activity within the 1-5 nm particle size range, in contrast to ethylene hydrogenation [2]. The size effects are explained by the hydrogenation reactions proceeding via di- σ -bonded pentene, which is favored on the terrace sites of large particles, and π -bonded ethylene.

The effect of silver on reactivity of Pd particles in acetylene hydrogenation has been examined. The combined STM, XPS and IRAS results show that silver segregates on the particle surface and basically blocks acetylene and hydrogen chemisorption. However, at the smallest Ag coverage, the selectivity towards ethane is found to be smaller than ethene, which is consistent with the promoting effect of silver observed on commercial Pd-Ag catalysts of selective hydrogenation.

References

1. A. Doyle, S. Shaikhutdinov, S.D. Jackson, H.-J. Freund, *Angew. Chem. Int. Ed.* **42**, 5240 (2003)
2. A. Doyle, S. Shaikhutdinov, H.-J. Freund, *Angew. Chem. Int. Ed.* **44**, 629 (2005)

Iron Oxide Supported Gold Nanoparticles: Structure and Reactivity

D. Starr, C. Lemire, R. Meyer, S. Shaikhutdinov, H.-J. Freund

Introduction

Surface chemistry of gold has recently received much attention owing to the unique catalytic properties of Au nanoparticles, particularly in the CO oxidation reaction [1]. In order to determine structure-reactivity relationships on gold catalysts we developed model systems involving Au metal particles deposited on well-ordered oxide films. Of particular interest is the role of the support in formation and stabilization of Au nanoparticles and their adsorption behaviour towards CO and O₂. Understanding of the surface structure of the iron oxide support is a crucial prerequisite for explanation of the reactivity of gold catalysts. Here we report on a comparative study of gold model catalysts supported on iron oxide (FeO, Fe₃O₄, Fe₂O₃) films.

Results

Adsorption of CO on the pristine iron oxide films grown on Pt(111) studied by TPD and IRAS revealed that the Fe₃O₄(111) surface is terminated by ½ monolayer (ML) of iron, with an outermost ¼ ML consisting of octahedral Fe²⁺ cations situated above a ¼ ML of tetrahedral Fe³⁺ ions. The most strongly bound CO, which desorbs at 230 K, is assigned to adsorption to Fe³⁺ cations present at the step edges [2]. For the α-Fe₂O₃(0001) surface, experimental and theoretical evidence is presented which shows that the hematite may be terminated with ferryl (Fe=O) groups, which has never been considered for iron oxide surfaces [3].

The combined STM, TPD and IRAS data for gold deposited on various supports indicate that interaction of CO with annealed Au surfaces is essentially identical and independent on the particle size, dimensions and nature of support. It has been concluded that the CO adsorption only includes highly uncoordinated surface atoms, from which CO may desorb at temperatures as high as 300 K [4]. Gold particles are found to be inert towards molecular oxygen under the conditions studied.

In order to examine the stability of the gold particles in a reactive atmosphere, the morphology of Au particles deposited on thin FeO(111) films at elevated pressures of CO, O₂, CO + O₂, and H₂ has been examined using in situ STM at room temperature. The Au particles are found to be quite stable in O₂ and H₂ environments at pressures up to 2 mbar. However, in CO and CO+O₂ atmospheres, the destabilization of Au particles located at the step edges occurs leading to the formation of mobile Au species, which migrate across the oxide surface. In addition, data clearly show the effects of ambient gas impurities, which may lead to erroneous conclusions, particularly about structural changes of the gold surfaces at elevated pressures.

References

1. M. Haruta, Chem. Record **3**, 75 (2003)
2. C. Lemire, R. Meyer, V. Henrich, S. Shaikhutdinov, H.-J. Freund, Surf. Sci. **572**, 103 (2004)
3. C. Lemire, S. Bertarione, et al., Phys. Rev. Lett., **94**, 166101 (2005)
4. C. Lemire, R. Meyer, S. Shaikhutdinov, H.-J. Freund, Surf. Sci. **552**, 27 (2004)

Group Five Model Catalysts: Supported Vanadia Clusters and Thin Niobia Films

S. Kaya, J.-L. Lu, A. Uhl, S. Guimond, D. Lahav, F. Mendes, D. Starr,
J. Weissenrieder, H. Kuhlenbeck, S. Shaikhutdinov, H.-J. Freund

Introduction

Group Five (V, Nb) compounds (G5-compounds) are widely used as catalysts for many important processes including methanol oxidation, oxidative dehydrogenation of alkanes, Fischer-Tropsch reaction, etc [1]. In these catalysts, vanadia is supported on a second metal oxide such as silica, titania, etc. Niobia can participate as either a support for metal particles or as an active component when added to other reducible oxides such as titania. In attempts to understand the reactivity of the G5-catalysts, we use model catalysts including metal or oxide particles deposited onto well-ordered oxide films. The controlled preparation of the model catalysts and determination of the atomic structure of the system are essential for providing a molecular level understanding of their reactivity. Here we focus on structural characterization of vanadia particles deposited on thin silica films and report on the preparation of well ordered niobia films.

Results

The silica films were grown on Mo(112) by Si deposition in oxygen ambient and subsequent annealing in vacuum. The structure of the film has been studied by scanning tunneling microscopy (STM), infrared reflection absorption spectroscopy (IRAS) and X-ray photoelectron spectroscopy (XPS). In excellent agreement with the experimental results, theoretical calculations (performed by Sauer's group in the HU, Berlin) show that the film consists of a two dimensional network of corner sharing $[\text{SiO}_4]$ tetrahedra, with one oxygen of each tetrahedron binding to the Mo(112) surface [2].

Vanadia clusters were deposited on the silica films by V evaporation in an oxygen ambient. Comparison of the STM and IRAS results observed for VO_x on the silica and thin alumina films corroborated with theoretical calculations clearly showed that the accepted interpretation of vibrational spectra, which are primarily used for structural characterization of the powdered vanadia catalysts, must be revised [3].

Thin niobia films were grown by Nb deposition onto oxygen implanted $\text{Cu}_3\text{Au}(100)$ and subsequent oxidation [4]. This results in a flat, well-ordered thin niobia film. Combining low energy electron diffraction, STM, angular resolved photoelectron spectroscopy using synchrotron radiation and DFT calculations we have determined the atomic structure of the film, which consists of $2/3$ ML of Nb between two hexagonal O-layers, where Nb^{5+} cations occupy the three-fold hollow sites. The top O atoms occupy close to bridge sites above the Nb sub-lattice. However, at increasing film thickness, HREELS reveals vibrations characteristic for Nb=O (niobyl) species observed on polycrystalline $\text{H-Nb}_2\text{O}_5$ powders. These studies may be linked to the studies of supported vanadia catalysts, where V=O species is believed to play a crucial role in oxidation reactions.

References

1. M. Ziolek, Catal. Today **78**, 47 (2003), I.E. Wachs, Catal. Today **100**, 79 (2005)
2. J. Weissenrieder, S. Kaya, J.-L. Lu, et al., Phys. Rev. Lett., in press.
3. N. Magg, B. Immaraporn, G. Giorgi, et al. J. Catal. **226**, 88 (2004)
4. J. Middeke, R.-P. Blum, M. Hafemeister, H. Niehus, Surf. Sci. **587**, 219 (2005)

Frequency modulated atomic force microscopy: Atomic resolution and distance dependence of tip-sample interaction

M. Heyde, M. Sterrer, M. Kulawik, G. Thielsch, H.-P. Rust, H.-J. Freund

Introduction

Metal oxides are of great technological importance because they are involved in a variety of applications, such as microelectronics or heterogeneous catalysis. The characterization of their properties on the atomic scale is therefore of special interest. However, the low conductivity inherent in most bulk oxides makes it difficult to investigate them by scanning tunneling microscopy (STM). Frequency-modulated atomic force microscopy (FM-AFM) does not encounter these problems and can be used to study both conducting and insulating samples on the atomic scale. The force detected by FM-AFM originates from several kinds of interaction between surface and tip. Though these interactions play a central role in contrast mechanisms, they are not well understood so far. Force spectroscopy and imaging in different regimes (e.g. repulsive or attractive) can be used to specify different force contributions. They are promising tools for a microscopic characterization of surfaces beyond topography measurements.

Results

A new-built low temperature ultra-high vacuum system is currently supplemented with a double tuning fork sensor for AFM and STM measurements [1]. The combined AFM/STM set-up has been tested successfully. It now shows now atomic resolution in both modes. For the detailed analysis and interpretation of surface structures, we benefit from the capability of our sensor to record AFM and STM images as well as spectroscopic data at the same surface area. Atomically resolved images of MgO on Ag(001) have been obtained [2]. Images acquired in the attractive and the repulsive regimes controlled to a constant frequency shift reveal contrast changes. This result emphasizes the importance of the tip-induced relaxation of the surface ions in the tip-surface interaction and in image contrast. For the detailed interpretation of tip-sample interactions, distance dependent frequency shift measurements have been performed. From the experimental data, the interaction force and energy between tip and sample are recovered. Clear differences in the interaction potential have been observed in comparative studies on metal (NiAl(110)) and oxide ($\text{Al}_2\text{O}_3/\text{NiAl}(100)$) surfaces, respectively [3]. The setup also allows us to gain specific information in the repulsive regime of the contact formation, where elastic and plastic stages have been identified. A detailed discussion of these results is given.

References

1. M. Heyde, M. Kulawik, H.-P. Rust, H.-J. Freund, *Rev. Sci. Instr.* **75**, 2446 (2004)
2. M. Heyde, M. Sterrer, H.-P. Rust, H.-J. Freund, *Appl. Phys. Lett.* (2005), accepted.
3. M. Heyde, M. Kulawik, H.-P. Rust, H.-J. Freund, *Phys. Rev. B* (2005), submitted

Atomic Chain Formation in the early Nucleation Stage of Gold on Al_2O_3 thin Films

M. Kulawik, N. Nilius, H. P. Rust, H.-J. Freund

Introduction

Thin oxide films grown on metal substrates are widely used as model systems to investigate the properties of bulk oxides, and play therefore an important role in catalysis research. Although bulk electronic properties already develop in rather thin oxide layers, their adsorption characteristics might still be modified by the limited thickness of the film. Recent theoretical work predicts, for instance, a strong influence of the metal support on the binding of electronegative ad-atoms on a thin MgO film deposited on Mo(001) [1]. The adsorption behavior obtained for thin oxide layers can therefore not generally be transferred to the respective bulk oxides, making a more careful investigation of the influence of the underlying metal desirable.

Results

Using low-temperature STM and STS, we have investigated the nucleation of Au atoms on a thin Al_2O_3 film grown on NiAl(110) [2]. In the low coverage regime, Au dimers and small linear chains containing up to five Au atoms are observed, in addition to isolated monomers. Independent of the orientation of the Al_2O_3 domains, self-assembled Au chains follow a distinct direction on the surface: They are almost aligned with the closed-packed rows of the NiAl substrate, indicating an influence of the metal support on the binding process. This assumption is corroborated by spectroscopic information obtained by conductance measurements with the STM. A pair of occupied and unoccupied states observed for Au monomers, splits into a set of energy levels for Au chains on the oxide film. Direct orbital interaction between neighboring chain atoms is excluded due to the large Au-Au separation of 5.6 Å. The coupling is therefore attributed to a substrate-mediated mechanism. Possible candidates are long-range interactions mediated by polaronic deformations of the Al_2O_3 lattice due to Au binding, or Coulomb interactions due to charge transfer between the NiAl support and Au ad-atoms in the chain.

References

1. G. Pacchioni, L. Giordano, M. Baistrocchi, Phys. Rev. Lett. **94**, 226104 (2005)
2. M. Kulawik, N. Nilius, H.-J. Freund, Phys. Rev. Lett. (2005), submitted

Self-Organization of Au Atoms on a polar FeO film

E. D. L. Rienks, N. Nilius, H.-P. Rust, H.-J. Freund

Introduction

The spatial arrangement of metal ad-atoms on solid surfaces is determined by the availability of suited binding sites and lateral interactions between the ad-atoms. On most oxide surfaces, the interplay between these two factors gives rise to the formation of compact 3D clusters. Nucleation is often found to take place at point or line defects. On polar oxide surfaces, the large surface dipole can have a significant effect on the adsorption characteristics. That contribution can be studied very effectively using a system that displays a surface dipole of varying magnitude. Using low-temperature STM and STS, we have found that a thin film of FeO grown on Pt(111) possesses these qualities.

Results

A lattice mismatch between the single-layer FeO film and the Pt substrate gives rise to a Moiré pattern. In this structure, the Fe atoms alternately occupy on-top, fcc and hcp positions on the Pt lattice. The surface potential in these distinct regions differs, as can be concluded from the unusually large contrast in STM images taken in the near field-emission regime ($U_{\text{sample}} > 4.5$ V). The strong contrast is caused by the fact that field-emission resonances occur at different energies at the three different locations in the Moiré unit cell. The interpretation of this effect in terms of a varying surface potential is supported by alternative measurements of the local barrier-height, a quantity that depends directly on the surface potential. On the polar FeO film with its inhomogeneous structure, modulations of the surface potential can be directly linked to local variations of the surface dipole.

Single Au atoms are deposited on the oxide film to probe the effect of the varying surface dipole on adsorption. The ad-atoms preferentially bind to the region of the Moiré cell with the largest surface dipole. This indicates that the role of electrostatic interaction in binding is significant. With increasing coverage, the Au atoms display a remarkably small tendency to form clusters. Instead, a hexagonal network of single atoms with a lattice constant of 2.5 nm is formed. Electrostatic repulsion between polarized or partially charged Au atoms can account for this phenomenon.

References

1. E. D. L. Rienks, N. Nilius, H.-P. Rust, H.-J. Freund, *Phys. Rev. B* **71**, 241404 (2005)
2. N. Nilius, E.D.L. Rienks, H.-P. Rust, H.-J. Freund, *Phys. Rev. Lett.* (2005), in press

Influence of Electromagnetic Interactions on Optical Properties of Ordered and Disordered Silver Particle Ensembles

H. M. Benia, N. Nilius, N. Ernst, H.-J. Freund

Introduction

The optical properties of metal particle ensembles are not only determined by size, shape, and environment of the particles and their dielectric properties, but additionally by the mean particle-particle separation on the surface. The latter influence is the result of a constructive coupling of in-plane dipoles as well as destructive interference of out-of-plane modes in the individual particles, and leads to a splitting of the collective excitation into two plasmon modes. Controlled experiments investigating this effect are sparse, because any variation of the particle density on the surface is usually connected to changes of the particle geometry. We have employed photon emission spectroscopy with an STM to study self-organized Ag nano-crystal arrays on HOPG as well as ensembles of Ag particles with controlled shapes and densities on a $\text{Al}_2\text{O}_3/\text{NiAl}(110)$ support. The combination of local topographic and optical measurements within one instrument enables direct exploration of the influence of electromagnetic interactions in the ensembles.

Results

Silver colloids, prepared by a reverse micelle technique [1], are characterized by a uniform size and self-assemble into a hexagonal super-lattice of 7 nm lattice constant on HOPG. Optical spectra of such ensembles reveal two emission peaks, assigned to plasmon dipoles oscillating parallel and perpendicular to the sample surface. The energy splitting of both modes provides a measure of the dipole-dipole coupling in the particle layer, while their relative intensities yield information on the long-range order in the network [2]. The dependence of dipole interactions on the particle separation is probed by fabricating Ag particle ensembles with different densities on an Al_2O_3 film. Particle densities are controlled by adjusting temperature and atom flux during deposition and by creating artificial nucleation sites on the oxide surface via Ar^+ sputtering. For dome-like particles, a pronounced blue shift of the plasmon mode is observed with increasing density, demonstrating the destructive interference of out-of-plane dipoles. For disk-like particles on the other hand, plasmon energies are constant for different number densities. The absent plasmon shift is attributed to a generally small out-of-plane polarizability of flat particles, in agreement to results obtained from model calculations.

References

1. M. P. Pileni, *J. Phys. Chem. B* **105**, 3358 (2001)
2. N. Nilius, H.-M. Benia, C. Salzemann, H.-J. Freund, A. Brioude, M.-P. Pileni, *Chem. Phys. Lett.* (2005) in press.

Structure and dynamics of proteins on planar surfaces

K. Jacobsen, T. Risse, W.L. Hubbell*

Introduction

Although it is commonly accepted that the exposition of proteins to man-made materials typically results in protein adsorption on the material surface, little is known about the interplay between the protein-surface interactions involved and the resulting conformational changes of the adsorbing protein caused by this process. In this study the site-directed spin labeling (SDSL) approach has been extended to the investigation of proteins adsorbed to planar surfaces. The method involves the selective introduction of an artificial spin-labeled side-chain to a predefined residue of the amino acid sequence and allows the determination of the structure and dynamics of adsorbed proteins by analysis of the electron paramagnetic resonance (EPR) spectra.

Results

The globular protein T4 Lysozyme (T4L) has been adsorbed to planar model surfaces to study the correlation between conformational changes of the protein and the physical and chemical properties of the surfaces. The vectorial tethering of T4L on a planar quartz-supported lipid bilayer consisting of a zwitterionic lipid shows a conservation of the secondary structure and only minor changes in the tertiary structure of the protein. Thus this surface may be classified as a situation of only weak protein-surface interactions. Furthermore, a macroscopic order of the adsorbed protein layer is proven by angular-dependent EPR-spectra which allow the determination of the protein orientation on the surface. Offering surfaces that are net negatively charged to the highly positively charged T4L leads to the observation of more drastic conformational changes. Here, the conformation of T4L adsorbing to a fluid quartz-supported lipid bilayer containing negatively charged lipids is compared to the structure of T4L adsorbed to the negatively charged but rigid quartz surface. A partial unfolding of T4L on the quartz surface can be revealed whereas structural changes involving the entire protein lead to the formation of protein aggregates on the negatively charged lipid bilayer. The adsorption process may also influence the substrate itself. This can be shown by the phase separation of the negatively charged lipid bilayer upon protein adsorption.

* Jules Stein Eye Institute, University of California Los Angeles, Los Angeles, USA

Construction of an UHV compatible W-band (94 GHz) ESR spectrometer for the characterization of paramagnetic surface species

W. Hänsel-Ziegler, E. Fischbach, T. Risse, H.-J. Freund

Introduction

In the last decade the group has explored the capabilities of ESR spectroscopy to characterize a variety of para- or ferromagnetic species on well defined surfaces. The systems cover a broad range of systems from adsorbed paramagnetic atoms and molecules, paramagnetic surface centers to small deposited ferromagnetic particles. For these investigations an ultrahigh vacuum (UHV) compatible ESR spectrometer operating at X-band (9 GHz) was used. At this frequency the experiments are limited by the absolute sensitivity (approximately 10^{11} spins/G (30 K)) as well as relaxation properties of the paramagnetic surface species. The latter limits the spectral resolution and prevents the application of pulse spectroscopic techniques. In order to address these issues we have adapted a commercial a high field ESR spectrometer operating at 94 GHz such as to allow the investigation of paramagnetic species on well defined surfaces under UHV conditions.

Results

The main challenge in adapting the high field EPR spectrometer to UHV conditions is the design of an appropriate resonator. The wavelength of the radiation (3 mm) would require the use of tiny single crystals (approx. 0.6 mm x 1 mm x 0.1 mm) if one would simply scale down the X-Band setup using a monomodal resonator. Therefore, we decided to use a Fabry-Perot resonator with one convex and one planar mirror, the latter being the single crystal under investigation. In order to investigate the sample under UHV conditions an appropriate seal between the microwave bridge operating at ambient pressures and the sample being in UHV has to be constructed. In the present set up the sample is sealed by a 0.1 mm thick quartz window being places in the nodal plane of the electric field component of the resonator separating the UHV chamber from a fine vacuum compartment containing the convex mirror. The choice of the material and the thickness of the window is dictated by necessity to have a material free of paramagnetic impurities which should be as transparent in this frequency regime as possible. The seal between the fine vacuum compartment and the microwave bridge is realized by a Keflar sheet pressed between two wave guide sections. The superconducting split coil magnet which is mounted on linear and rotary platform used has two orthogonal horizontal bores which allow the direction of the magnetic field to be switched between parallel and perpendicular orientation with respect to the surface. This allows the measurement of angular dependent spectra key to an extraction of orientation information of paramagnetic species on surfaces.

Color centers on the MgO surface

M. Sterrer, E. Fischbach, M. Yulikov, M. Heyde, N. Nilius, H.-P. Rust, T. Risse, and H.-J. Freund

Introduction

The role of defects for the physical and chemical properties of surfaces has long been recognized. In addition to line defects such as steps, point defects play an important role in this respect. A particularly important class of point defects in oxides is anion vacancies, often called color or F-centers. The properties of these centers strongly depend on the geometric position as well as the electron occupancy of the vacancies ranging from 0 to 2 for a divalent oxide such as MgO. Due to the large number of different positions and charged states, a detailed spectroscopic characterization of these species is challenging. In this contribution we will present a combined approach where atomic scale information of color centers on MgO thin films, used as model surfaces, obtained from scanning tunneling microscopy and spectroscopy (STM/STS) will be augmented by spectroscopic properties as measured by electron paramagnetic resonance (EPR) experiments in order to obtain a detailed characterization of these defects and elucidate their role for the nucleation of metal particles.

Results

STM experiments were carried out on 4 monolayer (ML) thick MgO films deposited on Ag(001). The formation of localized defects occurred due to both electrons tunneling from the STM tip and electrons created by an external filament. In both sets of experiments, two types of defects with defect levels in the band gap of MgO are observed which are located at the edges of MgO islands. One type of defect is characterized by occupied states 2 eV above the valence band with a strong dependence on the defect position. On the other hand, the second defect type exhibits an occupied state in the middle of the MgO band gap with an additional unoccupied state 1 eV below the conduction band. The good agreement with calculated energy levels of color centers on the surface of MgO allows the assignment of the observed defects to F^+ and F^0 centers, respectively.

EPR experiments on fresh prepared MgO thin films give no indication for the presence of paramagnetic F^+ centers. After electron bombardment, an EPR signal around the free spin value is observed which is assigned to surface color centers. A detailed analysis of the angular dependent EPR spectra reveals the position of the defects to be on edges of MgO islands. To elucidate the importance of these centers for the nucleation of metal particles, gold atoms adsorbed on the MgO film were investigated. The results of the two complementary techniques will discuss the properties of these atoms with respect to the different nucleation sites on the surface.

Sum Frequency Generation Spectroscopy and Reactivity Studies under Ambient Conditions

F. Höbel, A. Bandara, J. Silvestre-Albero, G. Rupprechter, H.-J. Freund

Introduction

In recent years there has been a growing interest to study chemical processes on vacuum-grown model catalysts under technically relevant conditions, i.e. at mbar or even higher pressure^{1,2}. Sum Frequency Generation (SFG) vibrational spectroscopy and gas chromatography were used to monitor adsorbed and reacting molecules on well-defined model catalysts at high-pressure (up to 1 bar). Systems studied include CO adsorption and hydrogenation on Pd-Nb₂O₅/Cu₃Au(100) model catalysts and 1,3-butadiene hydrogenation on Pd-Al₂O₃/NiAl(110) and Pd(111) and Pd(110). TDS, LEED and AES were employed as complementary methods under UHV.

Results

For CO adsorption on pristine Pd-Nb₂O₅ (110 K, 10⁻⁶ mbar CO) SFG detected on-top bonded CO (2105 cm⁻¹) and bridge bonded CO (1994 cm⁻¹), very similar to the Pd-Al₂O₃ system. However, when the temperature was increased to above 300 K irreversible changes occurred, i.e. most of the CO adsorption capacity was lost. Similar changes were also followed by SFG at mbar pressure. This effect is most likely due to interdiffusion between Pd and Nb₂O₅, as indicated by SFG and XPS, and can be partly reversed by hydrogen reduction.

Selective 1,3-butadiene hydrogenation was studied on single crystal and nanoparticle model catalysts at atmospheric pressure, using a UHV-high pressure cell^{3,4}. Catalytic measurements show the formation of 1-butene, trans-2-butene, cis-2-butene and n-butane as reaction products. By correlating the catalytic activity of Pd nanoparticles for 1,3-butadiene hydrogenation with the exact particle surface structure we are able to prove that “large” Pd particles behave identical to Pd(111) single crystals, while Pd particles below 4 nm do not. As a result, although 1,3-butadiene hydrogenation is known to be structure-sensitive, the reaction is in fact particle size independent if the correct morphology of the Pd nanoparticles is taken into account. The effect of CO traces on the reaction selectivity will also be demonstrated. SFG spectroscopy is planned for the future.

References

1. G. Rupprechter, T. Dellwig, H. Unterhalt, H.-J. Freund, *Topics in Catal.*, **15**, 19 (2001)
2. M. Morkel, G. Rupprechter, H.-J. Freund, *Surf. Sci. Lett.* **588**, L209 (2005)
3. J. Silvestre-Albero, G. Rupprechter, H.-J. Freund, *J. Catal.*, in press.
4. J. Silvestre-Albero, G. Rupprechter, H.-J. Freund, *Angew. Chem. Int. Ed.*, submitted.

PM-IRAS and XPS Spectroscopy of Methanol Decomposition and Oxidation on Pd(111)

M. Borasio, O. Rodríguez de la Fuente, G. Rupprechter, H.-J. Freund

Introduction

Polarization-Modulation Infrared Reflection Absorption Spectroscopy (PM-IRAS) provides a route for studying vibrations of adsorbed molecules at elevated pressure^{1,2}. To separate surface and gas phase contributions, PM-IRAS utilizes the polarization modulation of the incident infrared light and is based on the predominance of p- over s-polarized light at a metal surface. Our experimental setup combines a UHV preparation/characterization chamber with a UHV-high pressure cell optimized for the PM-IRAS geometry. X-ray photoelectron spectroscopy (XPS) is used for pre- and post-reaction surface analysis under UHV.

Results

Methanol decomposition on Pd(111) was studied by XPS and PM-IRAS both under ultrahigh vacuum (UHV) and mbar pressure. Annealing CH₃OH multilayers under UHV mainly lead to methanol desorption without reaction². However, at background pressures $\geq 10^{-6}$ mbar dehydrogenation products such as methoxy CH₃O, formaldehyde CH₂O, formyl CHO and CO could be spectroscopically identified at 300 K³. In addition, methanolic C-O bond scission lead to the formation of carbonaceous species CH_x which rapidly deactivated the catalyst surface and no products were observed by gas chromatography^{2,4}.

PM-IRAS was also used to follow methanol oxidation between 300 and 500 K, at a total pressure of 1 bar³. CO₂, H₂O and CH₂O were observed as reaction products with a reaction onset temperature of 400 K. On the Pd(111) surface only CO was detected during the reaction, which points to a low concentration of intermediates. The resonance frequency of CO was typical of adsorption on metallic Pd and also post-reaction XPS detected only metallic Pd, i.e. there were no indications of an involvement of Pd surface oxide. Reference studies of Pd(111) oxidation at 10⁻⁵ mbar oxygen indicated the onset of surface oxidation at ~600 K with clear shifts in the Pd3d and O1s lines.

References

1. G. A. Beitel, A. Laskov, H. Oosterbeek, E. W. Kuipers, J. Phys. Chem. **100**, 12494 (1996)
2. O. Rodríguez de la Fuente, M. Borasio, P. Galletto, G. Rupprechter, H.-J. Freund, Surf. Sci. **566-568**, 740 (2004)
3. M. Borasio, O. Rodríguez de la Fuente, G. Rupprechter, H.-J. Freund, J. Phys. Chem. Lett. B, submitted.
4. M. Morkel, V. V. Kaichev, G. Rupprechter, H.-J. Freund, I. P. Prosvirin, V. I. Bukhtiyarov, J. Phys. Chem. B **108**, 12955 (2004)

Reaction Kinetics on Supported Pd Nanoparticles
Prepared by e-Beam Lithography:
Molecular Beam Experiments and Microkinetic Simulations

M. Laurin, V. Johánek, S. Schauer mann, J. Hoffmann, A. Grant*, B. Kasemo*,
J. Libuda, H.-J. Freund

Introduction

Many heterogeneous catalysts are based on nanometer-sized metal particles finely dispersed on oxide supports. Experimentally, it is well established that reaction kinetics on such systems can differ strongly from single crystal surfaces. Understanding and controlling such effects remains one of the key challenges in catalyst development. Among the numerous potential origins are so-called “nanoscale” kinetic effects, which simply are the result of the limited size of the particles, i.e. without modification of their adsorption properties. Examples of such phenomena are communication effects resulting from the coupling of surface areas with different adsorption or reaction behavior via surface diffusion or coverage fluctuations in confined surface regions. Aiming at a microscopic understanding of such phenomena, we have recently started to perform molecular beam (MB) experiments on supported model catalyst prepared by electron beam lithography (EBL). This preparation method, which has been used only lately for reactivity studies in UHV, provides an exceptional level of control over structural parameters of the surface and opens up a broad spectrum of new kinetic experiments.

Results

Specifically, we focus on two effects: First, we investigate the diffusion of atomic oxygen under reaction conditions [1]. Towards this aim we combine multi-molecular beam experiments and angular-resolved detection of products. The experimental data is used to develop microkinetic reaction-diffusion models, which explicitly take into account the morphology of the model catalyst and the geometry of the MB experiment [2]. The kinetic models allow us to quantitatively reproduce the experimentally determined CO oxidation kinetics under both transient and steady-state conditions. From a comparison of experiment and simulation, it is possible to extract information on the diffusion rates of adsorbates under reaction conditions and on the distribution of local reaction rates on the surface of the Pd nanoparticles. As a second phenomenon, kinetic bistabilities are studied, which occur for CO oxidation on Pd and various other transition metal surfaces [3]. It is shown that such bistabilities are quenched on sufficiently small particles as a result of fluctuation induced transitions between the two reactive states. The rate of these transitions is amplified by the modified adsorption properties of the nanoparticles.

References

1. V. Johánek, M. Laurin, J. Hoffmann, S. Schauer mann, A. W. Grant, B. Kasemo, J. Libuda, H.-J. Freund, Surf. Sci. 561, L218 (2004)
2. M. Laurin, V. Johánek, A. W. Grant, B. Kasemo, J. Libuda, H.-J. Freund, J. Chem. Phys. 122, 084713 (2005), J. Chem. Phys., in press.
3. V. Johánek, M. Laurin, A. W. Grant, B. Kasemo, C. R. Henry, J. Libuda, Science 304, 5677 (2004)

* Department of Applied Physics, Chalmers Univ. of Technology, S-41296 Göteborg, Sweden

Reaction Kinetics on Oxide Supported Metal Nanoparticles: On the Role of Surface Oxygen, Subsurface Oxygen, Surface and Interface Oxides

T. Schalow, B. Brandt, M. Laurin, S. Schauermann, J. Libuda, H.-J. Freund

Introduction

For many heterogeneous reaction systems which involve oxygen there is an ongoing discussion on the chemical state of the oxygen species under reaction conditions. Often, a large number of surface structures, subsurface species, surface oxides and bulk oxides are observed as a function of the reaction conditions. In general, the role of the various species and structures in the kinetics of catalytic reactions is poorly understood. For supported nanoparticle systems, the situation is further complicated by the fact that the particles simultaneously expose many different sites and facets. Moreover, the surface and bulk oxidation kinetics of the metal particles depends on the particle size, the equilibrium particle morphology is expected to vary with oxygen pressure and the oxide support may be involved in the oxidation and reaction kinetics via spillover processes.

Results

In order to obtain deeper insights into such processes at the microscopic level, we follow a model approach: Supported Pd catalysts are prepared under UHV conditions on well defined oxide surfaces ($\text{Fe}_3\text{O}_4/\text{Pt}(111)$). Previously, these systems have been characterized with respect to their geometric and electronic structure. In this study, we probe the oxygen adsorption and oxidation employing molecular beam methods and time-resolved IR reflection absorption spectroscopy (TR-IRAS) under reaction conditions [1]. This approach provides detailed information on the adsorption and oxidation kinetics and on the role of the different oxygen species in the kinetics of oxidation reactions. Specifically, it is shown that at temperatures of 500 K and above, chemisorbed oxygen on the Pd particle surface is rapidly incorporated into a thin oxide layer at the particle/support interface. In comparison with surface oxide layers, which can also be formed on Pd surfaces under similar conditions, the interface oxide is strongly stabilized by interaction with the support. It is found that a dynamic equilibrium is established between oxygen chemisorbed on the metallic Pd surface and oxygen incorporated into the interface oxide layer. As demonstrated by isotopic exchange experiments, this equilibrium is fast in comparison with oxygen exchange with the Fe_3O_4 support. With respect to the kinetics of oxidation reactions on the model catalyst, it is important to note that the surface and interface oxide layers can act as an intrinsic oxygen buffer, which can reversibly store and release large amounts of oxygen. The kinetics of this storage channel is probed by studying the CO oxidation kinetics. Here, the interface and surface oxides are shown to be unreactive with respect to CO. Instead, the reaction mainly proceeds via decomposition of surface and interface oxides resulting in release of chemisorbed oxygen onto the metallic part of the surface.

References

1. T. Schalow, B. Brandt, M. Laurin, S. Guimond, D. Starr, H. Kuhlenbeck, S. K. Shaikhutdinov, J. Libuda, H.-J. Freund, *Angew. Chem. Int. Ed.*, accepted.

Two-photon Photoemission Study of Silver Nanoparticles on Thin Alumina Films

F. Evers, K. Watanabe, D. Menzel*, and H.-J. Freund

Introduction

Plasmon excitation of silver nanoparticles leads to enhancement of the photoelectron yield in two-photon photoemission (2PPE)¹. Such plasmon-enhanced electron dynamics should strongly influence surface photochemistry. However, compared to surfaces of bulk metals, information about the electron dynamics and the electronic structure at metal nanoparticle surfaces is still scarce. Using femtosecond laser pulses, we investigate the dynamics of hot electrons as well as the electronic structure of size-controlled silver nanoparticles deposited on thin alumina films by 2PPE and 1PPE.

Results and Discussion

2PPE spectra from silver nanoparticles deposited on Al₂O₃/NiAl(110) at room temperature have been measured at photon energy $h\nu=3.2$ eV as a function of dosage of Ag atoms. The 2PPE signal abruptly increased with Ag dosage and leveled off at about 0.9 nm mean thickness (mean particle diameter ~ 10 nm), where the total photoelectron yield is about 100 times larger than that from the bulk Ag(111). A broad feature near the Fermi edge growing with Ag dosage could be attributable to surface states on small (111) facets of the Ag nanoparticles similar to that on Ag(111). 1PPE spectra ($h\nu=5.3$ eV) also showed this feature which was quenched by NO adsorption, supporting that it originates from surface states. The 2PPE yield from silver nanoparticles measured as a function of photon energy showed a pronounced peak at $h\nu=3.6$ eV. This peak position corresponds to the plasmon excitation of silver nanoparticles². Time-resolved two-color 2PPE on 7-nm silver nanoparticles at $h\nu=3.6$ eV and 3.2 eV exhibited a hot electron relaxation time of ~ 40 fs at ~ 1 eV above the Fermi level, which is about twice as long as that measured on bulk silver surfaces. The particle size dependence of the electron relaxation will be investigated and compared with photochemistry.

References

1. F. Evers, C. Rakete, K. Watanabe, D. Menzel, and H.-J. Freund, Surf. Sci., in press.
2. N. Nilus, N. Ernst, and H.-J. Freund, Phys. Rev. Lett. **84**, 3994 (2000)

* Physik Department E20, Technische Universität München, Germany

Towards a Completely Self Consistent Embedded Cluster Approach: Calculation of Adsorbates on Metal Surfaces

D. Lahav, T. Klüner

Introduction

We present a new stage of the development towards a completely self consistent embedded cluster scheme. The theory allows the treatment of a cluster with ab initio methods (MP-n, CASSCF, CI) while the metallic environment is presented via an embedding operator which is described within the Density Functional Theory (DFT). While previous applications within this theory^{1,2} used a partially self consistent embedding operator, we present for the first time results using a completely self consistent embedding scheme.

Within this scheme, the adsorption energy of CO on Pd(111) was calculated on the Hartree-Fock, MP-2 and MP-4 levels of theory. Our results were compared with previous theoretical and experimental investigations.

Results

The results of the embedding theory using the completely self consistent embedding operator are in very good agreement with experimental adsorption energies for CO on Pd(111). The result of $E = -1.55\text{eV}$ of the new embedding scheme using Moeller-Plesset perturbation theory is in excellent agreement with the experimental value³ of

$E = -1.54\text{eV}$.

In variance to the partially self consistent embedding scheme it seems mandatory to treat parts of the kinetic potential of the embedding operator self consistently. We systematically studied various exchange-correlation and kinetic energy functionals, respectively and investigated the influence of the embedding density on the calculated adsorption energy.

References

1. T. Klüner, N. Govind, Y. A. Wang, and E. A. Carter, Phys. Rev. Lett. **86**, 5954 (2001)
2. T. Klüner, N. Govind, Y. A. Wang, and E. A. Carter, J. Chem. Phys. **116**, 42 (2002)
3. X. Guo, J. T. Yates, Jr. , J. Chem. Phys. **90**, 6761 (1989)

Quantitative Surface Structure Determination Using Scanned-Energy Mode Photoelectron Diffraction

E. A. Kröger, D.I. Sayago, M. Polcik, D.P. Woodruff,

F. Allegretti*, M. Knight*, C. L. A. Lamont**, G. Nisbet**, K. Hogan**

Introduction

Scanned-energy mode photoelectron diffraction (PhD) is a novel synchrotron-radiation-based method to determine quantitatively the local structure at surfaces in an element-specific and chemical-state-specific fashion. While the group continues to exploit this method to investigate the structure of increasingly complex small molecules (such as the smallest chiral amino acid, alanine) on metal surfaces, the focus of the FHI-based component of the collaboration is on transition metal oxide surfaces, and particularly VO_x . During the last 2 years work has focussed on two systems, both involving ultra-thin epitaxial films of VO_x , namely VO_2 on $\text{TiO}_2(110)$, and V_2O_3 on $\text{Pd}(111)$.

Results

Despite reports in the literature based on angle-scan X-ray photoelectron diffraction (XPD) that good epitaxy of a rutile-phase VO_2 occurs, our PhD data are indicative of very poor order, and a parallel study we have conducted using normal incidence X-ray standing waves now shows that the quality of these films beyond a single atomic layer is poor. However, on $\text{TiO}_2(110)$ the interaction of formic acid leads to coadsorbed formate and hydroxyl species, and the local adsorption geometry of both species have been determined from O 1s and C 1s PhD data [1]. Most recently, we have also determined the local adsorption geometry of molecular water on this surface. We find a significant discrepancy in the $\text{Ti-O}_{\text{water}}$ bondlength relative to current theory; this may be a key to the well-known problem in such theoretical calculations of correctly reproducing the inability of water to dissociate on un-defected $\text{TiO}_2(110)$.

By contrast to growth on $\text{TiO}_2(110)$, excellent films of V_2O_3 have been grown on $\text{Pd}(111)$. While the PhD technique is more naturally suited to studies of adsorbate structures than of clean surfaces, preliminary theoretical simulations of PhD data from the clean, as-prepared, $\text{V}_2\text{O}_3(0001)$ surface do indicate an encouraging sensitivity to the surface termination, and thus some potential to determine this experimentally. In parallel with this study of the clean surface, initial experiments on adsorbate structures have been initiated. PhD data collected from O 1s emission from surface hydroxyl species formed both by water dissociation and by exposure of the surface to atomic hydrogen show essentially identical modulations, and initial data evaluation indicates that surface hydroxylation is certainly not limited to the vanadyl oxygen atoms as has sometimes been suggested.

References

1. D. I. Sayago, M. Polcik, R. Lindsay, J. T. Hoeft, M. Kittel, R. L. Toomes, D. P. Woodruff, *J. Phys. Chem. B* **108**, 14316 (2004)

* University of Warwick, Warwick, U.K.

** University of Huddersfield, Huddersfield, U.K.

Department of Molecular Physics

Poster List 2005

- MP 1** **Infrared spectroscopy of gas phase peptides and proteins**
I. Compagnon, N. Polfer, J. Oomens, G. Meijer and G. von Helden
- MP 2** **Probing weak interactions in gas phase molecules and molecular complexes**
U. Erlekam, M. Frankowski, G. Meijer and G. von Helden
- MP 3** **Size, charge, and isomer specific vibrational spectroscopy of metal clusters**
A. Fielicke, Ch. Ratsch, J. Behler, M. Scheffler, G. von Helden and G. Meijer
- MP 4** **Size and charge effects on the binding of CO to small isolated transition metal clusters**
A. Fielicke, B. Simard, D. M. Rayner, G. von Helden and G. Meijer
- MP 5** **Mass-selective vibrational spectroscopy of gas phase cluster ions**
K. R. Asmis, M. Brümmer, G. Santambrogio, L. Wöste and G. Meijer
- MP 6** **Deceleration and trapping of OH radicals**
J. J. Gilijamse, S. Hoekstra, N. Vanhaecke, S. Y. T. van de Meerakker and G. Meijer
- MP 7** **Accumulating Stark-decelerated radicals in a magnetic trap**
S. Hoekstra, J. J. Gilijamse, N. Vanhaecke, W. Schöllkopf, S. Y. T. van de Meerakker and G. Meijer
- MP 8** **A sectional electrostatic storage ring for neutral molecules**
C. E. Heiner, H. L. Bethlem, D. Carty and G. Meijer
- MP 9** **A molecular fountain clock**
H. L. Bethlem, W. Ubachs and G. Meijer
- MP 10** **Decelerating and trapping polar molecules on a chip**
S. Meek, H. Conrad, H. L. Bethlem and G. Meijer
- MP 11** **Alternate gradient focusing and deceleration of a beam of large molecules**
K. Wohlfart, F. Filsinger, H. L. Bethlem, J. Küpper and G. Meijer

- MP 12** **An AC electric trap for molecules in high-field seeking states**
J. van Veldhoven, H. L. Bethlem, M. Schnell and G. Meijer
- MP 13** **A microwave trap for molecules in their absolute ground-state**
M. Schnell, P. Lützwow, J. van Veldhoven and G. Meijer
- MP 14** **A quasi-analytic model of a Stark accelerator/decelerator and of an AC electric trap**
K. Gubbels, M. Schleier-Smith and B. Friedrich
- MP 15** **Sympathetic cooling of cold molecules by Rb atoms**
S. Schlunk, A. Marian, A. - P. Mosk, P. Geng, W. Schöllkopf and G. Meijer
- MP 16** **Buffer gas loading and magnetic trapping of atoms and molecules**
M. Stoll, J. M. Bakker, G. Meijer and A. Peters
- MP 17** **The transition from coherent to incoherent photoelectron scattering in diatomic molecules: CO versus N₂**
M. Braune, S. Cvejanovic, O. Geßner, R. Hentges, S. Korica, T. Lischke, G. Prümper, A. Reinköster, D. Rolles, J. Viefhaus, U. Becker, B. Zimmermann, V. McKoy, B. Langer and R. Dörner
- MP 18** **New phenomena in valence and inner-shell photoionization of fullerenes**
A. Reinköster, S. Korica, M. Braune, R. Hentges, D. Rolles, J. Viefhaus, U. Becker, B. Langer, M. Stener and P. Decleva
- MP 19** **Molecular double Auger decay studied by electron time-of-flight coincidence spectroscopy**
J. Viefhaus, M. Braune, S. Korica, A. Reinköster, D. Rolles and U. Becker
- MP 20** **Chirality and structure in adsorbed layers: Tartaric acid on Cu(110)**
T. Kampen, J. W. Kim, J. H. Dil, P. M. Schmidt, K. Horn, M. Parschau and K.-H. Ernst
- MP 21** **Quantum size effects in self organized thin metal films**
J. H. Dil, T. U. Kampen and K. Horn

Infrared spectroscopy of gas phase peptides and proteins

Isabelle Compagnon* Nick Polfer*, Jos Oomens*, Gerard Meijer and Gert von Helden

Infrared spectroscopy is one of the key techniques to determine the conformational structures of peptides and protein molecules in solution. In infrared experiments, vibrational modes that are sensitive to the higher order structure, such as the C=O stretching modes (amide I) and the N-H bending modes (amide II), are used to obtain detailed structural information for small peptides or to obtain a global picture of the conformation for proteins.

A variety of techniques exist to obtain vibrational spectra of gas phase molecules. Frequently, however, these techniques are limited by the lack of availability of suitable infrared (IR) laser systems. A highly powerful and versatile source of tunable IR radiation is the free electron laser FELIX, located at the FOM Institute for Plasma Physics, Nieuwegein, The Netherlands. The combination of its various performance characteristics make this ideally suited to resonantly pump large amounts of vibrational energy into isolated gas-phase species. FELIX is continuously tunable from 2.5 to 250 microns. The light output comes in macropulses of 5 microsecond duration at a repetition rate of 10 Hz. Each macropulse contains micropulses that are 300 fs to 5 ps long and spaced by 1 ns. The bandwidth is Fourier transform limited. Macropulse energies can reach above 100 mJ.

We here present IR spectra of a small peptide containing two aminoacids (Z-Aib-Pro-NHMe), as well as of a protein containing 104 aminoacids (bovine heart cytochrome c). For the peptide, a comparison of the experimental spectrum to results from DFT calculations shows that the backbone is locally constrained to an α -helix by Aib and to a γ -turn by Pro. The observation of a γ -turn motif is intriguing since the condensed phase molecule has a β -turn and it emphasizes the subtle balance between intra- and inter-molecular forces, which is responsible for the relative stability of the different secondary structure motif [1].

The protein is observed to have a gas-phase structure that is similar to that in solution. Compared to solution, the amide I band is blue-shifted and the amide II band red-shifted, as expected for species in an environment with reduced hydrogen bonding. The band positions are suggestive of a mostly α -helical structure of the protein and their widths are comparable to those in solution, suggesting a similar conformational distribution [2].

References

1. I. Compagnon, J. Oomens, G. Meijer and G. von Helden, *J. Am. Chem. Soc.* (submitted).
2. J. Oomens, N. Polfer, D. T. Moore, L. van der Meer, A. C. Marshall, J. R. Eyler, G. Meijer and G. von Helden, *Phys. Chem. Phys.* **7**, 1348 (2005).

* FOM-Institute for Plasmaphysics „Rijnhuizen“, Nieuwegein, The Netherlands.

Probing weak interactions in gas phase molecules and molecular complexes

Undine Erlekam, Marcin Frankowski, Gerard Meijer and Gert von Helden

Free-electron lasers like FELIX, CLIO or FELBE are powerful tools in gas phase molecular physics research as they can deliver tunable radiation over the entire IR wavelength range [1]. However, they are bulky, expensive and commercially not available. Fortunately, the range up to about 10 μm (1000 cm^{-1}) can also be covered by table top lasers. In that range, the important X-H stretching vibrations (around 3 μm), C=O stretching and N-H bending vibrations (both between 5 and 7 μm) are present. We recently installed a laser system that delivers nanosecond pulses of narrow-band, tunable IR radiation in that range. At present, that laser system is tunable between 2 and 5 μm , and an extension to the 5-10 μm range is planned.

In the first experiments, this laser system has been used in combination with a compact molecular beam set-up to investigate "floppy" molecular complexes in the gas phase, with the aim to learn about weak intra- and intermolecular interactions. Such interactions are important in nature, for example in the formation of secondary and higher order structures of proteins or in base-base interactions in DNA.

The benzene dimer is the simplest model system for dispersive interactions between aromatic centers. This complex has received much attention over the last twenty years, yet many open questions concerning its structure and dynamics remain.

Here, we investigate the vibrational properties of the complex in its electronic ground state via mass-selective infrared ion dip spectroscopy. The benzene dimer forms in a supersonic expansion and is internally cooled. Ions are produced via resonance enhanced two-color photoionization and detected in a time of flight mass spectrometer. A few ns before UV excitation and ionization, the molecular beam is interrogated by the IR laser that is tuned in the range of $3000\text{-}3150\text{ cm}^{-1}$. When the photons from that laser are resonant with a molecular vibration, ground state population is depleted and a reduction in ion signal is observed. IR ion dip spectra are obtained by measuring the ion yield, while scanning the frequency of the IR laser.

IR and UV Spectra of $(\text{C}_6\text{H}_6)_2$ and $(\text{C}_6\text{H}_6)(\text{C}_6\text{D}_6)$ are measured. For the latter, depending on the UV excitation wavelength, two different IR spectra can be measured that are consistent with two non-equivalent, non-interconverting benzene molecules, in the dimer, such as for example in the T-shaped structure, which is the one obtained using quantum chemical methods.

A laser desorption setup to perform infrared experiments on volatile and non-volatile biomolecules in the gas phase is under construction and first results will be presented.

Reference

1. G. von Helden, A. Fielicke and G. Meijer, *Physik Journal* **4**, 39-44 (2005).

Size, charge, and isomer specific vibrational spectroscopy of metal clusters

André Fielicke, Christian Ratsch*[#], Jörg Behler*, Matthias Scheffler*, Gert von Helden and Gerard Meijer

We report on the vibrational spectra of neutral and charged metal clusters in the far infrared. These spectra are obtained via far infrared resonance enhanced multiple photon dissociation (FIR-MPD) of the complexes of metal clusters with rare gas atoms. The experiments make use of the Free Electron Laser for Infrared eXperiments (FELIX) in Nieuwegein, The Netherlands, as an intense and widely tunable far-infrared radiation source.

The measured FIR-MPD spectra of the gas phase complexes represent the infrared absorption spectra of the bare metal clusters. These spectra are unique for each cluster size and are true fingerprints of the cluster's structure. This FIR-MPD technique has been applied to cationic vanadium clusters [1,2] and cationic and neutral niobium clusters [3] containing 3 to more than 20 atoms. Interestingly, for some cluster sizes, the vibrational spectra of neutral and cationic niobium clusters differ rather strongly, indicating different geometric structures. For smaller sized clusters ($n \leq 15$), theoretical infrared spectra have been calculated using density functional theory and a comparison with the experimental spectra allows for the structure determination.

The experimental IR-MPD spectra do in most cases not depend on the number of attached rare gas atoms or the nature of the rare gas. However, the observed spectra for the neutral niobium cluster complexes Nb_9Ar_n ($n=1-4$) are different for different values of n . This is explained by the presence of two isomers of Nb_9 that have different affinities towards Ar and the isomer specific infrared spectra are obtained. In addition, for one of the isomers, the FIR spectrum is recorded without interferences from the other isomer using near threshold ionization. Again, by comparison with theory, the structures of the isomers are determined. Furthermore, an analysis of the charge distribution in the different cluster isomers gives an explanation of the different binding behavior of the isomers towards the Ar atoms [4].

References

1. A. Fielicke, A. Kirilyuk, C. Ratsch, J. Behler, M. Scheffler, G. von Helden and G. Meijer, *Phys. Rev. Lett.* **93**, 023401 (2004).
2. C. Ratsch, A. Fielicke, A. Kirilyuk, J. Behler, G. von Helden, G. Meijer and M. Scheffler, *J. Chem. Phys.* **122**, 124302 (2005).
3. A. Fielicke, G. von Helden and G. Meijer, *Eur. Phys. J. D* **34**, 83 (2005).
4. A. Fielicke, C. Ratsch, G. von Helden and G. Meijer, *J. Chem. Phys.* **122**, 091105 (2005).

* FHI, Theory Department.

[#] Dept. of Mathematics and California NanoSystems Institute, University of California, Los Angeles, USA.

Size and charge effects on the binding of CO to small isolated transition metal clusters

André Fielicke, Benoit Simard*, David M. Rayner*, Gert von Helden and Gerard Meijer

The adsorption of carbon monoxide is a common probe to characterize the surfaces of transition metals or of deposited transition metal nanoparticles. Furthermore, the interaction of CO with transition metals directly plays a central role in model studies of catalytic oxidations or, e.g., in the Fischer-Tropsch reaction. The characterization of the bonding situation of the CO can be achieved using vibrational spectroscopy of the $\nu(\text{CO})$ stretch, since the C-O bond strength is highly sensitive to the coordination of the CO and the electron density on the metal.

Here, the interaction of CO with rhodium clusters in the size range of 3–15 atoms is studied in the gas-phase using IR multiple photon dissociation spectroscopy (IR-MPD). The IR absorption spectra of neutral, cationic and anionic Rh_nCO complexes are measured in the frequency range of $\nu(\text{CO})$, between 1650 and 2200 cm^{-1} . We find that for most clusters adsorption in an atop position (μ^1) is preferred; however for some clusters CO in bridging (μ^2) or hollow (μ^3) sites can be identified as well. Comparison with DFT calculations carried out for the smallest cluster complexes $\text{Rh}_n\text{CO}^{+/0/-}$ ($n = 3, 4$) shows that the experimentally identified CO adsorption sites correspond to the energetically favored positions [1,2].

Further, we investigated the reaction of carbon monoxide with cationic and anionic gold clusters. Successive adsorption of CO molecules on the $\text{Au}_n^{+/-}$ clusters proceeds until a cluster size specific saturation coverage is reached. In case of the cations, structural information for the bare gold clusters is obtained by comparing the saturation stoichiometry with the number of available equivalent sites presented by candidate structures of Au_n^+ . By inference we also establish the structure of the saturated $\text{Au}_n(\text{CO})_m^+$ complexes. In addition, vibrational spectra of the $\text{Au}_n(\text{CO})_m^{+/-}$ complexes in the CO stretching region and in the region of the Au-C stretch and the Au-C-O bend are measured. The spectra further aid in the structure determination of the gold clusters, provide information on the structure of the carbonyl complexes and can be compared with spectra of CO adsorbates on deposited clusters or surfaces. The results provide a size- and charge-dependent basis to interpret values of $\nu(\text{CO})$ measured for CO on deposited gold clusters in terms of the charge states of the clusters [3].

References

1. A. Fielicke, G. von Helden, G. Meijer, B. Simard, S. Dénoimée and D. M. Rayner, *J. Am. Chem. Soc.* **125**, 11184 (2003).
2. A. Fielicke, G. von Helden, G. Meijer, D. B. Pedersen, B. Simard and D. M. Rayner, *J. Phys. Chem. B* **108**, 14591 (2004).
3. A. Fielicke, G. von Helden, G. Meijer, D. B. Pedersen, B. Simard and D. M. Rayner, *J. Am. Chem. Soc.* **127**, 8416 (2005).

*Steele Institute for Molecular Sciences, National Research Council, Ottawa, Canada.

Mass-selective vibrational spectroscopy of gas phase cluster ions

Knut R. Asmis, Mathias Brümmer*, Gabriele Santambrogio*, Ludger Wöste*
and Gerard Meijer

The vibrational spectroscopy of mass-selected, gas phase cluster ions remains a very challenging research area due to the combination of low number densities attainable in the gas phase and a lack of commercially available intense and widely tunable infrared light sources. Even though significant progress has been made recently in applying table-top, OPO-based laser systems to cluster ion spectroscopy, the intensity of the IR pulses in these experiments remains roughly three orders of magnitude below that of typical FEL radiation. Thus many experiments, in particular those requiring the absorption of multiple IR photons or those that probe below 800 cm^{-1} , remain limited to FEL facilities. Here, we present recent results of our research program involving the free electron laser FELIX, which currently focuses on two central topics: strong hydrogen bonding and transition metal oxide clusters.

The hydrogen bond interaction is key to understanding the structure and properties of water and biomolecules. However, our understanding of strong, low-barrier hydrogen bonds and their central role in enzyme catalysis, biomolecular recognition, proton transfer across biomembranes and proton transport in aqueous media remains sketchy. We recently measured gas phase IR spectra of several prototypical systems containing strong hydrogen bonds, directly probing the shared proton region of the underlying potential energy surface. These experiments demonstrate that the theoretical description of the vibrations of strong hydrogen bonds is considerably more complex than originally anticipated and not yet solved satisfactorily for larger than triatomic systems.

Transition metal oxides play an increasingly important role in heterogeneous catalysis. Recent gas phase reactivity studies on vanadium oxide cluster ions were aimed at understanding the nature of the reactive sites. The interpretation of the reactivity data requires information on the structure of the cluster ions. We employ IR photo dissociation spectroscopy in combination with electronic structure calculations to identify the geometric structure as well as structural trends as a function of cluster size in vanadium oxide cluster cations and anions. For the cluster anions we present the first spectroscopic evidence for the formation of polyhedral vanadium oxide cages in the gas phase [1]. The measured IR spectra are sensitive probes for charge localization of unpaired d-electrons and show a strong resemblance with the IR spectrum of a V_2O_5 surface already at medium cluster sizes.

Our most recent results will be discussed on the poster, including the vibrational spectra of the protonated ammonia clusters $\text{H}^+(\text{NH}_3)_{1-8}$, of bare vanadium oxide cluster anions as well as of complexes of SO_2 , and the first IR spectra of doubly-negatively charged ions, namely, $[\text{SO}_4(\text{H}_2\text{O})_{n>3}]^{2-}$ clusters.

Reference

1. K. Asmis, G. Santambrogio, M. Brümmer and J. Sauer, *Angew. Chem. Int. Ed.* **44**, 3122 (2005).

* Institut für Experimentalphysik, Freie Universität Berlin, Germany.

Deceleration and trapping of OH radicals

Joop J. Gilijamse, Steven Hoekstra, Nicolas Vanhaecke, Sebastiaan Y.T. van de Meerakker and Gerard Meijer

Over the last years our group has been developing methods to get improved control over the absolute velocity and over the velocity spread of molecules in a molecular beam. These methods rely on the, quantum state specific, force that polar molecules experience in inhomogeneous electric fields. This force is rather weak, typically some eight to ten orders of magnitude weaker than the force that the corresponding molecular ion would experience in the same electric field, but nevertheless suffices to achieve complete control over the molecular motion, using techniques akin to those used for the control of charged particles. In particular, we have developed a so-called 'Stark-decelerator', the equivalent of a linear accelerator (LINAC) for charged particles, by which one is able to transfer the high phase-space density that is present in the moving frame of a pulsed molecular beam to a reference frame at any desired velocity. With the Stark-decelerator, a part of the molecular beam can be selected and bunches of state-selected molecules with a computer-controlled (calibrated) velocity and with a narrow velocity distribution, corresponding to translational temperatures as low as a few mK, can be produced [1]. Slow bunches of molecules can subsequently be loaded in an electrostatic trap [2].

In the summer of last year, a new generation molecular beam deceleration and trapping machine, designed such that a large fraction of the molecular beam pulse can be slowed down and trapped, has become operational. We will report on the deceleration and electrostatic trapping of ground state OH radicals. Depending on the details of the trap loading sequence, typically 10^5 OH ($X^2\Pi_{3/2}$, $v=0$, $J=3/2$) radicals can be trapped for times up to several seconds at a density of 10^7 - 10^8 mol/cm³ and at a temperature in the 50-500 mK range [3]. The long interaction time afforded by the trap can be exploited to measure lifetimes of long-lived excited states of a molecule. This method is demonstrated and used to measure the infrared radiative lifetime of vibrationally excited OH radicals, thereby benchmarking the Einstein *A*-coefficients in the Meinel system of OH [4].

The poster will present a detailed description of the operation mechanism of the molecular beam deceleration and trapping machine. The prospects that these decelerated molecular beams offer for collision and reaction studies will be discussed.

References

1. H.L. Bethlem, G. Berden and G. Meijer, Phys. Rev. Lett. **83**, 1558 (1999).
2. H. L. Bethlem, G. Berden, F.M.H. Crompvoets, R.T. Jongma, A.J.A. van Roij and G. Meijer, Nature **406**, 491 (2000).
3. S.Y.T. van de Meerakker, P.H.M. Smeets, N. Vanhaecke, R.T. Jongma and G. Meijer, Phys. Rev. Lett. **94**, 023004 (2005).
4. S.Y.T. van de Meerakker, N. Vanhaecke, M.P.J. van der Loo, G.C. Groenenboom and G. Meijer, Phys. Rev. Lett. **95**, 013003 (2005).

Accumulating Stark-decelerated NH radicals in a magnetic trap

Steven Hoekstra, Joop J. Gilijamse, Nicolas Vanhaecke, Wieland Schöllkopf,
Sebastiaan Y.T. van de Meerakker and Gerard Meijer

We have recently demonstrated that our new generation molecular beam deceleration and trapping machine can be used to produce samples of trapped free radicals like OH. To be able to study molecular interactions and collective effects in these trapped cold molecular gases, the phase-space density (defined as the number of molecules per unit volume and per unit momentum space) needs to be increased. Accumulation of molecules from successive deceleration cycles in the trap would be the ideal method for this. However, increasing the phase-space density is not possible when only conservative forces are applied (Liouville's theorem); simply opening the trap to allow molecules from the next deceleration cycle to enter can not be performed without losing or heating the molecules that are already stored.

On this poster we will present a novel scheme that we intent to apply to re-load polar molecules in a trap, to circumvent this fundamental obstacle. This scheme will enable large densities of cold molecules, in particular NH and ND radicals, to be accumulated in a magnetic trap. The essence of the method is that we decelerate and stop these molecules, after they are prepared in a long-lived electronically excited state, using their interaction with electric fields. By applying an intense laser-field we then optically pump the NH radicals on a spin-forbidden transition to another electronically excited state, from where they decay via spontaneous emission to their electronic ground state. In their electronic ground state the NH and ND radicals can be readily trapped in inhomogeneous magnetic fields. The laser-induced spontaneous decay thus provides a unidirectional path to load the magnetic trap, in which molecules can then be accumulated [1]. Once the number density in the trap is high enough, various cooling schemes will be explored to further increase the phase-space density. The NH/ND radical has very promising properties both for evaporative cooling (the selective boiling off of the hottest trapped particles) and for direct laser cooling.

The two crucial steps for this project, namely (i) the production of a pulsed beam of NH radicals in the metastable $a^1\Delta$ state and (ii) the optical pumping of the NH radicals on the (never previously observed!) $A^3 \leftarrow a^1\Delta$ transition, have both been demonstrated, and a detailed spectroscopic analysis of the rotational line-intensities on this spin-forbidden transition has been undertaken [2]. More recently, we have also decelerated the metastable NH radicals in our new beam machine, and a quadrupole magnetic trap, to be mounted directly behind the Stark-decelerator, has been constructed and tested.

References

1. S.Y.T. van de Meerakker, R.T. Jongma, H.L. Bethlem and G. Meijer, Phys. Rev. A **64**, 041401(R) (2001).
2. S.Y.T. van de Meerakker, B.G. Sartakov, A.P. Mosk, R.T. Jongma and G. Meijer, Phys. Rev. A **68**, 032508 (2003).

A sectional electrostatic storage ring for neutral molecules

Cynthia E. Heiner, Hendrick L. Bethlem, David Carty and Gerard Meijer

An impressive amount of control over neutral molecules using electromagnetic fields has been demonstrated in recent years, offering unique possibilities for various experiments aimed at unravelling molecular properties and interactions. Among these advancements is an electrostatic storage ring for neutral molecules [1]. A ring has the innate advantage of making the molecules interact repeatedly with either the electric fields and/or other molecules, at very well-defined times and locations. The flexibility of the ring, however, has not yet been fully exploited. The prototype electrostatic storage ring had the geometry of an electrostatic hexapole focuser, bent in the shape of a torus. In this toroidal trap, bunches of molecules were confined in circular orbits, but there was no possibility to keep the molecules together tangentially; the molecules gradually spread out until they filled the entire ring.

Control over the velocity of the packet of molecules inside the storage ring, e.g. the ability to maintain a high number density of molecules per bunch, is crucial for future collision studies. A sectional storage ring allows for a bunching scheme to counteract the spreading out of the packet of molecules along the ring [2], similar to bunching schemes used in charged particle storage rings. Moreover, a sectional storage ring offers the possibility of designating certain segments to perform specific tasks, e.g. optimized for injection, detection, or bunching.

On the poster we will present the first results that have been obtained with our sectional storage ring, which consists out of two hexapole half-rings. For these experiments, a packet of deuterated ammonia molecules in a single rovibrational state is decelerated in a Stark-decelerator to laboratory velocities in the 80 - 100 m/s range. Prior to entering the ring, the longitudinal velocity spread of the molecules is reduced with a buncher to less than 1 m/s, corresponding to a translational temperature of less than 1 mK in the moving frame. Hexapoles on either side of the buncher are used to shape the transverse velocity distribution of the molecules for optimum coupling into the ring. It is experimentally demonstrated that this injection beam-line also enables the simultaneous production of two decelerated and longitudinally cooled packets of molecules with different velocities, and that both of these packets can subsequently be coupled into the storage ring. The most recent results on the re-bunching of the packet of molecules inside the storage ring, along with the respective simulations, will be presented.

References

1. F.M.H. Crompvoets, H.L. Bethlem, R.T. Jongma and G. Meijer, *Nature* **411**, 174 (2001).
2. F.M.H. Crompvoets, R.T. Jongma, H.L. Bethlem, A.J.A. van Roij and G. Meijer, *Phys. Rev. Lett.* **89**, 093004 (2002); F.M.H. Crompvoets, H.L. Bethlem and G. Meijer, *Adv. in At. Mol. Opt. Phys.* **52**, Chapter 5 (2005).

A molecular fountain clock

Hendrick L. Bethlem, Wim Ubachs* and Gerard Meijer

Frequency is the most accurately measurable quantity in physics. High-resolution spectroscopic measurements on atoms and molecules therefore serve as stringent tests of various fundamental physics theories. Ultimately, the resolution of any spectroscopic experiment is limited by the interaction time between the particles that are to be examined and the measuring device, due to the limited size of the interaction region in combination with the non-zero velocity of the examined particles. Obviously, the only two ways to increase the interaction time are to either increase the size of the interaction region or to decelerate, or even trap, the particles. The former has been most successfully implemented in Ramsey-type experiments. In the case of atoms, samples of trapped atoms, either confined "physically" (as in the H-atom maser) or by electro-magnetic fields, as well as Zeeman-slowed beams and atomic fountains have been used for high-resolution spectroscopy. We have recently demonstrated the use of Stark-decelerated molecular beams for high-resolution spectroscopy in a proof-of-principle experiment [1].

In this project, performed in collaboration with the Laser Centre at the Free University of Amsterdam, The Netherlands, we intent to further increase the obtainable spectral resolution by several orders of magnitude by setting up a molecular fountain clock. In this device a beam of molecules is decelerated and cooled using a Stark-decelerator and a buncher, and the slow molecules are subsequently directed upwards. The upward velocity will be such that the molecules fly upwards some 30 cm before they will fall back under gravity, thereby passing a microwave cavity twice; as they move up and as they fall down. The effective interrogation time in such a scheme includes the entire flight time between the two traversals through the driving field and is typically half a second. This long interrogation time allows for a very high accuracy.

One of the prime molecules that will be investigated is ammonia, in its various isotopomeric forms. The frequency of the microwave transition in ammonia is a measure for the rate at which the protons tunnel through the barrier between the two equivalent configurations of the molecule and is exponentially dependent on the ratio of the proton mass to the electron mass. The inversion frequency is therefore a very sensitive probe for a possible variation of this ratio.

On the poster we will present a detailed design of the molecular beam machine with the molecular fountain. The anticipated signal intensities and the expected spectroscopic accuracy as deduced from three-dimensional trajectory calculations will be discussed.

Reference

1. J. van Veldhoven, J. Küpper, H.L. Bethlem, B. Sartakov, A.J.A. van Roij and G. Meijer, *Eur. Phys. J. D* **31**, 337 (2004).

* Laser Centre, Free University of Amsterdam, Amsterdam, The Netherlands

Decelerating and trapping polar molecules on a chip

Samuel Meek, Horst Conrad, Hendrick L. Bethlem and Gerard Meijer

By utilizing the forces that polar molecules experience in inhomogeneous electric fields, a variety of molecular-optical elements have been experimentally demonstrated. In almost all experiments performed thus far, the dimensions used for the various elements are rather large, with electrodes typically being several mm apart, implying that voltages of tens of kV need to be applied to reach the required high electric fields. We have recently demonstrated that by applying modest voltage differences to micrometer-sized gold electrodes, deposited on a sapphire substrate, equally high electric fields to manipulate polar molecules can be produced. In particular, we have constructed a switchable micro-structured electrostatic mirror for polar molecules, which we have used for normal incidence reflection of a beam of ammonia molecules [1]. The large electric field gradients that can be produced in these micro-structured elements offer great prospects for a variety of molecular manipulation tools, including lenses, mirrors, guides, conveyor belts, decelerators, storage rings and traps, all integrated on a compact surface area.

In this project we plan to construct and demonstrate a decelerator and an electrostatic trap, using a periodic array (periodicity 40 μm) of micro-structured linear electrodes (width 10 μm ; length up to 10 mm) deposited on an approximately 40-mm-long planar insulator substrate. By applying appropriate voltages to the various electrodes, the superposition of oppositely directed electric fields results in local electric field minima some 30 μm above each third electrode, i.e. with a periodicity of 120 μm . The depth of each electric field minimum is about 20 kV/cm in the plane of the electrodes and 4 kV/cm in the perpendicular direction. This electric field minimum can be moved continuously in perpendicular direction, and in the plane above the electrodes by smoothly varying the voltages that are applied to the electrodes. Polar molecules in low-field-seeking quantum states can be confined, slowed down and eventually trapped in these travelling electric field minima, provided that their translational energy in the moving frame is sufficiently low; typically, it has to be below 10 mK. To be spatially captured in the travelling electric field minima, the molecules must initially be within a tube-like region approximately 5-10 μm in diameter and up to 10 mm in length. One complication is that the electric field minimum experiences a slight displacement of about 1 μm in the direction perpendicular to the plane of the electrodes while moving across the electrodes. Because of the non-harmonic shape of the potential well, this causes a coupling of the motion in these two directions, and this can, depending on the initial phase-space position of the molecules, lead to loss of molecules from the potential minima.

Experiments will be performed using a pulsed beam of laser-prepared metastable CO ($a^3\Pi_1$, $v=0$, $J=1$) molecules. The CO molecules, which have a radiative lifetime of 3.7 ms, will be decelerated from their original velocity of around 300 m/s to a standstill in a fraction of a ms, and they can subsequently be trapped and observed on the chip via spatially resolved fluorescence imaging. On the poster, the experimental setup is described in detail, and two-dimensional trajectory calculations are presented.

Reference

1. S.A. Schulz, H.L. Bethlem, J. van Veldhoven, J. Küpper, H. Conrad and G. Meijer, *Phys. Rev. Lett.* **93**, 020406 (2004).

Alternate gradient focusing and deceleration of a beam of large molecules

Kirstin Wohlfart, Frank Filsinger, Hendrick L. Bethlem, Jochen Küpper and Gerard Meijer

Polar molecules in low-field seeking states are now almost routinely decelerated in our laboratory using a Stark decelerator. It would be a major advantage if that would be possible for molecules in high-field seeking states as well, if only because the absolute ground state of any molecule is a high-field seeking state. In particular, this would make large polar molecules, for which all rotational states are practically high-field seeking due to their small rotational constants and their correspondingly high density of states, amenable for deceleration and trapping experiments. It might appear straightforward to apply the electric field deceleration method to molecules in high-field seeking states by simply letting the molecules fly out off, instead of into, regions of a high electric field. For the motion of the molecules in the forward direction, this is indeed true. However, since Maxwell's equations do not allow for a maximum of the electric field in free space, e.g. on the molecular beam axis, transverse stability cannot be maintained easily; molecules in high-field seeking states have the tendency to crash into the electrodes, where the electric fields are the highest.

The same situation is encountered in charged particle accelerators where this problem has been resolved by applying the alternate gradient (AG) focusing method. This principle can be applied to polar molecules when using electrostatic dipole lenses. These lenses focus the molecular beam in one direction but simultaneously defocus the beam in the orthogonal direction. By alternating the orientation of these lenses, an electric field geometry with an overall focusing effect in both directions can be created. By switching these lenses on and off at the appropriate times, AG focusing and deceleration of a molecular beam can be achieved simultaneously [1,2].

Earlier this year, a dedicated AG decelerator molecular beam machine has become operational in our laboratory. With this machine we aim to decelerate large poly-atomic molecules like benzonitrile, as well as different conformational structures of amino-acids like, for instance, tryptophan. The AG decelerator has a modular design, and at present only the first (out of three) unit of the decelerator, consisting out of 27 electric field stages, is in use. First test experiments have been performed on the focusing and deceleration of metastable CO molecules. More recently, focusing and deceleration of benzonitrile in its lowest rotational state has been demonstrated.

For the quantum state selective detection of benzonitrile and other large molecules laser induced fluorescence detection using a newly installed cw narrowband laser system is applied. Individual rovibronic transitions of benzonitrile molecules are recorded with a linewidth of about 10 MHz shortly after the molecules exit the AG decelerator. The time-of-flight distributions of benzonitrile molecules in individual quantum states are obtained in real-time by keeping the laser frequency in resonance and by recording the laser induced fluorescence signal using photon counting techniques.

References

1. H.L. Bethlem, A.J.A. van Roij, R.T. Jongma and G. Meijer, *Phys. Rev. Lett.* **88**, 13003 (2002).
2. M.R. Tarbutt, H.L. Bethlem, J.J. Hudson, V.L. Ryabov, V.A. Ryzhov, B.E. Sauer, G. Meijer and E.A. Hinds, *Phys. Rev. Lett.* **92**, 173002 (2004).

An AC electric trap for molecules in high-field seeking states

Jacqueline van Veldhoven, Hendrick L. Bethlem, Melanie Schnell and Gerard Meijer

During the last years, trapping of molecules using optical fields, magnetic fields and electric fields has been experimentally demonstrated. In the largest and deepest traps that can be realized, traps created by static inhomogeneous magnetic and/or electric fields, polar molecules can be confined when they are in low-field seeking quantum states. There is a special interest in these polar molecules, as they are promising for a variety of fundamental physics studies and applications. For most of these investigations, however, trapping of molecules in high-field seeking states is required. For instance, only when polar molecules are trapped in their absolute ground-state, which is high-field seeking for any molecule, increasing the phase-space density via evaporative cooling is expected to be possible; the strong dipole-dipole interaction between polar molecules is predicted to lead to high trap loss rates due to inelastic collisions for most molecules in low-field seeking states, thereby hampering the evaporative cooling process. Furthermore, when heavier diatomic molecules, e.g., those that are important for measurements on the electric dipole moment of the electron, or biomolecules are to be trapped, a trap for molecules in high-field seeking states is the only viable option. In principle, optical trapping can be used for molecules in high-field seeking states, but typical trap depths (≈ 1 mK) and trapping volumes (10^{-5} cm³) are then rather small, however [1].

Creating a maximum of the static electric field in free space in three dimensions, which would allow trapping of molecules in high-field seeking states, is fundamentally impossible. In two dimensions such a field maximum can be created. In a cylindrically symmetric geometry, for instance, a static electric field can be made with a maximum in the radial direction and a minimum in the axial direction, or vice versa. Switching between these two saddlepoint configurations results in a field that is alternately exerting a focusing and a defocusing force in each direction for molecules in high-field (and low-field) seeking states. At the right switching frequency the overall effect is focussing, and confinement in three dimensions can thus be obtained.

We here report on the trapping of ammonia molecules in both high-field and low-field seeking states in such a novel AC electric trap. For ground state ammonia molecules the depth of the AC electric trap is about 10 mK, and the trapping volume is about 20 mm³. We have studied the stability of the AC electric trap, which really is the equivalent of a Paul trap for charged particles, as a function of switching frequency, and we have characterized the spatial distribution and the temperature of the trapped cloud of molecules [2].

References

1. R. Grimm, M. Weidemüller and Y.B. Ovchinnikov, *Adv. At. Mol. Opt. Phys.* **42**, 95 (2000).
2. J. van Veldhoven, H.L. Bethlem and G. Meijer, *Phys. Rev. Lett.* **94**, 093001 (2005).

A microwave trap for molecules in their absolute ground-state

Melanie Schnell, Peter Lützow, Jacqueline van Veldhoven and Gerard Meijer

Complementary to the project on the development of an AC electric trap for molecules in high-field seeking states, we have started a project on the development of a large and deep ‘optical’ trap for ground-state molecules, using near-resonant microwave radiation. In this case, molecules in high-field seeking states will be trapped in the amplitude maximum of the standing wave microwave field in an open Fabry-Perot type resonator. For such a trap the depth is determined by the dipole moment of the molecule, by the detuning of the trapping frequency from the molecular resonance frequencies and by the strength of the microwave field. Since very small detunings are possible and since microwave amplifiers up to several kW are commercially available, trap depths of about 0.1-1 K are anticipated [1].

In our experimental approach, we plan to load molecules into the microwave trap with a Stark-decelerator, and we will bring the molecules to a near standstill at the centre of the resonator using an electrostatic mirror. A weak, resonant, microwave field will then be used to optically pump the slow molecules to the high-field seeking state, after which the strong, detuned, microwave field for trapping will be abruptly switched on. The molecule that we plan to use for testing of the microwave trap is the NH_3 molecule, which appears to be an ideal candidate for various reasons. First, we have extensive experience with producing and detecting decelerated beams of (various isotopomers of) ammonia. In these decelerated beams only the low-field seeking hyperfine levels of the upper component of the $|J,K\rangle = |1,1\rangle$ inversion doublet are populated. Second, there is a strong inversion transition around 24 GHz for NH_3 , and this transition frequency is far removed from the frequencies from all other possible transitions that can originate from the $|J,K\rangle = |1,1\rangle$ level. Therefore, the inversion doublet can be considered as an isolated two-level system. Third, the transition frequency of around 0.8 cm^{-1} implies that the intensity maxima of the microwave field in the resonator will be some 6 mm apart, and that the actual trapping volume will be about $(2 \text{ mm})^3$. This trapping volume is almost perfectly matched to the volume of the decelerated packet of molecules at the exit of the decelerator. The only slight disadvantage of using NH_3 as a test molecule is that in the 24 GHz region microwave amplifiers are less readily available.

A crucial element in this project is the design of the electrostatic mirror, which requires the mounting of electrodes as close as possible to the axis of the microwave cavity without significantly deteriorating the Q-factor of the cavity too much. Design studies of this electrostatic mirror as well as test experiments indicate that this requirement can indeed be fulfilled. On the poster, the proposed loading, trapping and detection scheme for testing the microwave trap will be detailed. Prospects of the use of the microwave trap for high-resolution spectroscopic studies and for evaporative cooling experiments will be discussed.

Reference

1. D. DeMille, *Eur. Phys. J. D* **31**, 375 (2004).

A quasi-analytic model of a Stark accelerator/decelerator and of an AC electric trap

Koos Gubbels, Monika Schleier-Smith and Bretislav Friedrich

We present (a) a quasi-analytic model of a linear *Stark accelerator/decelerator* for polar molecules in both their low- and high-field seeking states and examine the dynamics of the acceleration/deceleration process and its phase stability; (b) a quasi-analytic model of a *stable anharmonic AC trap*.

The requisite time-dependent inhomogeneous Stark field, as implemented in current experiments, is Fourier-represented and the representation used to build a model which encompasses the complete physics of the longitudinal motion in the *Stark accelerator/decelerator* [1]. The electric field is found to consist of a superposition of partial waves with well-defined phase velocities. These phase velocities are $(2n-1)/(2k-1)$ -multiples of a fundamental phase velocity L/T , with $n, k=1, 2, 3 \dots$ and L and T the spatial and temporal periods of the field. The analysis of the acceleration/deceleration dynamics shows that a given wave will "give a ride" to molecules whose velocities are close to the phase velocity of that wave. The dynamics of any such ride is found to be isomorphic with that of the oscillations of a biased pendulum. A packet of molecules can also get a ride by a wave which results from an interference of (mainly adjacent) waves. In this case, the molecules can have velocities which are also even multiples of the fundamental velocity. The general properties of the velocity of molecules in a phase-stable accelerator/decelerator reveal a similarity with a flying accordion [1].

We propose a deep, *stable anharmonic AC trap* for polar molecules in high-field seeking states. A dynamic maximum of electric field strength in free space is produced by switching between vertical and horizontal fields, each produced by a pair of concave electrodes. For concave electrodes, the curvature of the field perpendicular to a given electrode pair exceeds in magnitude the curvature of the field parallel to the pair. This ensures that, within a single switching cycle, the average force attracting molecules in high-field seeking states into the trap in the plane of the electrodes is greater than the force that is pushing them out. Stable trapping along the longitudinal axis is ensured by the fringe fields at either end of the electrode assembly. The key features of the trap are captured by a quasi-analytic model and are compared with the properties of traps made up of harmonic as well as anharmonic fields produced by convex electrodes. Trap depths of about 50 mK/Debye appear feasible. A 2D-version holds the promise of achieving up to 500 mK/Debye.

Reference

1. B. Friedrich, Eur. Phys. J. D **31**, 313 (2004).

Sympathetic cooling of cold molecules by Rb atoms

Sophie Schlunk, Adela Marian, Allard P. Mosk*, Peter Geng, Wieland Schöllkopf
and Gerard Meijer

Cooling and trapping of molecules is considerably more difficult than for atoms, mainly because laser cooling, the work-horse in the field of cold atoms, has not yet been demonstrated for molecules, due to their complex multi-level structure. In addition, cooling a molecular gas by forced evaporation or by sympathetic cooling with atoms, i.e., by using the atoms as a coolant for the molecules, has not been demonstrated at sub-mK temperatures. For efficient sympathetic cooling of molecules with atoms, a sufficiently large ratio (≥ 200) of elastic to inelastic collision rates is needed; inelastic collisions can spoil the thermalization process between the two species, leading to loss of atoms and/or molecules. For most atom-molecule collisions however, the corresponding low-temperature cross-sections can not be predicted by theory because of their extreme sensitivity to details of the, not sufficiently well known interaction potentials.

In this project we will experimentally study cold atom-molecule collisions by overlapping a magnetically trapped cloud of Rb atoms with a cloud of polar molecules confined in an electrodynamic trap. Simultaneous cooling and trapping of atoms and molecules in a single vacuum chamber seems impractical due to the large number of magnetic field coils, electrodes and laser beams required. Therefore, in our approach, atoms and molecules will first be cooled and trapped separately and then the cold atom-cloud will be moved to overlay with the molecular cloud.

A beam of polar molecules (NH_3 , CO^* , OH, NH are all feasible) is decelerated and loaded into an AC electric trap, in which the molecules can be trapped in their lowest energy state. The Rb atoms are cooled in a separate vacuum chamber by a standard magneto-optical trap (MOT) loaded from a Zeeman-slower. After transfer to a magnetic trap and adiabatic compression achieved by increasing the magnetic field, a Rb density on the order of 10^{11} atoms/cm³ and a temperature of about 1 mK are expected. The cold Rb cloud can then be moved into the UHV chamber where the molecules are trapped by mounting the magnet coils on an accurate translation stage [1]. As the trapped atoms are in (magnetically) low-field seeking states, collisions with molecules in which the spin of the Rb atom is changed will release Zeeman energy, and hence, cause trap loss and/or heating, which can be observed by absorption imaging of the Rb atoms.

Reference

1. H.J. Lewandowski, D.M. Harber, D.L. Whitaker and E.A. Cornell, *J. Low Temp. Phys.* **132**, 309 (2003).

* Technical University Twente, Enschede, The Netherlands

Buffer gas loading and magnetic trapping of atoms and molecules

Michael Stoll, Joost M. Bakker, Gerard Meijer and Achim Peters*

Buffer gas loading of molecules into a cryogenic He-filled cell and subsequent magnetic trapping of the thermalized molecules has been proven to be a powerful method for the production of samples of trapped cold molecules; the largest number densities of trapped molecules that have been obtained thus far have been produced via this method [1]. The method is rather generally applicable to paramagnetic species, and has recently been used, for instance, for the study of a variety of rare-earth atoms, magnetically trapped at mK temperatures [2].

We have set up a buffer gas loading and magnetic trapping project in our laboratory to be able to directly compare the performance of this method to that of the Stark-deceleration and AC/DC electric field trapping of molecules. It also provides an alternative to that of the Stark deceleration method which is applicable to a complementary set of molecules. In our present set-up we use a superconducting quadrupole magnet in combination with a ^3He - ^4He dilution refrigerator. From the various methods available for introducing atoms and molecules into the buffer gas cell, we have focused for now on laser ablation of a solid precursor material. Over the last two years the dilution refrigerator setup has been built and the first milestone has been achieved: chromium atoms have been loaded into the magnetic trap at temperatures of ~ 1.5 K and they have been trapped for about ~ 0.5 seconds.

In the coming year we will perform our first experiments aimed at cooling and trapping molecules, with an initial focus on molecules with large magnetic moments. Critical issues in the selection of the best candidate molecule are its production, detection efficiency, and the generally largely unknown, collision properties of the molecules with helium atoms. Once molecules are trapped, their collisional properties will be the first thing to be investigated, as knowledge of these properties is essential for future evaporative cooling studies to reach temperatures in the low mK range. We are considering the possibility to combine the buffer gas loading method with Stark deceleration: a high flux effusive molecular beam can be extracted from the cryogenic cell and this beam can subsequently be decelerated and loaded in an electric or magnetic trap.

References

1. J. D. Weinstein, R. deCarvalho, T. Guillet, B. Friedrich and J. M. Doyle, *Nature* **395**, 148 (1998).
2. C.I. Hancox, S.C. Doret, M.T. Hummon, L.J. Luo and J.M. Doyle, *Nature* **431**, 281 (2004).

*Humboldt Universität zu Berlin, Germany

The transition from coherent to incoherent photoelectron scattering in diatomic molecules: CO versus N₂

Markus Braune, Slobodan Cvejanovic, Oliver Geßner, Rainer Hentges, Sanja Korica, Thoralf Lischke, Georg Prümper, Axel Reinköster, Daniel Rolles, Jens Viefhaus, Uwe Becker, Björn Zimmermann^{*}, Vincent McKoy^{*}, Burkhard Langer[#] and Reinhard Dörner[§]

Recently, some fundamental questions of quantum mechanics have been revisited by macroscopic double-slit experiments: Using polarization filters as *quantum markers* they provide information on which way the photon passes the slits. The original interference pattern is lost and two shifted, bell-shaped curves are observed. However, if that *which-way* information is subsequently *erased* the interference fringes return [1].

We have shown that core electron photoemission of diatomic hetero- and homonuclear molecules is a microscopic quantum marker experiment in momentum space. In analogy to the characteristic features of macroscopic double-slit experiments we see in the case of N₂ for the *gerade* and *ungerade* channels of the N₂:N(1s) photoelectron emission two oscillations with a frequency proportional to the inverse bond length. They are shifted by π with respect to each other and correspond to the π -shifted fringes and anti-fringes in the macroscopic experiment. The contrary is true for the diffraction behaviour of CO. Here, oscillations with a frequency proportional to the inverse bond length are not observed, instead two scattering channels referring to electron emission away from or into the molecule are appearing. They oscillate approximately with twice the inverse bond length's frequency and are also shifted by π , pointing to single and double photoelectron scattering at the neighboring atom in the molecule. The sum of the two resembles exactly the sum of the *g* and *u* oscillations in N₂, again in complete equivalence to the macroscopic experiment. Surprisingly this faster oscillation shows also up in the sum of *g* and *u* photoelectron channels. It arises from the transition of coherent two-center scattering to incoherent one-center scattering above 50 eV, where the de Broglie wavelength of the photoelectron becomes shorter than twice the bond length. In contrast to this dynamic core hole localization we have shown that isotope substitution in the N₂ molecule leads to partial static core hole localization due to the inversion symmetry violation experienced by the molecule through "asymmetric" vibrations [2]. Both localization processes may be considered as a decoherence process as observed in macroscopic two-slit experiments with atoms and fullerenes.

References

1. S.P. Walborn, M.O. Terra Cunha, S. Padua and C.H. Monken, Phys. Rev. A **65**, 033818 (2002); ditto, American Scientist **91**, No. 4, 336 (2003).
2. D. Rolles, M. Braune, S. Cvejanovic, O. Geßner, R. Hentges, S. Korica, B. Langer, T. Lischke, G. Prümper, A. Reinköster, J. Viefhaus, B. Zimmermann, V. McKoy and U. Becker, Nature (in press).

^{*}California Institute of Technology, Pasadena, CA, USA.

[#] Max-Born-Institut für Nichtlineare Optik und Kurzzeitspektroskopie, Berlin, Germany.

[§] Institut für Kernphysik, Universität Frankfurt, Germany.

New phenomena in valence and inner-shell photoionization of fullerenes

Axel Reinköster, Sanja Korica, Markus Braune, Rainer Hentges, Daniel Rolles, Jens Viefhaus, Uwe Becker, Burkhard Langer*, Mauro Stener[#] and Piero Decleva[#]

The oscillation in the partial cross sections of C_{60} carries structural information on the cage size and the delocalized electron distribution [1]. Extended measurements in the gas phase and in an amorphous solid exhibit the same oscillatory structure for the photoelectron intensity ratio between the HOMO and HOMO-1 level [2]. This points to a very similar electronic structure in both phases of C_{60} . The same experiments for C_{70} evidence an interesting and unexpected difference between the two phases: The intensity ratio of HOMO and HOMO-1 exhibits a distinct offset for the gas phase measurements compared to the solid state data. Theoretical calculations performed within the LCAO approximation [3] reveal good agreement for both data sets, if one assumes, that in the *gas* phase the (+16a')-orbital is unoccupied. For *solid* C_{70} on the contrary this LUMO structure becomes filled from the substrate due to the small HOMO-LUMO gap. This result demonstrates, how strong substrate-fullerene interaction can become, if electron transfer is energetically possible.

The (multiple) ionization and the subsequent fragmentation of gas phase C_{60} was studied with synchrotron radiation covering a large photon energy range (26–130 eV) [4]. C_{60}^{q+} ions ($q=1-3$) and several smaller C_{60-2m}^{q+} fragments are formed in the interaction. Our attention was especially focused on the fragmentation dynamics, which probably proceeds via emission of neutral C_2 particles. In addition to 'normal' (non-coincident) electron and ion time-of-flight spectroscopy we investigated this topic with the help of an electron-ion-coincidence measurement. Here, different fragments, like C_{58}^{2+} or C_{56}^{2+} , can already be identified by their outgoing electrons, although the fragmentation takes place on a longer time scale than the ionization. Furthermore, our results indicate for the majority of the events such a mechanism: a fast electronic excitation followed by an energy transfer to the vibrational modes and a subsequent (successive) evaporation of C_2 fragment(s). However, certain fragmentation events originate from particular two-electron ejection processes leading to distinct bond breaking.

References

1. A. Rüdell, R. Hentges, U. Becker, H.S. Chakraborty, M.E. Madjet and J.M. Rost, Phys. Rev. Lett. **89**, 125503 (2002).
2. S. Korica, D. Rolles, A. Reinköster, B. Langer, J. Viefhaus, S. Cvejanovic and U. Becker, Phys. Rev. A **71**, 013203 (2005).
3. P. Decleva, S. Furlan, G. Fronzoni and M. Stener, Chem. Phys. Lett. **348**, 363 (2001).
4. A. Reinköster, S. Korica, G. Prümper, J. Viefhaus, K. Godehusen, O. Schwarzkopf, M. Mast and U. Becker, J. Phys. B: At. Mol. Opt. Phys. **37**, 2135 (2004).

* Max-Born-Institut für Nichtlineare Optik und Kurzzeitspektroskopie, Berlin, Germany.

[#] Dipartimento di Scienze Chimiche, Università di Trieste, Trieste, Italy.

Molecular double Auger decay studied by electron time-of-flight coincidence spectroscopy

Jens Viefhaus, Markus Braune, Sanja Korica, Axel Reinköster, Daniel Rolles
and Uwe Becker

Double Auger decay represents a process in close analogy to double photoionization [1] that can only be described in an atomic model properly including electron correlations. In contrast to the normal Auger lines formed by electrons of discrete energies, the energy spectra in direct double Auger decay show a continuous intensity distribution, where the sum of the kinetic energies of the two electrons equals the excess energy. It was shown that electron time-of-flight coincidence spectroscopy allows to disentangle direct double Auger transitions from Auger cascade processes [2,3]. First exploratory investigations followed by more systematic studies were performed for all rare gases and a variety of small molecules. They all show that double Auger emission is very general and by no means a negligible process, which often contributes a 10–20% fraction to the total Auger yield. In the case of Ar $2p$ inner-shell ionization at a photon energy of 270 eV the double Auger process is responsible for about 20% of the observed Auger electron intensity [2]. This rather high yield for a higher order process stimulated further studies on other targets namely small molecules and fullerenes. The coincidence study for the case of SF₆ molecules, showed clear signatures for double Auger decay into triply charged SF₆³⁺ final states populated after S($2p$) and F($1s$) core ionization. This and other results for N₂ after N($1s$) ionization show that the double Auger decay is not restricted to atoms, but it is also of importance in the case of small molecules. We furthermore extended the study by using the fullerene C₆₀ as a prototype of a large molecule. The energy and angular distributions of the emitted electrons of different atoms, molecules and fullerenes will be presented. These allow to obtain information on the electron correlations giving rise to the double Auger process particularly with respect to the symmetry of the associated two-electron continuum state. These studies may open a new field of Auger spectroscopy on highly correlated materials in the same way Auger spectroscopy served as a probe of "single particle dominated" solid matter in the past.

References

1. R. Dörner, V. Mergel, O. Jagutzki, L. Spielberger, J. Ullrich, R. Moshhammer and H. Schmidt-Böcking, Phys. Rep. **330**, 95 (2000).
2. J. Viefhaus, S. Cvejanovic, B. Langer, T. Lischke, G. Prümper, D. Rolles, A.V. Golovin, A.N. Grum-Grzhimailo, N.M. Kabachnik and U. Becker, Phys. Rev. Lett. **92**, 083001 (2004).
3. J. Viefhaus, A.N. Grum-Grzhimailo, N.M. Kabachnik and U. Becker, J. Electron Spectrosc. Relat. Phenom. **141**, 121 (2004).

Chirality and structure in adsorbed layers: Tartaric acid on Cu(110)

Thorsten U. Kampen, Jeong Won Kim^{*}, Jan Hugo Dil, Philipp M. Schmidt,
Karsten Horn, Manfred Parschau[#] and Karl-Heinz Ernst[#]

In heterogeneous catalysis of chiral compounds, metal surfaces are often covered with specific chiral molecules to serve as "modifiers" for the preferred synthesis of a particular enantiomer. Hence the identification of the chiral nature of molecules in the adsorbed phase is a desirable goal. However, this has proven difficult; conventional surface science techniques are not directly sensitive to the chiral nature of the adsorbate. Here, we report on the characterization of adsorbed chiral molecules with respect to handedness and chemical composition using circular dichroism in core level photoemission spectroscopy excited with circular polarized x-rays.

In the adsorption of different enantiomers of tartaric acid Cu(110), two different phases are observed, depending on surface coverage: a low coverage bitartrate phase {9 0, 1 2} structure and a high coverage monotartrate phase with {4 1, 2 5} structure. For a given coverage, the LEED patterns of layers consisting out of the (R,R) or (S,S) enantiomers are mirror images of one another. This is a result of the interplay between the molecular structure of the adsorbate and the Cu(110) surface geometry.

The circular dichroism in core level photoemission of tartaric acid adsorbed on Cu(110) changes sign with going from the (R,R) to the (S,S) enantiomer; it is absent for the achiral (R,S) isomer, demonstrating that the dichroism is caused by the chiral molecular environment of the photoionized atoms. These observations complement those from the system butanediol/Si(100) which we had studied earlier, but for which structural information was lacking. We use an in-plane geometry to distinguish the dichroism induced by the chiral center from that of the experimental geometry which may arise even in the case of achiral (e.g. linear) adsorbed molecules.

An intriguing effect takes place in the adsorption of achiral (R,S)-tartaric acid, in that it leads to two-dimensional enantiomorphic structures, observable as mirror domains in LEED. Co-adsorption ("doping") of (R,S)-tartaric acid with small amounts of (S,S)- or (R,R)-tartaric acid, however, suppresses the formation of one enantiomorphic domain and drives the entire monolayer into homochirality.

^{*} Nano-Surface Group, Korea Research Institute of Standards and Science, Korea

[#] EMPA – Institute for Materials Science and Technology, Switzerland

Quantum size effects in self organized thin metal films

Jan Hugo Dil, Thorsten U. Kampen and Karsten Horn

Quantum size effects (QSE) begin to appear as the size of a small object becomes comparable to the de Broglie wavelength of electrons confined in it. These effects can have a profound effect on various nanoscale physical properties, among them the formation of islands of magic or preferred height [1], anomalous oscillations in the direction and magnitude of the Hall effect [2] and oscillations in the superconductivity temperature [3]. The reduced coupling with the substrate makes metal films on semiconductors an attractive field of study. Such epitaxial films, which are indispensable for any QSE study, are more difficult to grow, however. This problem can be overcome by depositing the metal films at sufficiently low substrate temperatures to avoid island growth, followed by an additional gentle annealing.

Our angle-resolved photoemission studies of Pb films grown on Cu(111) show "magic" heights, the occurrence of which is attributed to total energy minimization, i.e. those states in which the energy difference between the highest quantum well state (QWS) and the Fermi level is at maximum are most stable. A similar observation is found for Pb films on single crystalline graphite films. The band structure of these QWS matches with DFT calculations of a free standing Pb slab where the quantized $6p_z$ bands show a free electron-like dispersion with an effective mass (m^*) similar to that of the bulk bands. The situation is totally different for Pb films grown on the $\sqrt{3}\times\sqrt{3}$ reconstructed Pb/Si(111) surface. Here, the $6p_z$ -related quantum well bands show a dispersion with large effective masses ranging from 10 to $3.5 m_e$ (becoming smaller with increasing thickness). In a simple picture, flat bands are directly related to an enhanced localization of the electrons parallel to the surface; however, other aspects of the band structure are in conflict with this picture. A variation of the reflection phase as a function of $k_{||}$ appears equally unlikely, since similar systems do not exhibit this effect. An in-plane localization cannot be attributed to the structural properties of the overlayer, since STM and LEED data indicate an atomically flat film extending over several hundred nanometers. It appears likely that the specific structure of the Pb/Si interface is responsible for the smaller QWS dispersion, since the related system In/Si does not exhibit this effect.

References

1. Z. Zhang, Q. Niu and C. K. Shih, Phys. Rev. Lett. **80**, 5381 (1998).
2. M. Jalochowski, M. Hoffmann and E. Bauer, Phys. Rev. Lett. **76**, 4227 (1996).
3. Yang Guo, Y-F.Zhang, X-Y. Bao,T.-Z. Han, Z. Tang, L.-X. Zhang,W.-G. Zhu, E. G. Wang, Q. Niu, Z. Q. Qiu, J.-F. Jia, Z.-X. Zhao and Q.-K. Xue, Science 306, 1915 (2004).

Department of Physical Chemistry

Poster List

- PC 1 Chaos in activator-inhibitor systems**
M. Eiswirth and A. Senses
- PC 2 Nonautocatalytic oscillators and olfactory response**
A. Senses, M. Eiswirth, J. Reidl, J. Starke, P. Borowski, M. Zapotocky
- PC 3 Are enzymes molecular machines?**
H.-Ph. Lerch, V. Casagrande, Y. Togashi, R. Rigler, A. S. Mikhailov
- PC 4 Corrosion onset as a nonequilibrium critical phenomenon**
L. Organ, J. L. Hudson, A. S. Mikhailov
- PC 5 Imaging metastable pitting corrosion on stainless steel**
M. Dornhege, C. Punckt, H. H. Rotermund
- PC 6 Quantitative measurement of the deformation of ultra-thin platinum foils during adsorption and reaction of CO and O₂**
C. Punckt, P. Sanchez Bodega, J. Wolff, H. H. Rotermund
- PC 7 Combining microstructures and local addressability in a surface chemical reaction**
C. Punckt, Q. Liang, I. G. Kevrekidis, H. H. Rotermund
- PC 8 Hydroxide adsorption at Ag(hkl) electrodes using cyclic voltammetry, in situ second harmonic generation, and ex situ electron diffraction**
B. Pettinger, S. I. Horswell, A. I. N. Pinheiro, E. R. Savinova, M. S. Zei
- PC 9 Tip-enhanced Raman spectroscopy**
B. Pettinger, K. F. Domke, J. Steidtner, D. Zhang

Chaos in Activator-Inhibitor Systems

M. Eiswirth and A. Senses

Introduction

Chaotic behaviour has been observed in a large number of systems, including many chemical reactions. The aim of the present study is to systematically determine the mechanistic basis of chaos in chemical oscillators. The starting point are minimal oscillators containing exactly one positive feedback loop (autocatalysis, the species on which are referred to as activators) and one negative loop containing at least one additional species (referred to as inhibitor).

Results

Minimal activator-inhibitor systems have been extended using one additional species causing exactly one additional feedback loop. There are a total of 8 possibilities, namely positive or negative 2-loops consisting of the additional species and the activator or inhibitor, as well as four 3-loops with different directions and signs containing all three species. The type of feedback loops can readily be seen in the Jacobian matrix. All such combinations exhibited period doubling and chaos, hereby the systems can be classified into 2 groups depending on where the chaotic region is located in the 2-parameter bifurcation diagrams. The numerical results can be rationalized in terms of Shil'nikov orbits and the codimension-2 points from which these emerge (Takens-Bogdanov- resp. Guckenheimer-Gavrilov points). Application to realistic systems is pointed out using the oxidase-peroxidase oscillator.

Nonautocatalytic Oscillators and Olfactory Response

A. Sensse, M. Eiswirth, J. Reidl*, J. Starke*, P. Borowski**, M Zapotocky**

Introduction

In olfactory cilia, intracellular calcium oscillations have been observed which are not based on any autocatalysis such as calcium-induced calcium release (CICR), but seem to be based on direct negative regulation of cyclic nucleotide-gated channels [1,2].

Results

Using stoichiometric network analysis [3] we clarified the conditions under which nonautocatalytic oscillations can arise in (bio)chemical reaction networks. The results were applied to oscillations in cilia in a model including opening of Ca channels by cAMP, active Ca pumps and blocking of channels by Ca/calmodulin. Then a numerical 4-variable model was developed which is in quantitative agreement with experiment, both with respect to oscillations and to fast adaptation of the olfactory response. The resulting system is refractory (adaptation) without exhibiting excitability, and compared to an earlier system (CO oxidation on Pt), which can show excitability without a refractory zone [4].

References

1. J. Reisert and H.R. Matthews, *J. Physiology* **535**, 637 (2001)
2. T. Leinders-Zufall, C.A. Greer, G.M. Shephard, and F. Zufall, *J. Neurosci.* **18**, 5630 (1998)
3. M. Eiswirth, J. Bürger, P. Strasser, and G. Ertl, *J. Phys. Chem.* **100**, 19118 (1996)
4. M. Bär and M. Eiswirth, *Phys. Rev. E* **48**, 1635 (1993)

** , Institut für Angewandte Mathematik, Univ. Heidelberg

** MPI für Physik komplexer Systeme, Dresden

Are Enzymes Molecular Machines?

H.-Ph. Lerch*, V. Casagrande, Y. Togashi, R. Rigler**, A. S. Mikhailov

Introduction

Enzymes are single-molecule protein catalysts. In the classical Michaelis-Menten view of an enzyme, enzymic action is localized in its active center, while the rest of the protein merely plays a role of a support. Modern experimental evidence suggests that catalytic turnover cycles of an enzyme may include slow functional conformational motions involving the whole protein. Such ordered internal motions, initiated by ligand binding, are not aimed to perform mechanical work, as in molecular motors. Instead, their function consists in transporting a substrate to an active center inside a molecule or in gradually approaching a molecular configuration favorable for a chemical catalytic conversion event.

Single-molecule experiments based on fluorescence correlation spectroscopy (FCS) provide a unique opportunity to monitor catalytic turnover cycles of individual enzyme molecules. Because of their complexity, such experiments have so far been performed only for several different enzymes. Applying special statistical analysis, we have earlier shown that functional conformational motions are present in the enzyme horseradish peroxidase¹.

If enzymes operate as cyclic molecular machines and are allosterically activated or inhibited by their own products, a population of enzyme molecules in a micrometer-size fluid reactor can undergo a spontaneous transition to a coherent regime where turnover cycles of individual enzymes are strongly correlated (see ² and references therein).

Results

Re-examining statistical data of well-known single-molecule FCS experiments for the enzyme cholesterol oxidase³, we have found that functional conformational motions were also involved in a turnover cycle of this enzyme and have constructed a theoretical model of its single-molecule dynamics⁴. Fully stochastic numerical simulations and mean-field modeling of chemical reactions in extended spatial arrays of allosterically interacting enzymes are furthermore performed. They reveal that synchronization of single turnover cycles can spontaneously in such molecular arrays and various wave patterns of coherent enzymic activity can be observed.

References

1. H.-Ph. Lerch, A. S. Mikhailov, B. Hess, Proc. Natl. Acad. Sci. **99**, 15410 (2002)
2. A. S. Mikhailov, B. Hess, J. Biol. Phys. **28**, 655 (2002)
3. H. P. Lu, L. Xun, X. S. Xie, Science **282**, 1887 (1998)
4. H.-Ph. Lerch, R. Rigler, A. S. Mikhailov, Proc. Natl. Acad. Sci. **102**, 10807 (2005)

* Present address: Department of Chemistry, Stanford University, USA.

** Institute of Imaging and Applied Optics, Swiss Federal Institute of Technology, Lausanne, Switzerland, and Department of Medical Biochemistry and Biophysics, Karolinska Institute, Stockholm, Sweden.

Corrosion Onset as a Nonequilibrium Critical Phenomenon

L. Organ*, J. L. Hudson*, A. S. Mikhailov

Introduction

Corrosion in stainless steels develops abruptly, as temperature, salt concentration or applied potential are increased. Its onset is accompanied by the formation of metastable pits, i.e., microscopic corrosion seeds of a size of a micrometer that remain active for about a second and then undergo passivation. Each pit leads to a small spike in the total electric current. The traditional view on corrosion onset is that it proceeds through stabilization of individual pits.

About ten years ago, we have suggested¹ that the principal role in the sudden corrosion onset is rather played by interactions between metastable pits, when each pits enhances the probability of appearance of a next pit on the surface. In the first phenomenological model¹, spatial effects were neglected and only temporal memory of the stochastic pitting process was taken into account. The predictions of this model were consistent with the results of statistical analysis of the experimental data series for the electric current². Subsequently, a more realistic model of corrosion onset, taking into account release and diffusion of aggressive species in a pit and weakening of the protective oxide layers in its neighbourhood, has been proposed and experiments on corrosion in spatially coupled electrode arrays were performed³.

Results

Detailed numerical simulations have been performed using the stochastic spatially extended model. They have revealed that, because of a positive feedback in this system, the corrosion onset effectively represents an autocatalytic explosion in the number of metastable pits^{4,5}. Thus, it can be viewed as a nonequilibrium cooperative critical phenomenon. The transition to the regime of high pitting activity proceeds through propagation of the fronts, similar to the waves of spreading infection. The stabilization of pits occurs only at a later stage, when the whole surface is highly active. These theoretical predictions were tested and confirmed⁴ in specially designed optical microscopy experiments that were carried in our Department in a close contact between the experimental and the theoretical groups. The gained new understanding of corrosion onset in stainless steels opens a way for better control and suppression of corrosion processes.

References

1. B. Wu, J. R. Scully, J. L. Hudson, A. S. Mikhailov, *J. Electrochem. Soc.* **144**, 1614 (1997)
2. T. T. Lunt, S. T. Pride, J. R. Scully, A. S. Mikhailov, J. L. Hudson, *J. Electrochem. Soc.* **144**, 1640 (1997)
3. T. T. Lunt, J. R. Scully, V. Brisamarello, A. S. Mikhailov, J. L. Hudson, *J. Electrochem Soc.* **149**, 163 (2002)
4. Ch. Punckt, M. Bölscher, H. H. Rotermund, A. S. Mikhailov, L. Organ, N. Budiansky, J. R. Scully, J. L. Hudson, *Science* **305**, 1133 (2004)
5. L. Organ, A. S. Mikhailov, J. L. Hudson, *Electrochem. Acta* (2005) (accepted)

* Department of Material Science and Engineering, University of Virginia, USA.

Imaging Metastable Pitting Corrosion on Stainless Steel

M. Dornhege, C. Punckt, H. H. Rotermund

Introduction

Stainless Steel is protected against corrosion by means of an oxide layer naturally forming in the presence of humidity and oxygen. But this protection may break down locally, especially when exposed to protons and chloride ions. This gives rise to the appearance of individual microscopic metastable pits which are sites having an extent of up to a few micrometers where the surface erodes locally. However, after a few seconds the oxide layer inside the pit rebuilds and the corrosion stops¹. This metastable pitting process is regarded as the onset of pitting corrosion, which can lead to severe damage of the material.

In recent years there has been growing evidence that the metastable pits have spatial and temporal influence on each other, which might be mediated through the release of aggressive ions. These ions weaken the protective oxide layer and thus enhance the nucleation rate of metastable pits. Based on those assumptions a stochastic reaction-diffusion model was developed under the guidance of A. Mikhailov and J. Hudson² (see Poster PC 3). An autocatalytic reproduction of pitting sites with front-like spreading was found in their numerical simulations³. Those results stimulated us to adopt Ellipso-Microscopy for Surface Imaging (EMSI) to the liquid/solid interface and thus to try to observe metastable pitting corrosion *in situ*.

Results

We succeeded to directly visualize different aspects of the corrosion process by applying two complementary imaging methods simultaneously. While EMSI was used to detect the weakening and rebuilding of the protective oxide layer, contrast enhanced optical microscopy enabled us to follow the formation and spatial distribution of individual pits⁴. Recently we found an expanding region of a weakened oxide layer accompanied by a succeeding front like spreading of the pit nucleation zone and an exponential growth of the number of pitting sites. Thus, the existence of propagating fronts during metastable pitting corrosion of stainless steel could clearly be proven. The results corroborate our belief that the transition to higher corrosion rates can be explained by an autocatalytic reproduction of individual metastable pits.

References

1. G. S. Frankel, J. Electrochem. Soc. **145**, 2186 (1998)
2. B. Wu, J. R. Scully, J. L. Hudson, A. S. Mikhailov, J. Electrochem. Soc. **144**, 1614, (1997)
3. L. Organ, J. R. Scully, A. S. Mikhailov, J. L. Hudson, Electrochim. Acta, (in Press)
4. C. Punckt, M. Bölscher, H. H. Rotermund, A. S. Mikhailov, L. Organ, N. Budiansky, J. R. Scully, J. L. Hudson, Science **305**, 1133 (2004)

Quantitative measurement of the deformation of ultra-thin platinum foils during adsorption and reaction of CO and O₂

C. Punckt, P. Sanchez Bodega, J. Wolff, H. H. Rotermund

Introduction

An ultrathin Pt-foil with a thickness of 300 nm and 4 mm diameter has a heat capacity of only 10 $\mu\text{J/K}$. Thus, even small amounts of heat deposited within the very thin metal foil cause a significant temperature increase. This effect was used for the microcalorimetric determination of heats of adsorption of different gases on Ni and Pt single crystal surfaces¹⁻². During the adsorption of, for example, CO and O₂ on Pt(110) heat in the order of 200 kJ/mole is released into the metal. If the rim of a Pt(110) single crystal foil is mounted on a substrate, then a temperature difference between the substrate and the foil induced by adsorption and reaction of CO and O₂ can cause thermoelastic stress. This under certain conditions leads to even macroscopic deformations of the metal foil³. It should be possible to measure the amount of heat which is released during the adsorption and/or reaction of CO and O₂ on a catalytic Pt(110)-foil, following the deformation of the foil quantitatively by means of interferometry. Therefore an imaging Michelson-interferometer was set up in order to detect small deformations of the ultrathin Pt catalyst down to 10-20 nm. The catalytic foil was placed in an UHV-chamber equipped with LEED and Ar⁺-sputtering for sample analysis and preparation. The partial pressures of CO and O₂ could be controlled by the computer.

Results

The profile of the Pt(110) foil could be measured with an accuracy of about 10 nm. Adsorption of CO and O₂ causes a clear mechanical response of the Pt-foil. Depending on sample temperature and partial pressures of the reactants fronts and pulses of deformation were found. The system could be calibrated by using continuous and chopped laser light. A change of the optical properties of the catalytic surface in the presence of adsorbates causes difficulties which will be avoided in a future setup.

References

1. N. al Sarraf, J. T. Stuckless, and D. A. King, *Nature* **360**, 243 (1992)
2. A. Stuck, C. E. Wartnaby, Y. Y. Yeo, J. T. Stuckless, N. al Sarraf, D. A. King, *Surf. Sci.* **349**, 229 (1996)
3. F. Cirak, J. E. Cisternas, A. M. Cuitino, G. Ertl, P. Holmes, I. G. Kevrekidis, M. Ortiz, H. H. Rotermund, M. Schunack, J. Wolff, *Science* **300**, 1932 (2003)

Combining microstructures and local addressability in a surface chemical reaction

C. Punckt, Q. Liang*, I. G. Kevrekidis*, H. H. Rotermund

Introduction

The interplay of spontaneous pattern formation and heterogeneities or geometrical boundaries in nonlinear systems is a topic of intense research in many different fields ranging from catalysis to biology¹⁻⁴. Pattern-forming reaction-diffusion systems show a wealth of intrinsic spatiotemporal patterns. However, by using microstructured systems (i. e. systems with obstacles, slits, gratings, channels, labyrinths etc.) it is possible to analyze the individual components of the dynamics in detail both in experiment and theory. We use microlithography to create fixed inert, no-flux, insulating boundaries on a Pt(110) single crystal and observe the evolution of pulse patterns within the remaining reactive structures under excitable conditions during the catalytic oxidation of CO. Additionally, local addressing of surface activity by means of a focussed laser beam allows for controlled initiation of single reaction waves in the experiment and also permits direct control of reaction waves that propagate on the microstructured sample.

Results

Under the condition of low excitability reaction-pulses do not appear in the experiment naturally (i. e. they do not nucleate at system-intrinsic defects) but are none the less still stable. “Artificial” pulses were generated by focussing laser light at defined locations on the microstructured sample thus establishing sufficiently strong temperature heterogeneities for pulse nucleation. The propagation of these pulses was followed, and we found that due to interaction with the geometry of the applied microstructures pulses lost or gained stability. Pulses that had lost stability could be “rescued” by short shots with the laser, complete surface domains could be switched from stable to unstable pulse propagation, and some microstructures showed frequency filtering properties. The experimental findings were accompanied by numerical studies with a well established three-variable model⁵ in the group of I. G. Kevrekidis at Princeton University.

References

1. M. D. Graham, I. G. Kevrekidis, K. Asakura, J. Lauterbach, K. Krischer, H. H. Rotermund, G. Ertl, *Science* **264**, 80 (1994)
2. O. Steinbock, Á. Tóth, K. Showalter, *Science* **267**, 868 (1995)
3. K. Suzuki, T. Yoshinobu, H. Iwasaki, *J. Phys. Chem. A* **104**, 5154 (2000)
4. H. A. Stone, A. D. Stroock, A. Ajdari, *Annu. Rev. Fluid Mech.* **36**, 381 (2004)
5. K. Krischer, M. Eiswirth, G. Ertl, *J. Chem. Phys.* **96**, 9161 (1992)

Hydroxide Adsorption at Ag(hkl) Electrodes using Cyclic Voltammetry, in Situ Second Harmonic Generation, and ex Situ Electron Diffraction

B. Pettinger, S.L. Horswell, A.L.N. Pinheiro, E.R. Savinova, M.S. Zei

Introduction

The adsorption of hydroxide on the (111), (110), and (100) faces of silver electrodes from mixed NaOH/NaF solution is investigated using cyclic voltammetry, in situ second harmonic generation (SHG) and ex situ electron diffraction. The comparison of the information obtained from each technique allows us to develop a detailed picture of the structures and electronic effects at the three low index Ag(hkl)/alkaline electrolyte interfaces.

Results

Cyclic voltammograms for the three low index silver planes in alkaline electrolytes are compared for the first time. They show two pairs of anodic and cathodic peaks in the potential interval below the equilibrium Ag/Ag₂O potential and are attributed to the specific adsorption of hydroxide ions followed by submonolayer oxide formation. The differences in the cyclic voltammograms for the (111), (110), and (100) planes are ascribed to different (i) work functions, (ii) surface atomic densities, and (iii) corrugation potentials for these surfaces. Ex situ low energy electron diffraction (LEED) and reflection high energy electron diffraction (RHEED) show that disordered adlayers are formed on Ag(111) and Ag(100). This is in contrast to Ag(110), where OH⁻ is found to be adsorbed at potentials negative of the potential of zero charge, forming small antiphase domains of c(2 x 6) symmetry. Further adsorption leads to longer-range order and the removal of antiphase domain boundaries and is associated with a current peak in the cyclic voltammogram (CV). A c(2 x 2) pattern gradually replaces the c(2 x 6) pattern as the potential, and the OH-coverage, is increased. At the beginning of the second current wave, another symmetry change takes place which is accompanied by a sharp change in the LEED pattern from a c(2 x 2) pattern to a (1 x 1) pattern with strong background, indicating a disordered adlayer. However, RHEED results show that some patches of c(2 x 2) structure remain on the surface. This later effect holds also for the (100) face. The isotropic (for the (111), (110), and (100) planes) and anisotropic (for the (110) and (111) planes) contributions to the SHG intensity were calculated by fitting the experimental data and are discussed in terms of their dependence on the charge density at the interface, on hydroxide adsorption, and on submonolayer oxide formation.

References

1. S. L. Horswell, A.L.N. Pinheiro, E.R. Savinova, B. Pettinger, M.S. Zei, G. Ertl, J. Phys. Chem. B **108**, 18640 (2004).
2. S. L. Horswell, A.L.N. Pinheiro, E.R. Savinova, M. Danckwerts, B. Pettinger, M.S. Zei, G. Ertl, Langmuir **20**, 10970 (2004).

Tip-Enhanced Raman Spectroscopy

B. Pettinger, K.F. Domke, J. Steidtner, D. Zhang

Introduction

Tip-enhanced Raman spectroscopy (TERS) is a versatile analytical tool for the detection and identification of (sub)monolayer adsorbates at single crystalline surfaces. The combinatory technique of Raman spectroscopy and scanning tunneling microscopy (STM) is based on near-field processes associated with localized surface plasmons, which are excited in the cavity between gold STM tip (in tunneling contact) and substrate. Only the adsorbates located underneath the tip apex experience the locally confined enhanced electromagnetic field and give rise to intense characteristic Raman bands.

Results

Intensive studies on the tip etching process have brought about a reproducible, rapid and easy to handle routine to produce sharp Au STM tips with a smooth surface, which are essential for the required field enhancement and localization. Typically, scanning electron microscope (SEM) images show tip radii of approximately 20-30 nm.¹

In comparison to band intensities from normal Raman scattering, a more than 10^6 -fold enhancement is observed for TERS. Very intense scattering has been observed for malachite green isothiocyanate at Au(110), Au(111) and Pt(110) samples. For this resonant dye, about 200 molecules underneath the tip are sufficient to be 'seen' by TERS. The huge enhancement also permits to obtain TER signals from molecules which are not in optical resonance with the exciting laser line, such as CN^- at Au(111), thiophenole at Au(110) and Pt(110) or mercaptopyridine adsorbed at Au(111).²⁻⁴ In addition, TERS has been employed to investigate the four DNA bases and their adsorption geometry at a Au(111) surface. The spectral differences for coadsorbed adenine-thymine base pairs indicate orientational changes at the surface due to molecular interactions (e.g. H-bonding). By monitoring the ClO_4^- stretch vibration, the dependence of the TER band intensities on the distance between tip and metal substrate has been determined. For a tip radius of 20 nm, the initial TER signal drops to $1/e^2$ within 10 nm retraction of the tip. This illustrates the very local nature of TERS. It is thus a very sensitive vibrational spectroscopy with spatial resolution in the nanometer regime, which yields both chemical and topographic information on the state of the surface (K.F. Domke, J. Steidtner, D. Zhang).

References

1. B. Ren, G. Picardi, B. Pettinger, *Rev. Sci. Instrum.* **75**, 837 (2004)
2. B. Pettinger, B. Ren, G. Picardi, R. Schuster, G. Ertl, *Phys. Rev. Lett.* **92**, 096101 (2004)
3. B. Ren, G. Picardi, B. Pettinger, R. Schuster, G. Ertl, *Angew. Chem. Int. Ed.* **44**, 139 (2004)
4. B. Pettinger, B. Ren, G. Picardi, R. Schuster, G. Ertl, *J. Raman Spectrosc.* **36**, 541(2005)

Theory Department

Poster List

Recent work done in the *Theory Department* and in Karsten Reuter's "*Independent Junior Research Group*" (*IG*) is displayed on 27 posters. A selection of 20 poster abstracts is given in the following, where those of the *IG* are indicated by the superscript ^(IG), as e.g. TH^(IG) 1.

All posters are displayed in building T and **the poster site** is given below (left column).

Poster Site

Poster Title and Authors

Structure

- | | | |
|--------------------|---|---|
| TH ^(IG) | 1 | When Seeing is Not Believing: Oxygen on Ag(111), a Simple Adsorption System?
Angelos Michaelides, Karsten Reuter, and Matthias Scheffler |
| TH ^(IG) | 2 | A First-Principles Multi-Scale Approach to the Ordering Behavior of Adsorbates under the Influence of a Step
Yongsheng Zhang, Jutta Rogal, and Karsten Reuter |
| TH ^(IG) | 3 | Alloy Segregation in Reactive Environments: An <i>Ab Initio</i> Atomistic Thermodynamics Study
John R. Kitchin, Karsten Reuter, and Matthias Scheffler |
| TH | 4 | How to Identify Different Oxygen at V₂O₃(0001) Surfaces: DFT Cluster Studies Help to Interpret Oxygen 1s NEXAFS Spectra
Christine Kolczewski and Klaus Hermann |
| TH | 5 | Is the Catalytic Epoxidation of Allylic Alkenes on Cu(111) Governed by Geometric Effects?
Christine Kolczewski, Federico J. Williams, Rachael L. Cropley, Klaus Hermann, and Richard M. Lambert |
| TH | 6 | Simulations of Nanoporous Carbon for Styrene Catalysis
Johan M. Carlsson, Suljo Linic, and Matthias Scheffler |
| TH | 7 | Understanding Growth of InAs/GaAs Nanostructures in Atomistic Detail
Thomas Hammerschmidt, Peter Kratzer, and Matthias Scheffler |

Dynamics

- TH** 10 **Toward a Deeper Understanding of “Dry” and “Wet” NaCl**
Bo Li, Angelos Michaelides, and Matthias Scheffler
- TH^(IG)** 11 **Oxygen Dissociation at Al(111): The Role of Spin Selection Rules**
Jörg Behler, Sönke Lorenz, Karsten Reuter, and Matthias Scheffler
- TH^(IG)** 12 **The Steady State of Heterogeneous Catalysis, Studied with First-Principles Statistical Mechanics**
Karsten Reuter and Matthias Scheffler
- TH^(IG)** 13 **Atomic-Scale Insight into High-Pressure CO Oxidation Catalysis at Pd(100): Relevance of Sub-Nanometer Thin Surface Oxides**
Jutta Rogal, Karsten Reuter, and Matthias Scheffler

Magnetic Systems

- TH** 14 **Stabilization Mechanisms on Oxide Surfaces: Fe₃O₄(001)**
Rossitza Pentcheva, Wolfgang Moritz, and Matthias Scheffler
- TH** 16 **Half-Metallicity at the (001) Surface of Co₂MnSi and Magnetic Properties of Thin Co₂MnSi Films on Si(001)**
S. Javad Hashemifar, Hua Wu, Peter Kratzer, and Matthias Scheffler

Biophysics

- TH** 17 **Potential-Energy Surface of Infinite Polypeptides: An Approach to Study the Secondary Structure of Proteins**
Joel Ireta and Matthias Scheffler
- TH** 18 **The α to 3_{10} Helix Transition in Alanine Polypeptides**
Radu A. Miron, Joel Ireta, and Matthias Scheffler
- TH** 20 **Thermodynamic Stability of the Secondary Structure of Proteins: A DFT-GGA Based Vibrational Analysis**
Lars Ismer, Joel Ireta, and Jörg Neugebauer
- TH** 21 **Diffusion Monte Carlo Applied to Non-Covalent Bonding: Hydrogen Bonded and Stacked DNA Base Pairs, and More**
Martin Fuchs, Claudia Filippi, Joel Ireta, and Matthias Scheffler

Methods

- TH^(IG) 22** **Accurate First-Principles Determination of the Stable Adsorption Sites of Molecules on Metal Surfaces**
Qing-Miao Hu, Karsten Reuter, and Matthias Scheffler
- TH 23** **Combining Quasiparticle Energy Calculations with Exact-Exchange Density-Functional Theory**
Patrick Rinke, Abdallah Qteish, Jörg Neugebauer, Christoph Freysoldt, and Matthias Scheffler
- TH^(IG) 25** **Efficiency and Flexibility of Numeric Atom-Centered Basis Sets for Fast All-Electron Calculations**
Volker Blum, Ralf Gehrke, Jörg Behler, Karsten Reuter, and Matthias Scheffler

When Seeing is Not Believing: Oxygen on Ag(111), a Simple Adsorption System?

Angelos Michaelides, Karsten Reuter, and Matthias Scheffler

Solving atomic structures is a common activity for the natural scientist. A structure, whether of relevance to molecular biology, chemical physics, catalysis, or another area, is considered “solved” when an atom-by-atom structural understanding of the molecular or solid state systems involved has been obtained. In surface science such efforts are mostly directed at clean and adsorbate covered single-crystal surfaces that are e.g. of relevance to heterogeneous catalysis or the semiconductor industries. After some 50 years of surface science, many such surface structures have now been solved, including several cases with highly complex, large surface unit-cell reconstructions.

Here we argue that despite conventional wisdom one seemingly simple structure, namely oxygen on Ag(111), has evaded solution [1]. We make this claim in the face of more than thirty years of experimental investigations and two previous density-functional theory (DFT) studies [2,3] that largely confirmed a unique structural model for oxygen on Ag(111). Indeed previous experiments on this system even included scanning tunneling microscopy (STM) in which the overlayer was imaged with apparent atomic resolution [4]. However, new DFT results presented here and a careful review of published experimental data indicate that previous conclusions are significantly incomplete and that the structure of this overlayer must be reconsidered. Our main conclusion is that the accepted model, an Ag₂O-like surface-oxide, is either incorrect or is a metastable structure. Several other structures equally stable to or more stable than the existing model have been identified making it unclear why a single almost defect-free overlayer is apparently observed under ultra-high vacuum (UHV) conditions. A clear implication of the present results, however, is that this system is likely to be much more complex than anticipated and, in particular, at the high temperatures and high pressures characteristic of industrial catalysis the Ag surface is likely to comprise a complex coexistence of related sub-nanoscale oxide overlayers, each built, perhaps, from a set of novel Ag₃O₄ building blocks identified here.

- [1] A. Michaelides, K. Reuter, and M. Scheffler, *J. Vac. Sci. and Technol.*, accepted.
- [2] A. Michaelides, M.-L. Bocquet, P. Sautet, A. Alavi, and D.A. King, *Chem. Phys. Lett.* **367**, 344 (2003).
- [3] W.X. Li, C. Stampfl, and M. Scheffler, *Phys. Rev. Lett.* **90**, 256102 (2003).
- [4] C. Carlisle, D.A. King, M.-L. Bocquet, J. Cerdá, and P. Sautet, *Phys. Rev. Lett.* **84**, 3899 (2000).

A First-Principles Multi-Scale Approach to the Ordering Behavior of Adsorbates under the Influence of a Step

Yongsheng Zhang, Jutta Rogal, and Karsten Reuter

Exposing undercoordinated atoms, steps are believed to play a decisive role in the oxide formation at transition metal (TM) surfaces. Despite this suggested importance, first-principles investigations qualifying this role in the oxidation behavior are scarce. This is mostly due to the limitations of electronic structure calculations in tackling the large system sizes and huge configuration spaces involved. The aim of the present work is to overcome these limitations, by developing a multi-scale approach coupling density-functional theory (DFT) calculations with mesoscopic Monte Carlo simulations.

Focusing on the on-surface O adsorption as initial step in the oxidation process, we specifically investigate the effect of (111) steps at a Pd(100) surface. Since this is a system with site-specific adsorption, a lattice gas Hamiltonian (LGH) can be used to provide the energetics of any given adsorbate configuration. Even in mesoscopic simulation cells the computational costs are then low enough to allow extensive canonical Monte Carlo simulations evaluating the adsorbate ordering behavior, e.g. as a function of the temperature and oxygen pressure in the environment. The crucial ingredient to make such simulations quantitative is to suitably parametrize the LGH by DFT calculations. When addressing the ordering behavior under the influence of a step this means in practice to determine all relevant lateral interactions among adsorbed oxygen atoms, both at terrace sites and at sites close to or at the step.

For this we systematically studied O adsorption at Pd(100) and the series of Pd(11 N) vicinals (with $N = 3, 5, 7$), which exhibit (111) steps and (100) terraces of increasing width. We find the adsorption energetics in the middle of the terraces at Pd(117) to be already virtually indistinguishable from that at Pd(100). Large scale DFT calculations of O configurations at Pd(117) and Pd(100) in various supercells can therefore be employed to extract all required LGH interactions, i.e., those interactions influenced by an isolated step are taken from the vicinal surface and those of undisturbed terrace sites from the low-index surface. Since adsorption at step sites is computed to be distinctly more favorable compared to terrace sites, we expect step decoration with O atoms already at oxygen gas pressures where no adsorbate phase can be stabilized at the (100) terraces. As a first step, these effects are discussed on the basis of the computed (T, p) surface phase diagram of O/Pd(100).

Alloy Segregation in Reactive Environments: An *Ab Initio* Atomistic Thermodynamics Study

John R. Kitchin^(*), Karsten Reuter, and Matthias Scheffler

Due to their often unique materials and chemical properties alloys are a key focus of modern materials science research. Their surface properties as e.g. catalytic behavior or corrosion resistance depend sensitively on the detailed surface composition and structure, which can be particularly affected by segregation of component species to the surface. Especially in the intended use of alloys in realistic, reactive environments (with partial gas phase pressures of the order of atmospheres and possibly elevated temperatures), preferential segregation of those alloy components that interact more strongly with the gas phase species is intuitive. This may lead to a chemical surface composition that differs largely from the nominal alloy bulk composition and is furthermore a direct function of the surrounding environment. A quantitative atomic scale understanding of alloy surface functionalities in materials applications can therefore neither be achieved on the basis of the formal bulk composition, nor on the structure and stoichiometry present under ultra-high vacuum (UHV) conditions. Instead, it is crucial to explicitly consider the alloy surface in contact with the reactive environment.

In order to determine the alloy surface termination under realistic environmental conditions we employ the *ab initio* atomistic thermodynamics approach based on density-functional theory. Specifically, we address the effect of an oxygen gas phase on the segregation behavior at the (111) surface of Ag₃Pd. The results reveal a segregation reversal with increasing oxygen content in the gas phase. While at low oxygen chemical potentials as typical for UHV conditions, a clean silver-terminated surface exhibits the lowest surface energy, increasingly Pd-enriched surface configurations become stable when going to higher pressures. The critical oxygen chemical potential required to induce Pd segregation depends furthermore sensitively on the bulk alloy reservoir; a higher oxygen chemical potential is required to induce Pd segregation in surfaces in equilibrium with a slightly Ag-rich bulk Ag₃Pd reservoir than for those in equilibrium with a slightly Pd-rich bulk. This underscores the intimate relation between bulk, surface, and environment that challenges any quantitative modeling of alloy material functions.

(*) Permanent address: Department of Chemical Engineering, Carnegie Mellon University, Pittsburgh, U.S.A.

How to Identify Different Oxygen at $V_2O_3(0001)$ Surfaces: DFT Cluster Studies Help to Interpret Oxygen 1s NEXAFS Spectra

Christine Kolczewski and Klaus Hermann

The identification and study of reactive oxygen sites at transition metal oxide surfaces is of basic scientific interest but also of great technological importance due to the use of these materials as catalysts. Here spectroscopic techniques such as photoemission or near-edge x-ray absorption fine structure (NEXAFS) can contribute to distinguish between specific reaction sites with atomic resolution. However, these experimental techniques rely heavily on theoretical input as to the interpretation of spectral details. Our study shows that DFT cluster methods can be successful in calculating O 1s NEXAFS spectra of different bulk and surface oxygen of complex transition metal oxides in quantitative agreement with experimental data [1].

Here we consider as a catalyst material rhombohedral vanadium sesquioxide, V_2O_3 , which offers different intrinsic terminations of its (0001) surface containing three types of reactive oxygen sites: two-, three-, and four-fold coordinated. Further, recent experiments on $V_2O_3(0001)$ after oxygen exposure [1] have postulated a termination containing singly coordinated vanadyl oxygen. Here we have calculated [2] angle resolved O 1s NEXAFS spectra of all non-equivalent oxygen types for the different surface terminations of $V_2O_3(0001)$ where corresponding superpositions yield total spectra, to be compared with experiment, while the component spectra allow us to distinguish between differently coordinated oxygen. The calculations are based on density-functional theory together with surface cluster [3] where core excitations and dipole transition matrix elements are considered within Slaters transition state approach.

A comparison of our theoretical data with experimental angle resolved NEXAFS spectra of $V_2O_3(0001)$ [1] is found to yield overall excellent agreement. A decomposition of the theoretical spectra shows pronounced differences for differently coordinated oxygen which allows us to interpret all main details of the experimental spectra. Therefore, our theoretical studies can be used to identify differently coordinated surface oxygen based on experimental NEXAFS spectra.

- [1] A.-C. Dupuis, M. Abu Haija, B. Richter, H. Kuhlenbeck, and H.-J. Freund, *Surf. Sci.* **539**, 99 (2003).
- [2] C. Kolczewski and K. Hermann, *TheorChemAcc*, online (2005).
- [3] C. Kolczewski and K. Hermann, *J. Chem. Phys.* **118**, 7599 (2003).

Is the Catalytic Epoxidation of Allylic Alkenes on Cu(111) Governed by Geometric Effects?

Christine Kolczewski, Federico J. Williams^(*), Rachael L. Cropley^(*),
Klaus Hermann, and Richard M. Lambert^(*)

Epoxides are valuable chemical intermediates in a number of important catalytic reactions. Examples are ethene and propene epoxides. While Ag catalysts are successful to produce ethene epoxide they are useless for propene epoxidation since in the latter case oxidation leads almost entirely to combustion. This behavior is assumed to reflect the presence of labile allylic hydrogen atoms in propene whose abstraction by oxygen at the Ag surface leads to combustion of the alkene. We have examined this hypothesis and other geometric details of the epoxidation process in theoretical and experimental studies on model systems where the Cu(111) surface serves as substrate and one hydrogen of the propene adsorbate is substituted by a phenyl ring in order to facilitate stabilization at the surface. This leads to three isomers of phenylpropene, C₉H₁₀: trans-methylstyrene (TMS), α -methylstyrene (α -MS) and allylbenzene (AB) whose properties are studied experimentally by temperature programmed reaction (TPR) and NEXAFS measurements. The TPR experiments show that epoxidation is the most efficient for α -MS on Cu(111) while AB shows no and TMS only weak epoxidation. Angle resolved NEXAFS measurements yield quite different spectra for the three adsorbates but do not allow a unique identification of their geometries.

We have also studied these systems theoretically by density functional theory calculations using Cu₇₃-C₉H₁₀ clusters. Optimized geometries of the three adsorbates show that their phenyl rings lie always flat on the surface. Allylbenzene adsorbs with its propenyl side chain pointing away from the surface. Thus, surface oxygen cannot reach the side chain to initiate epoxidation which explains the TPR result for AB. In contrast, the side chains of the TMS and α -MS adsorbates stabilize closer to the surface which facilitates epoxidation in agreement with experiment. In addition, the allylic hydrogen atoms of the α -MS adsorbate lie further away from the surface than those of TMS which makes hydrogen abstraction by surface oxygen less likely for α -MS and explains the relative epoxidation rates found in TPR. The present geometric findings are confirmed by our theoretical angle resolved C 1s NEXAFS spectra which yield excellent agreement with the measured spectra for the three adsorbates.

^(*) Permanent address: Department of Chemistry, University of Cambridge, U.K.

Simulations of Nanoporous Carbon for Styrene Catalysis^(*)

Johan M. Carlsson, Suljo Linic^(**), and Matthias Scheffler

Nanoporous carbon materials (NPC) exhibit unusual properties distinct from other sp^2 bonded carbon materials. It has for instance been shown that NPC can act as a catalyst for oxidative dehydrogenation (ODH) of ethylbenzene [1]. The origin of the catalytic activity is still unclear, since the atomic structure of NPC can take a variety of forms, depending on the preparation conditions and the starting material. However, TEM observations [2] and neutron diffraction experiments [3] suggest that NPC derived from hydrocarbons has the form of crumpled graphene sheets with a significant amount of non-hexagonal rings in the structure.

We have therefore carried out an extensive study of NPC and how oxygen can assist ODH of ethylbenzene. The building blocks of NPC were first identified by a systematic study of defects in graphene: the “motifs”. Our density-functional theory (DFT) calculations revealed that the atomic relaxation transforms defects into combinations of non-hexagonal rings. These motifs lead to strain and local buckling of the structure. They also induce defect states close to the Fermi level, leading to that some of them being charged, which may facilitate molecule dissociation. Curvature modifies the properties of the motifs by lowering their formation energy in nanotubes and mixing the defect states with the π -band, such that the defect states lose their localized character. These motifs can then be combined to build a model of a NPC material with a certain concentration of non-hexagonal rings in the structure. NPC materials with up to 1% motifs appear to have a comparable heat of formation to single wall nanotubes.

Our analysis of the dominant structural building blocks is supported by subsequent calculations, which show that the motifs are able to dissociate oxygen, which leads to the formation of functional C-O groups. The carbonyl group appears among these C-O groups to be the most promising candidate as active site for ODH of ethylbenzene. The heat of reaction for the ODH reaction at the carbonyl groups is found to be slightly endothermic in agreement with the elevated temperatures needed to run the reaction [1].

(*) In collaboration with the Department of Inorganic Chemistry at the FHI.

(**) Present address: Department of Chemical Engineering, University of Michigan, Ann Arbor, U.S.A.

[1] G. Mestl *et al.*, *Angew. Chem. Int. Ed.* **40**, 2066 (2001).

[2] P.J.F. Harris, A. Burian, and S. Duber, *Phil. Mag. Lett.* **80**, 381 (2000).

[3] V. Petkov *et al.*, *Phil. Mag. B* **79**, 1519 (1999).

Understanding Growth of InAs/GaAs Nanostructures in Atomistic Detail

Thomas Hammerschmidt, Peter Kratzer, and Matthias Scheffler

The utilization of self-assembled quantum dots (QDs), e.g. for optoelectronic devices, requires uniform and highly reproducible properties of the QDs. These are determined by their geometry and chemical composition, and hence a detailed understanding of QD growth is necessary. From a thermodynamic point of view, the formation of QDs is governed by the balance between energy gain due to strain relief and energy cost due to formation of QD side facets and edges. In order to account for both contributions, and in extension to the hybrid approach previously devised in our department [1,2], we developed a carefully parameterized, analytical many-body potential of the Tersoff type [3]. It reproduces many properties of Ga, As, In, GaAs, and InAs bulk structures, and of GaAs and InAs surfaces, as obtained from experiment or density-functional theory calculations, with good overall accuracy. This enables us to systematically study the energetics and atomic structure of realistic QD nanostructures to clarify the role of thermodynamic effects.

In particular, we identify the driving force behind the experimentally observed sequence of shapes with increasing QD size [4], and for the growth correlations in QD stacks [5]. We use STM images of InAs QDs obtained in the PC department [6] and in other groups [4] to set up InAs QD nanostructures in atomic detail, apply our potential to relax them, and compare the resulting total energies. To investigate the experimentally observed shape sequence of ‘hut’-like QDs dominated by {317} facets and ‘dome’-like QDs dominated by {101} facets, the energies of homogeneous InAs films and differently sized InAs QDs with either shape are compared. We identify three regimes: For coverages below about 1.9 monolayers of InAs the film is most stable, followed by small ‘hut’-like QDs and larger ‘dome’-like QDs. This is in line with the experimentally deduced critical coverage for the 2D to 3D growth transition [6], and the shapes of small and larger QDs [4]. We can also explain the growth correlation in QD stacks: Our calculated potential-energy surfaces of free-standing QDs in different lateral positions above overgrown QDs show an energy gain of about 20 meV per In atom for the experimentally observed vertical QD alignment.

- [1] E. Pehlke, N. Moll, A. Kley, and M. Scheffler, *Appl. Phys. A* **65**, 525 (1997).
- [2] Q.K.K. Liu, N. Moll, M. Scheffler, and E. Pehlke, *Phys. Rev. B* **60**, 1708 (1999).
- [3] J. Tersoff, *Phys. Rev. B* **39**, 5566 (1989).
- [4] G. Costantini *et al.*, *Appl. Phys. Lett.* **85**, 5673 (2004).
- [5] H. Heidemeyer, U. Denker, C. Müller, and O.G. Schmidt, *Phys. Rev. Lett.* **91**, 196103 (2003).
- [6] J. Márquez, L. Geelhaar, and K. Jacobi, *Appl. Phys. Lett.* **78**, 2309 (2001).

Toward a Deeper Understanding of “Dry” and “Wet” NaCl

Bo Li, Angelos Michaelides, and Matthias Scheffler

The interaction of water with NaCl is of general importance to many aspects of daily life as well as to disparate fields of scientific endeavor such as atmospheric chemistry, catalysis, and biophysics. Remarkably, however, our understanding of water/NaCl interfaces, especially at the atomic level, is severely lacking. In order to put our understanding of this key system on a firmer footing we have attacked it with density-functional theory (DFT) and *ab initio* molecular dynamics calculations.

As a starting point, “dry” flat and defective NaCl surfaces have been examined. This involved a characterization of monoatomic steps, single vacancies (colour centers), and Na and Cl adatoms on NaCl(100). Through use of the Cl₂ chemical potential their relative stabilities are assessed as a function of temperature and pressure enabling, amongst other things, predictions of the concentrations of different kinds of defects at finite temperatures and pressures. For the first time, the step formation energies of (100) (stoichiometric) and (111)-like (non-stoichiometric) steps on NaCl(100) are evaluated from first principles, revealing that (100)-like steps are more stable than their (111)-like counterparts at all relevant temperatures and pressures (i.e., experimentally accessible temperatures and pressures). In addition the interaction energy between neighbouring steps on a NaCl(100) terrace is found to be remarkably small, dropping to almost zero once the steps are more than one lattice constant apart.

Based on these initial studies and new knowledge of dry NaCl(100), the wetting of NaCl by water was then examined. From static DFT calculations, the structures and energetics of water adsorption on flat and defective NaCl(100) has been determined in the sub-monolayer, monolayer and multilayer regimes. Seemingly simple but important questions such as at what sites water molecules prefer to adsorb at low coverage and how the adsorbed water molecules hydrogen bond to each other at the NaCl surface have been answered. For the latter question, *ab initio* MD simulations have helped to reveal how the hydrogen bond structure and dynamics of thin water films is modified by the NaCl interface.

Oxygen Dissociation at Al(111): The Role of Spin Selection Rules

Jörg Behler, Sönke Lorenz, Karsten Reuter, and Matthias Scheffler

The dissociative adsorption of O₂ at Al(111) remains a basic and puzzling enigma in surface science. Already for the sticking curve, the disagreement between experiment [1] and results of first-principles calculations can hardly be more dramatic. Similarly, there is still no understanding for the early scanning tunneling microscopy observation [2] that for very low coverages and conditions where thermal diffusion is not relevant the distribution of adsorbed O atoms is random, i.e. there is no correlation of the two atoms that originate from the same O₂ molecule. We suggest that this is caused by hitherto unaccounted spin selection rules, which give rise to a highly non-adiabatic behavior in the O₂/Al(111) interaction.

Qualifying this assessment, we developed and implemented a locally-constrained DFT method into the DMol³ code, which enables us to compute diabatic potential energy surfaces (PESs) corresponding to different charge and spin states of the impinging molecule. This way we can analyze the trajectories of O₂ molecules that travel in the initial spin-triplet configuration up to distances close to the surface where hybridization with metal-surface states becomes significant. Since the computed spin-triplet PES exhibits energy barriers towards dissociation, molecular dynamics runs yield indeed a significantly reduced sticking coefficient in good agreement with the experimental data [3].

Such spin selection will be particularly important for systems with a low density of states at the Fermi level; for transition metals we expect that the high density of *d* states can more easily take up the spin. If the spin is not easily taken up as in the case of Al(111), spin selection rules lead to a very low sticking probability for thermal O₂ molecules in the triplet ground state, while O₂ molecules prepared in the singlet configuration should adsorb with high probability. Analyzing the approaching O₂ molecule in greater detail reveals furthermore that for molecules that approach in an orientation perpendicular to the surface (or close to this) the spin is shifted to the atom that is further away from the surface. We believe this to be the onset of adsorption by the abstraction mechanism. In this way, one O atom can adsorb in a singlet state, while the spin is carried away with the other O atom that is either repelled back into the vacuum or to a distant site at the surface.

- [1] L. Österlund, I. Zorić, and B. Kasemo, *Phys. Rev. B* **55**, 15452 (1997).
- [2] H. Brune, J. Wintterlin, R. J. Behm, and G. Ertl, *Phys. Rev. Lett.* **68**, 624 (1992).
- [3] J. Behler, B. Delley, S. Lorenz, K. Reuter, and M. Scheffler, *Phys. Rev. Lett.* **94**, 036104 (2005).

The Steady State of Heterogeneous Catalysis, Studied with First-Principles Statistical Mechanics

Karsten Reuter and Matthias Scheffler

A first-principles modeling of heterogeneous catalysis that quantitatively describes the activity over a wide range of realistic environmental situations of varying temperatures and pressures is a daunting task. Since one is dealing with a thermodynamically open system, even steady-state conditions, where the conversion of the chemicals at the solid surface proceeds at a stable rate, are determined by kinetics. A quantitative computation of the steady-state rate requires therefore to explicitly follow the time evolution of a large enough surface area, fully treating the statistics of all relevant underlying atomic-scale processes.

We tackle this challenge by a first-principles statistical mechanics setup [1], where we first use density-functional theory (DFT) together with transition state theory (TST) to accurately obtain the energetics of all relevant processes. Subsequently the statistical mechanics problem is solved by kinetic Monte Carlo (kMC) simulations. This two-step approach enables us to gain microscopic insight into the system, following its full dynamics from picoseconds up to seconds and explicitly considering the detailed statistical interplay of all elementary processes, i.e., by fully accounting for the correlations, fluctuations, and spatial distributions of the chemicals at the catalyst surface.

In the application to CO oxidation at a RuO₂(110) model catalyst, we compute the composition and structure of the catalyst surface in reactive environments ranging from ultra-high vacuum (UHV) to technologically relevant conditions with pressures of the order of atmospheres and elevated temperatures. For all these conditions the obtained conversion rates are in unprecedented quantitative agreement with existing experimental data. The catalytic activity is narrowly peaked in environments, where the surface kinetics builds a disordered and dynamic adsorbate composition at the surface. In the full concert of the large number of processes occurring in this active state, the chemical reaction with the most favorable energy barrier contributes only little to the overall CO₂ production. Moreover, the strong process interplay makes the resulting optimum mix at the catalyst surface also highly adaptive and renders the corresponding maximum conversion rates in this active state quite insensitive to modest errors in the individual process rates. This challenges established concepts like the idea of one rate-determining step or the necessity of chemical accuracy for the description of individual processes, and clearly illustrates the new quality and novel insights gained by such first-principles statistical mechanics methodology.

[1] K. Reuter, D. Frenkel, and M. Scheffler, *Phys. Rev. Lett.* **93**, 116105 (2004).

Atomic-Scale Insight into High-Pressure CO Oxidation Catalysis at Pd(100): Relevance of Sub-Nanometer Thin Surface Oxides

Jutta Rogal, Karsten Reuter, and Matthias Scheffler

At ambient conditions, transition metals (TMs) are covered by oxide films that form spontaneously in our oxygen-rich atmosphere. There is increasing awareness that this could similarly happen under the conditions of oxidation catalysis, and oxide films forming in the reactive environment will then actuate or at least affect the catalytic behavior that is traditionally ascribed to the pristine TM substrates [1]. With the bulk oxides too unstable, at more noble metals like Pd, Pt, and Ag the focus is primarily on the relevance of so-called “surface-oxides”, i.e., sub-nanometer thin oxidic films or islands.

In the present study we specifically address CO oxidation at a Pd(100) model catalyst where *in situ* experiments suggest a continuous formation and reduction of ultra-thin oxidic structures under steady-state high-pressure conditions [2]. As a first step, we employ *ab initio* atomistic thermodynamics to analyze the oxidation of the surface in an O₂ gas phase up to ambient pressures. In accordance with surface X-ray diffraction data, we identify a $(\sqrt{5} \times \sqrt{5})R27^\circ$ surface-oxide structure as the most stable phase over a wide range of temperatures and pressures [3]. Accounting also for the other reactant we next consider the surface structure and composition in a *constrained* equilibrium with an O₂ and CO gas phase. Under high-pressure gas phase conditions representative of technological CO oxidation the surface oxide results then again as the most stable structure.

More specifically, the system is under these conditions quite close to a transition to a CO-covered metal surface. Under steady-state operation this suggests possible oscillations between metallic and oxidic state, which could then lead to a wealth of intriguing surface phenomena like a particular relevance of phase boundaries or even spatio-temporal pattern formation. Addressing such effects requires at least to explicitly account for the on-going reactions, i.e., to go beyond the constrained equilibrium approach. We are presently investigating such kinetic effects under steady-state conditions by *ab initio* kinetic Monte Carlo simulations.

- [1] K. Reuter, *Nanometer and sub-nanometer thin oxide films at surfaces of late transition metals*. In: Nanocatalysis: Principles, Methods, Case Studies. (Eds.) U. Heiz, H. Hakkinen, and U. Landman, Springer, Berlin 2005.
- [2] B.L.M. Hendriksen, S.C. Bobaru, and J.W.M. Frenken, Surf. Sci. **552**, 229 (2004).
- [3] E. Lundgren *et al.*, Phys. Rev. Lett. **92**, 046101 (2004).

Stabilization Mechanisms on Oxide Surfaces: Fe₃O₄(001)

Rossitza Pentcheva^(*), Wolfgang Moritz^(*), and Matthias Scheffler

Knowledge and understanding of the mechanisms that lead to the stabilization of a polar oxide surface are essential in order to control their reactivity, as well as their magnetic and electronic properties. Besides its importance in geophysics and mineralogy, magnetite is a prospective material for the development of spintronic devices. To resolve a long standing controversy on the surface termination of Fe₃O₄(001), we performed density-functional theory (DFT) calculations within the generalized gradient approximation (GGA) for a variety of stoichiometric and non-stoichiometric terminations. The surface phase diagram constructed in the framework by *ab initio* atomistic thermodynamics [1] reveals that a hitherto ignored modified bulk termination is the lowest energy configuration over a broad range of oxygen pressures [2]. The stabilization of the surface involves a novel mechanism. While most of the previous studies proposed an ordering of surface vacancies as the origin of the experimentally observed ($\sqrt{2} \times \sqrt{2}$)R45°-reconstruction, here it is explained as a *Jahn-Teller* distortion of the surface atoms forming a *wave-like-pattern* along the [110]-direction. DFT-geometries are used as input for quantitative x-ray diffraction (XRD) and LEED-I/V-analyses [2,3]. To improve the efficiency of the latter for oxide surfaces, we have generated phase shifts from the *ab initio* calculations. Both the LEED- and XRD-results support the theoretically predicted model. Recent STM-images [4,5] are interpreted in the light of STM-simulations in the Tersoff-Hamann model. Significant changes in the electronic and magnetic properties, e.g. a *halfmetal-to-metal* transition from bulk to the surface, accompany the Jahn-Teller-stabilization of the Fe₃O₄(001)-surface. The reduction of the spin-polarization at the surface is consistent with recent spin-polarized photoemission measurements [5]. Finally, we explore the influence of on-site correlation effects on the surface stability and electronic structure as well as the possibility of long-range charge order within the LDA+U-formalism.

(*) Permanent address: Department of Earth and Environmental Sciences, University of Munich, Germany.

- [1] X.G. Wang *et al.*, Phys. Rev. Lett. **81**, 1038 (1998);
K. Reuter and M. Scheffler, Phys. Rev. B **65**, 035406 (2002).
- [2] R. Pentcheva *et al.*, Phys. Rev. Lett. **94**, 126101 (2005).
- [3] R. Pentcheva *et al.*, in preparation.
- [4] B. Stanka, W. Hebenstreit, U. Diebold, and S.A. Chambers, Surf. Sci. **448**, 49 (2000).
- [5] M. Fonin *et al.*, Phys. Rev. B, in print.

Half-Metallicity at the (001) Surface of Co_2MnSi and Magnetic Properties of Thin Co_2MnSi Films on $\text{Si}(001)$

S. Javad Hashemifar^(*), Hua Wu^(**), Peter Kratzer, and Matthias Scheffler

Materials for spintronics applications have recently attracted much interest. Apart from dilute magnetic semiconductors, thin ferromagnetic metal films are interesting to be used for injection of a spin-polarized current into a semiconductor substrate. One promising candidate for spintronics applications is the ferromagnetic half-metal Co_2MnSi , which, in its bulk phase, has a Curie temperature as high as 985 K and displays a gap at the Fermi level in the minority spin channel. At surfaces and interfaces, however, it is conceivable that electronic states in the gap arise which modify or destroy the half-metallic properties of this material.

To investigate this possibility, we performed all-electron density-functional calculations for the $\text{Co}_2\text{MnSi}(001)$ surface using the spin-polarized generalized gradient approximation and the full-potential LAPW/APW+lo method. Our analysis of the surface energies of different surface terminations shows that terminations by a layer of only Mn atoms, only Si atoms, or a mixture of both is thermodynamically stable, depending on the chemical environment used for surface preparation. The surface electronic structure is strongly affected by the type of surface termination. In particular, terminating the surface by a monolayer of Mn atoms preserves the half-metallic behavior, while surface states destroy this property for other terminations [1].

Next, we investigated the properties of ultra-thin $\text{Co}_2\text{MnSi}(001)$ films (one to three monolayers) grown epitaxially on the $\text{Si}(001)$ surface. We find magnetic moments of the Mn atoms in the range of 2.7–3.5 μ_B , similar in size as in bulk Co_2MnSi , and strong ferromagnetic coupling of the Mn magnetic moments both within the same layer and between layers. Moreover, the calculations reveal that the Co_2MnSi thin films are stable against decomposition into elementary silicides. At the $\text{Co}_2\text{MnSi}/\text{Si}(001)$ interfaces we studied so far, our calculations find a finite density of states at the Fermi energy for *both* spin channels, but the half-metallic behavior recovers a few layers away from the interface [2].

(*) Permanent address: Physics Department, Isfahan University of Technology, Iran.

(**) Present address: II. Physikalisches Institut, Universität zu Köln.

[1] S.J. Hashemifar, P. Kratzer, and M. Scheffler, Phys. Rev. Lett. **94**, 096402 (2005).

[2] H. Wu, P. Kratzer, and M. Scheffler, Phys. Rev. B, submitted.

Potential-Energy Surface of Infinite Polypeptides: An Approach to Study the Secondary Structure of Proteins

Joel Ireta and Matthias Scheffler

The biological function of proteins crucially depends on their structural conformation. Only a specific conformation, the so-called native state, is biologically active and stable (or at least metastable with sufficient lifetime) under typical environmental conditions. In fact some diseases in mammals, like the Creutzfeld-Jacob or Alzheimer diseases, are associated to the transformation of the helical structure to sheet conformation (misfolding of the secondary structure) of certain sections of proteins found in nerve cells. Therefore studies on the structural transitions of the secondary structure may help to understand the function or possible malfunction of proteins. Moreover structural details of the secondary structure are still matter of controversy, for example the occurrence of helices different from the α -helix in the folding/unfolding event of helical conformations, or the origin of the deviation from a flat structure (twist) of sheet conformations. Our objective is to study the structural changes that an infinitely long polypeptide may assume under different (external) conditions. We use density-functional theory (DFT) to calculate the potential-energy surface (PES) of polyalanine and polyglycine chains. Neglecting the solvent-polypeptide interaction allows us to study the intrinsic properties of the peptides connected to the structural changes.

The PES for both polyalanine and polyglycine reveal *i*) a folded region where structures form hydrogen bonds between non nearest-neighbor peptide units; and *ii*) an unfolded region where nearest-neighbor interactions are dominant. The folded region is found to have three minima corresponding to three distinct helical conformations, namely the 3_{10} -helix, i.e., 3 peptide units per turn and 10 atoms in the ring formed by the hydrogen bonds, the 3.6_{13} -helix or α -helix and the 4.4_{16} -helix or π -helix [1]. The unfolded region contains two minima corresponding to the 2_7 conformation, i.e., 2 peptide units and 7 atoms in the ring formed by the hydrogen bonds, and the fully extended structure. The 3_{10} -helix and the 2_7 conformation appear as transition states along the unfolding path of an α -helix under uniaxial strain. The PES for polyalanine also reveals a twist in the fully extended structure, feature that is actually a fingerprint of sheet conformations in protein crystals and fibril amyloids. The twist appears to be associated to changes in the nitrogen hybridization. These results show that an infinitely long polypeptide is a realistic model for studying the basic structural motifs of the secondary structure of proteins.

- [1] J. Ireta, J. Neugebauer, M. Scheffler, A. Rojo, and M. Galván, J. Am. Chem. Soc., submitted.

The α to 3_{10} Helix Transition in Alanine Polypeptides

Radu A. Miron, Joel Ireta, and Matthias Scheffler

The folding of polypeptide chains into helical conformations is one of the key processes determining protein structure and functionality. In most studies to-date, this process is interpreted using a two-state model, where polypeptide chains can exist either as α helices, forming hydrogen bonds between *4th* nearest neighbor residues, or in the random coil state with no particular structure. However, recent results show that the two-state model can not explain non-exponential relaxation patterns in proteins [1] and the occurrence of other helix types. In particular, the existence of the 3_{10} helix, with hydrogen bonds between *3rd* nearest neighbor residues, has been often ignored, not least because many force fields used to interpret experimental results do not show the 3_{10} helix as a stable structure. However, both density-functional theory (DFT) calculations and experimental techniques able to discern the hydrogen-bonding patterns in helices show that the 3_{10} helix may be an important constituent in the folded state and as a folding kinetic intermediate [2].

As a first step towards realistically modeling the folding, we investigate the thermodynamic and kinetic stability of finite polyalanine chains in vacuum. The absence of solvent allows us to identify intrinsic peptide properties, such as the occurrence of the 3_{10} helix, before the influence of solvent is accounted for. Comparing DFT-GGA and empirical force-field calculations, we find that the AMBER force field renders an adequate reproduction of the two helical states. Both methods show that for chains smaller than 10 residues only the 3_{10} helix exists as a stable structure in vacuum. Further, we run molecular dynamics simulations using AMBER to probe the nanosecond-time scale dynamics of helices up to 20 residue long. Between 12 and 16 residues we uncover a length-dependent structural transition, whereby the α minimum becomes increasingly favored, and only longer chains obey the traditional view of pure α helices. Intermediate-length helices exhibit many local minima as mixtures of α and 3_{10} domains. Interconversion among helical states is very fast and occurs on picosecond-time scale at room temperature. We construct a suitable coordinate space where the evolution of these domains can be mapped along a few generalized coordinates. For chains of around 14 residues, the associated free-energy surfaces exhibit two important minima representing mostly- α and mostly- 3_{10} configurations separated by a barrier of less than $2k_B T$ at room temperature. Our results confirm the necessity of including the 3_{10} helix in realistic coarse-grained models of proteins.

[1] E. Abrams, Phys. Rev. E **71**, 051901 (2005).

[2] J. Ireta, J. Neugebauer, M. Scheffler, A. Rojo, and M. Galván, J. Am. Chem. Soc., submitted; K. A. Bolin and G. L. Millhauser, Acc. Chem. Res. **32**, 1027 (1999).

Thermodynamic Stability of the Secondary Structure of Proteins: A DFT-GGA Based Vibrational Analysis

Lars Ismer, Joel Ireta, and Jörg Neugebauer^(*)

About 90 percent of residues in proteins can be found in locally regular conformations, such as helices, sheets, and turns, named the secondary structure. The discovery of these structural motifs has stimulated scientific research for more than five decades. Nevertheless, open questions remain regarding their intrinsic stability which is a rather delicate balance between enthalpic and entropic contributions of the peptide chain. Our goal is to study these thermodynamic aspects of stability on the level of accuracy provided by density-functional theory (DFT).

Therefore, we have calculated harmonic vibrational spectra and free energies of isolated, infinite polyalanine (Ala) and -glycine (Gly) chains in various helical conformations, including α -, 3_{10} -, and π -helices and in the fully extended structure (FES), which serves as a reference state for the stability analysis. This study of isolated peptide chains may serve as a reliable reference point for studies which include complex environmental effects. The calculations were done by employing DFT in the generalized gradient approximation (GGA). To verify the reliability of this approach, we compared the obtained phonon dispersion relation and specific heat of the Ala α -helix with available experimental data and found good quantitative agreement (deviations for frequencies $< 5\%$) [1]. The helical structure motifs are found to be energetically preferred over the FES at 0K, owing to the formation of hydrogen bonds [2]. However, this stability is strongly reduced by the vibrational contributions to the free energy, mainly by vibrational entropy, with increasing temperature. Furthermore, vibrational entropy also affects the relative stability of the helical motifs leading to a significant destabilisation of the π -helix with respect to α -helix and 3_{10} -helix at room temperature. This result is remarkable, as it might explain, why the π -helix is seldom observed in proteins compared to the other helical motifs. In good agreement with the experimental observation the α -helix is the lowest free energy conformation for temperatures below a critical temperature T_c , where a transition to the FES takes place. The thermodynamic trends are found to be similar for Gly and Ala. However, T_c for Gly (~ 400 K) is substantially lower than that for Ala (~ 460 K) indicating a lower intrinsic tendency of glycine to form helices. These differences are mainly due to a larger flexibility of polyglycine in the FES.

^(*) Permanent address: MPI für Eisenforschung GmbH, Düsseldorf, Germany.

[1] L. Ismer, J. Ireta, S. Boeck, and J. Neugebauer, Phys. Rev. E **71**, 31911 (2005).

[2] J. Ireta, J. Neugebauer, M. Scheffler, A. Rojo, and M. Galván, J. Am. Chem. Soc., submitted.

Diffusion Monte Carlo Applied to Non-Covalent Bonding: Hydrogen Bonded and Stacked DNA Base Pairs, and More

Martin Fuchs, Claudia Filippi^(*), Joel Ireta, and Matthias Scheffler

Density-functional theory (DFT) calculations are a powerful tool for studying biomolecules. Hydrogen bonding is a key aspect in such systems where, moreover, also Van der Waals dispersion forces may play an important role. For these “non-covalent” interactions the accuracy of standard functionals like generalized gradient approximations (GGA) can be rather uncertain. Benchmarking DFT is thus essential. Accurate total energies of molecules or solids can be obtained by diffusion Monte Carlo (DMC) calculations. DMC remains computationally feasible even in larger systems where usual correlated methods like coupled cluster are impractical. While already applied with success to chemically bonded systems, little is known about how DMC performs for non-covalent bonds.

Here we apply DMC to biomolecular model systems [1] that showcase the performance of present day DFT [2]: formamide-water, tautomerizing via proton transfer; formamide chains, displaying cooperative strengthening of hydrogen bonds; (methyl-) formamide dimers, where GGAs may miss dispersion interactions dependent on the hydrogen bond geometry. For all these systems our DMC hydrogen bond strengths agree well with post-Hartree-Fock results. In addition we calculate adenine-thymine, a DNA base pair where hydrogen bonding and stacking interactions compete. GGAs and hybrid functionals are adequate for the hydrogen bonded conformers, but fail to bind the stacked pair. Second order perturbation theory (MP2) markedly overestimates the stacking energy compared to coupled cluster [CCSD(T)]. Our DMC results confirm those from CCSD(T) studies [3].

In these (state-of-the-art) DMC calculations, using the fixed-node approximation and localization of non-local pseudopotentials, the trial wavefunction must be carefully optimized. We explore a new method [4] to (energy) optimize simultaneously both the orbitals and the correlation factor in a Slater-Jastrow wavefunction. We obtain significantly lower DMC total energies than in the usual practice, that is, to use Hartree-Fock or DFT orbitals and (variance) optimize only the Jastrow factor. Yet both optimization schemes yield almost equivalent hydrogen bond energies, i.e., we find DMC total energy *differences* are more robust than absolute energies.

(*) Permanent address: Instituut Lorentz for Theoretical Physics, Univ. Leiden (NL).

[1] M. Fuchs, C. Filippi, J. Ireta, and M. Scheffler, in preparation.

[2] J. Ireta, J. Neugebauer, and M. Scheffler, *J. Chem. Phys. A* **108**, 5692 (2004).

[3] P. Jurečka and P. Hobza, *J. Am. Chem. Soc.* **125**, 15608 (2003).

[4] F. Schautz and C. Filippi, *J. Chem. Phys.* **120**, 10931 (2004).

Accurate First-Principles Determination of the Stable Adsorption Sites of Molecules on Metal Surfaces

Qing-Miao Hu, Karsten Reuter, and Matthias Scheffler

Density-functional theory (DFT) with present-day jellium-based local-density or gradient-corrected exchange-correlation (xc) functionals has matured into a widely employed tool for the quantitative description of materials on the atomic scale. Despite its undisputed success, there are, however, notorious cases, where this approach fails, even for seemingly quite simple systems. One extensively discussed example is the inability to predict the correct adsorption site of CO on most close-packed transition metal (TM) surfaces, including Pt(111) and Cu(111) [1,2].

Unfortunately, electronic structure methods, which could overcome this problem through an improved xc treatment, scale very unfavorably for extended systems. Since prominent errors in present-day DFT functionals like the electron self-interaction appear to be “nearsighted”, an alternative and more efficient approach could therefore be to only locally correct the xc error [3], i.e., in the CO/TM(111) case within a small cluster around the adsorption site. In the present study we illustrate this idea, by locally correcting the xc energy by a hybrid functional (B3LYP) and many-body perturbation theory (HF+MP2) calculations performed on small clusters. The key is to use appropriate energy differences and appropriately chosen clusters around the adsorption site. Consistent with the understanding of a primarily “nearsighted” error in present-day DFT functionals, we find that the xc *correction* (not the total energy) converges rapidly with cluster size.

For the example of low-coverage adsorption of CO at Cu(111), for which both local-density and gradient-corrected functionals predict the wrong stable adsorption site, we indeed obtain the correct on-top site with this approach. As a second system, we present calculations for the CO/Ag(111) system, where the correct on-top site is already favored by normal gradient-corrected functionals. Here, the xc correction does not affect the energetic order between the two sites and leads only to an increased stability of the on-top configuration. These results are explained in a simple physical picture [4] which indicates that a similar failure of standard DFT calculations as in the CO/Cu(111) case can be expected for a much wider class of molecular adsorption systems. The local xc correction approach presented here is then a suitable tool to overcome this deficiency.

- [1] P.J. Feibelman *et al.*, J. Phys. Chem. B **105**, 4018 (2001).
- [2] M. Gajdos, A. Eichler, and J. Hafner, J. Phys. Cond. Mat. **16**, 1141 (2004).
- [3] C. Filippi, S.B. Healy, P. Kratzer, E. Pehlke, and M. Scheffler, Phys. Rev. Lett. **89**, 166102 (2002).
- [4] G. Kresse, A. Gil, and P. Sautet, Phys. Rev. B **68**, 073401 (2003).

Combining Quasiparticle Energy Calculations with Exact-Exchange Density-Functional Theory

Patrick Rinke, Abdallah Qteish^(*), Jörg Neugebauer^(**), Christoph Freysoldt,
and Matthias Scheffler

The success of photoemission spectroscopy (PES) and its inverse counterpart (IPES) owes much to the interpretation of the photo-electron spectra in terms of single-particle excitations or *quasiparticles*. For solids Hedin's *GW* approximation has become the method of choice for an *ab initio* calculation of the quasiparticle energy spectrum. *GW* is typically applied as a perturbation to density-functional theory (DFT) in the local-density approximation (LDA). However, for systems with semi-core *d*-electrons this approach proves to be problematic if pseudopotentials are used.

In this work we therefore combine *GW* with DFT in the exact-exchange (EXX) approach and present a systematic *ab initio* study of the electronic structure of selected II-VI compounds and group-III nitrides in the zinc-blende structure. We show that EXX gives an improved description of the *d*-electron hybridization compared to the LDA. Moreover, we find that it is essential to use the newly developed EXX pseudopotentials [1] in order to treat core-valence exchange consistently. In combination with *GW* we achieve very good agreement with available photoemission data. Since the DFT energies and wavefunctions serve as input for the *GW* calculation we conclude that for these materials EXX constitutes the better starting point [2].

Amongst the group-III nitrides, InN assumes a special place because the magnitude of its bandgap is still discussed controversially. If one believes LDA or LDA-based *GW* calculations InN should be metallic, however, our EXX-based *GW* calculations yield a semiconductor with a small band gap in agreement with recent experiments [3]. The success of our approach for InN shows that we are now in a position to make predictions for a wide range of materials, for which the existence of a bandgap has not been conclusively determined experimentally.

(*) Permanent address: Physics Department, Yarmouk University, Irbid, Jordan.

(**) Permanent address: Max-Planck-Institut für Eisenforschung, Düsseldorf, Germany.

- [1] M. Moukara, M. Städele, J.A. Majewski, P. Vogl, and A Görling, J. Phys.: Condens. Matter **12**, 6783 (2000).
- [2] P. Rinke, A. Qteish, J. Neugebauer, C. Freysoldt, and M. Scheffler, New J. Phys. **7**, 126 (2005).
- [3] J. Wu *et al.*, Appl. Phys. Lett. **80**, 3967 (2002); T. Takachi, H. Okamoto, M. Nakao, H. Harima, and E. Kurimoto, Appl. Phys. Lett. **81**, 1246 (2002).

Efficiency and Flexibility of Numeric Atom-Centered Basis Sets for Fast All-Electron Calculations

Volker Blum, Ralf Gehrke, Jörg Behler, Karsten Reuter, and Matthias Scheffler

First-principles electronic structure calculations are rapidly becoming a commodity to resolve atomic-scale physical questions. Most prominently, the plane-wave based pseudopotential (PWPP) method constitutes an appealingly simple framework to systematically converge any physical target quantity to arbitrary basis set accuracy. However, the accuracy of PP calculations is still limited by the PWPP itself, e.g. through the controlled physical approximations in the PP construction, or through new physics whose interplay with PPs is yet untested. These uncertainty factors are all resolved in full-potential (FP) calculations, which however are more tricky than their PWPP counterpart, because no basis set of plane-wave-like convergence accuracy *and* simplicity exists. Rather, the construction of systematic FP basis sets (e.g. augmented plane waves [1]) is fraught with complex decision making processes and often imposes some prohibitive computational cost. Custom-optimized, localized atom-centered basis functions $\phi_{nlm}(\mathbf{r}) = u_{nl}(r)Y_{lm}(\Omega)$ (e.g. Gaussian [2], Slater-type [3] or numerical atom-centered orbitals (NAOs) [4]) are an attractive alternative, but these are expressly not systematically complete, and hence there is no guaranteed simple strategy to achieve basis set convergence.

We have investigated the routine feasibility of meV-level total-energy convergence in NAO-based FP electronic structure calculations by a step-wise selection of individual radial basis functions from a large pool of plausible basis function candidates (confined atomic, ionic, or hydrogenic radial functions), using as examples simple molecular or cluster systems such as N₂, Cu₂, Cu₄ and Cu₁₀. The target quantity is the sum of eigenvalues $E_s = \sum_i \epsilon_i$ for fixed non-selfconsistent atomic superposition potentials, a choice which promises maximum efficiency for routine use (no time penalty and additional numerical uncertainties of a selfconsistent procedure). We confirm that meV-level absolute convergence of E_s is possible with ~ 50 basis functions per atom for N₂ and Cu₂, but the required basis size increases for the larger systems Cu₄ and Cu₁₀, illustrating the importance of an easily customizable case-by-case basis convergence strategy. This project is the basis of a larger effort to create the infrastructure for reliable self-consistent FP NAO-based first-principles calculations with no hidden internal limitations on the achievable convergence accuracy, and with easy extendability to advanced electronic-structure developments.

- [1] D. J. Singh, *Plane Waves, Pseudopotentials and the LAPW Method* (Kluwer, 1994).
- [2] R. Poirier *et al.*, *Handbook of Gaussian Basis Sets* (Elsevier, 1985).
- [3] E. van Lenthe and E. J. Baerends, *J. Comput. Chem.* **24**, 1142 (2003).
- [4] B. Delley, *J. Chem. Phys.* **92**, 508 (1990).